EVALUATION OF SLOPE STABILITY CONDITIONS BY NUMERICAL ANALYSIS, A CASE OF OTOLO-SAWLA ASPHALT ROAD PROJECT, SOUTHERN PART OF ETHIOPIA

MSc IN GEOTECHNICAL ENGINEERING

NATNAEL BEREDED BAYOU

HAWASSA UNIVERSITY, HAWASSA, ETHIOPIA

NOVEMBER, 2020

EVALUATION OF SLOPE STABILITY CONDITIONS BY NUMERICAL ANALYSIS, A CASE OF OTOLO-SAWLA ASPHALT ROAD PROJECT, SOUTHERN PART OF ETHIOPIA

NATNAEL BEREDED BAYOU

A THESIS SUBMITTED TO THE DEPARTMENT OF CIVIL ENGINEERING, FACULTY OF CIVIL ENGINEERING AND BUILT ENVIRONMENT, SCHOOL OF GRADUATE STUDIES HAWASSA UNIVERSITY

HAWASSA, ETHIOPIA

IN PARTIAL FULFILLMENT OF THE
REQUIREMENTS FOR THE
DEGREE OF

MASTER OF SCIENCE IN CIVIL ENGINEERING
(GEOTECHNICAL ENGINEERING)

NOVEMBER, 2020

HAWASSA UNIVERSITY

SCHOOL OF GRADUATE STUDIES

ADVISORS' APPROVAL SHEET

This is to certify that the thesis entitled "Evaluation of Slope Stability Conditions by Numerical Analysis, A Case of Otolo-Sawla Asphalt Road Project, the southern part of Ethiopia" submitted in partial fulfillment of the requirements for the degree of Master's with specialization in Geotechnics, the Graduate Program of the School of Civil Engineering, and has been carried out by Natnael Bereded Bayou Id. No GPGeotR/021/11, under our supervision. Therefore, we recommend that the student has fulfilled the requirements, and hence here can submit the thesis to the school.

Yoseph Birru (PhD)	_____	_____
Name of major advisor	Signature	Date
Mr. Bereket Bezabih	_____	_____
Name of co-advisor	Signature	Date

HAWASSA UNIVERSITY

SCHOOL OF GRADUATE STUDIES

EXAMINERS' APPROVAL SHEET

We, the undersigned, members of the Board of Examiners of the final open defense by Natnael Bereded Bayou have read and evaluated his thesis "Evaluation of Slope Stability Conditions by Numerical Analysis, A Case of Otolo-Sawla Asphalt Road Project, and Southern part of Ethiopia", and examined the candidate. This is, to certify that the thesis has been accepted in partial fulfillment of the requirement for the degree.

_____	_____	_____
Name of Major Advisor	Signature	Date
_____	_____	_____
Name of Internal Examiner	Signature	Date
_____	_____	_____
Name of the Chairperson	Signature	Date
_____	_____	_____
Name of External examiner	Signature	Date
_____	_____	_____
SGS Approval	Signature	Date

DECLARATION

I hereby declare that this thesis is my original work and has not been presented for a thesis degree in any other university, and all sources of material used for this thesis have been duly acknowledged.

Name: Natnael Bereded Bayou

Signature _____

This MSc in Geotechnical Engineering or equivalent thesis has been submitted for examination with my approval as a thesis advisor.

Name: Yoseph Birru (PhD)

Signature: _____

Place Hawassa University,

Institute of Technology,

Hawassa.

Date November, 2020

ACKNOWLEDGMENT

First and for most, ‘’praise be to GOD for His Unspeakable Gift’’.

I am very grateful to my major advisor Yoseph Birru (Ph.D.) who has helped me with his guidance throughout the thesis work. I am very grateful to my co-advisor Bereket Bezabih for his critical guidance and support within the whole thesis paper. For the development and finalization of the thesis, I feel a deep sense of gratitude to Zala Woreda Main Administration, for their willingness to support me and for accepting my paper to collect the sample and for transportation facility adjustment. Especially, Uda Urcho, for support and encouragement throughout my site work.

My special thanks go to Ethiopian Road Authority for giving me this incredible scholarship and for funding the research fee and also covering my half school fee. Last but not least, I would also extend my sincere appreciation to everyone who has contributed whether directly or indirectly to this thesis, including my classmates and family members. Especially, Birtukan Uda, Bereket Uda, Hana Uda, Getayawkal Natnael, and Yilikal Natnael, this thesis work would have been impossible without your guidance, advice, and support.

TABLE OF CONTENTS

LISTS OF ABBREVIATIONS ACRONYMS

2D	Two dimensional
AASHTO	American Association of State Highway and Transportation Officials
ASTM	American Society for Testing Materials
E	Elastic Modulus
FEM	Finite Element Method
FOS	Factor of Safety
GPS	Geographic Positioning System
H	Slope Height
IDP	Incremental Displacement Profile
LEM	Limit Equilibrium Method
LI	Liquidity Index
LL	Liquid Limit
MDD	Maximum Dry Density
OMC	Optimum Moisture Content
PI	Plasticity Index
PL	Plastic Limit
SNNPRS	South Nation Nationality People Regional state
SRFEA	Strength Reduction Finite Element Analysis
USCS	Unified Soil classification System
FS	Failed Slope
ES	Existing Slope

LIST OF TABLES

LIST OF FIGURE

LIST OF TABLES IN THE APPENDIX

LIST OF FIGURES IN THE APPENDIX

ABSTRACT

Slope instability related issues in engineered, as well as natural slopes, are common challenges to geotechnical enginers. Due to the slope instability, so many associated risks arise around the cut slope so that it is advisable to analyze the slope stability ahead of excavation. Once slope failure occurs, traffic flow gets obstructed and which ultimately limits the road serviceability level impacting the economy. This thesis presents the investigation, analysis, cause identification, and remedial measures for failed slope and checks stability of the existing slope. Seven cut slope related instability locations were selected along with Otolo-Sawla Asphalt Road Project located in the Southern part of Ethiopia. In this thesis, disturbed samples were taken from a test pit dug in the slope section by hand excavation. In the case of existing slope locations, three samples were taken based on the slope angle and the material forming the slope through field observations. Laboratory tests were conducted to determine the index properties and engineering properties of the soil-forming the selected slope sections. The main objective of this thesis was to investigate slope stability conditions of the Otolo-Sawla asphalt road project using a numerical method considering selected slopes at varied geological and geographical locations. A suggestion of remedial measures to stop further failure of the slope section can be analyzed by modeling with commercial software PLAXIS 2D. Under this thesis, the factor of safety for the identified slope failure was determined using Finite Element software (PLAXIS 2D) based on the strength reduction approach. Based on the analysis the causes for failed slopes were identified as poor slope material, excessive slope height, and high groundwater levels. In this thesis the order of sensitivity of factors affecting the slope stability obtained as $\varphi > H > c > \gamma > k > E > \mu$. A stability check for the existing slopes was carried out and was found slightly stable. On the results from the analysis, the failed slope sections should be reconstructed with a slope angle less than 50% and an adequate drainage system should be provided. Existing slopes near the failed slopes are prone to failure because of similar soil properties and groundwater influence. The provision of geosynthetic for adequate drainage has been recommended as a remedial solution to avoid failure of the existing slopes near the failed slopes.

Keywords: Factor of safety, Finite element method, PLAXIS, Slope stability, Strength reduction technique.

1. INTRODUCTION

1.1. Background

A slope is defined as a surface of which one end or side is at a higher level than another; a rising or falling surface. Earthen embankments are usually constructed over the natural ground for carrying roads or railways over them. They may be constructed along rivers to act as levees, or along drains to act as the drain banks. The sides of the embankment cannot be made to stand vertical, they are to be sloped. Gentler the slope less likely the slope is to fail by slippage. However such flat slopes require more material and space for their construction. They will become uneconomical. A steeper slope may be unsafe. We need to explore the problem from a point of safety and economy and find a safe steepest slope, as Geotechnical Engineers. In the process, we are required to understand what are the forces that cause slippage and forces that hold the soil in equilibrium against failure.

Many road projects which are under construction traversing on an escarpment, mountainous and rolling terrain many times pose slope instability problems thanks to earth cuttings which are required by the road design standard. This problem is especially attributed to seasonal change of moisture on the slopes during the wet (rainy) season because the presence of water causes both increased stresses(through seepage forces) and loss of shear strength within the slope or failure surface. Under mountainous terrains conditions, cut slope instability problems are the foremost common and troublesome of major geotechnical difficulties encountered in such construction projects. And most of the time, there's a general lack of focus for detailed investigation and style for mitigation of slope instability related problems during the design of road projects. The problem of cut slope instability won't become apparent until excavation works are started or finalized to the specified lines and grades, however at later stages the trouble to correct these problems leads to project cost overruns and delay in the completion time of the project (Getinet, 2016).

Unexpected landslides in highly populated areas can cause huge losses to life and property. For already existing slopes, the factor of safety is getting to be calculated and thus the stability check for the slope is completed. Also, the potential failure surface under gravity loading is often acknowledged. For slopes unstable under varying amounts of precipitation or loading conditions, suitable remedial measures like drainage provision, slope angle adjustment, use of geogrids, and anchoring are often suggested. In the case of failed slopes,

the rationale for failure could be identified by studying various properties of the soil condition and slope geometry. A suggestion of remedial measures to stop further failure of the slope section can be analyzed by modeling with commercial software such as PLAXIS 2D.

1.2. Statement of the Problem

Excavation on slope instability may result from failure to control seepage forces in and at the toe of the slope, too steep slopes for the shear strength of the material being excavated, and insufficient shear strength of the soil. Slope instability may occur suddenly, as the slope is being excavated, or after the slope has been standing for some time (Guyer, 2013). The problem was intense mainly during the rainy season. Due to the slope instability, there are so many associated risks that arise around the cut slope so that it is advisable to analyze the slope stability ahead of excavation. Once slope failure occurs, traffic flow gets obstructed and which ultimately limits the road serviceability level impacting the economy. Hence to solve the problem of slope failure, it is advisable to identify the cause for failure of slope and propose the remedial measure. Besides, there was no research and other investigation done on slope stability along the road section to identify, analyze, and recommend proper remedial measures.

The application of numerical methods has been illustrated using the case study of the Otolo-Sawla asphalt road project that is located in the southern part of Ethiopia. These conditions can be modeled and analyzed in numerical software that can depict the behavior of slopes under a different set of conditions with results that are close to practical. The existing stable slope was also evaluated for the vulnerability of failure on-site observation and laboratory test results.

1.3. Objective

1.3.1. General Objective

The main objective of this thesis is to investigate slope stability conditions of the Otolo-Sawla asphalt road project using numerical method considering selected slopes at varied geological and geographical locations.

1.3.2. Specific Objectives

- To determine the index and engineering properties of soils found in slope sections at selected stretches along Otolo-Sawla Road.
- To study the stability of slope using the finite element method for particular soil type and slope condition.
- To identify causes of failure in failed locations and establish vulnerability levels on the rest of existing slopes.
- To suggest remedial measures on identified causes from slope stability analysis.

1.4. Scope of the Study

This thesis addresses the described objects and recommends the remedial measures on identified causes particularly on samples recovered from selected stretches on Otolo-Sawla road. To determine the stability of rock and soil slope, a critical slope section was selected and analyzed using the deterministic method and sensitivity analysis. However, due to constraining time, resources, and financial limitations, the analyses were applied only to selected slopes which showed potential instability. Therefore, during the present study only seven (7) critical slope sections were selected and studied. Besides, there was no borehole log data to determine subsurface lithology, instead, trial test pits with a maximum depth of 1.5m were used.

Concerning the stability analysis, the factor of safety is analyzed using the finite element method. The required analysis is carried out by using finite element software PLAXIS 2D. PLAXIS 2D software requires six input parameters such as cohesion, angle of internal friction, unit weight, Young's modulus, Poisson's ratio, and permeability value. In this study, the values for Young's modulus, Poisson's ratio, and permeability were taken for typical soils from Bowles, (1997) and U.S. Army Corps of Engineers, (1990) based on slope forming material due to the limitation of budget, time, and limitation on free movement due to COVID-19. The use of the results of the analysis and proposed remedial measures of this study are limited to the respective selected slope locations while the method of investigation and analysis can be adopted at other cut slope locations of road projects.

1.5. Significance of the Investigation

The slope failure of the road from Otolo-Sawla along steep cut is causing the operational limit for the road selected. Therefore, this work is significant to solve the problems by

recommending the remedial measures on the analysis result and field conditions. The existing stable slope section is also checked for its vulnerability to failure and allows it to take action before failure. The project road will shorten the additional 270km trip from Arbaminch to Sawla, through Arbaminch -Sodo- Sawla, by nearly half-length and will also connect the towns and many villages of the two ethnic groups, Gamo and Gofa zones with a total estimated length of 138.3kms but the road faces slope stability problem.

1.6. Organization of the Thesis

This thesis work contains five chapters, references, and appendices, each with detailed coverage of specific topics. Chapter one contains the general background of the thesis, problem statement, objective, significance of the study, the scope of the thesis, and the organization of the study. Chapter two contains a literature review of the general slope stability concepts and remedial measures. Chapter three covers material and methods of investigation, testing, characterization, and analysis of the respective cut slope landslides locations. In Chapter four, results and discussion were presented. Under Chapter five, a summary and conclusion were presented. Finally, detailed laboratory test results, Analysis output, and site photos were presented in appendices.

2. LITERATURE REVIEW

2.1. Introduction

Slope failure occurs when the downward movements of slope forming material due to gravity and shear stresses exceed the shear strength. Therefore, factors that tend to extend the shear stresses or decrease the shear strength increase the probabilities of failure of a slope. Increased pore pressure, cracking, decomposition of clayey rock fills, creep under sustained loads, leaching, strain softening, weathering and cyclic loading are common factors that decrease the shear strength of rock mass. In contrast to the present, the shear stress in rock mass may increase due to additional loads and increase in water pressure in cracks at the top of the slope, increase in soil weight due to increased water content, excavation at the bottom of the slope, and seismic effects (Ayalew, 1999).

In addition to those reasons factors contributing to the failure of a slope are properties of the rock mass, (slope geometry), state of stress, temperature, and erosion. In Ethiopia, road development is one of the major concerns of investors. However, the problem of slope instability was also widespread along roads that cross mainly through the mountainous region of the country. Most parts of the north, south, and western regions of the Ethiopian plateau face a record of slope instability both in superficial materials and at bedrocks due to the cutting of hills and roadsides (Ayalew, 1999).

2.2. Slope Stability Studies in Ethiopia

In Ethiopia, the problem of slope instability is widespread mainly along the roads which pass through mountainous regions of the country. To investigate the causative factor and recommend possible remedial measures different researchers conducted different investigations.

According to Jemal (2005) limit equilibrium method slope stability analyses conducted along the main road from Gohatsion to Dejen towns by identifying geological and geotechnical properties of geological material that compose the slope section. The study identified slope instability problems in the form of rockfall, toppling, planar, and wedge mode of rock failure in rock slope sections and circular mode of failure in the soil slope section. The problems were severe in the area on the sides of the road mainly during the rainy season.

Modified landslide hazard zonation techniques were adopted to investigate landslide hazards in Mersa and Wurgessa area. The analyses result revealed that a combination of inherent causative and triggering factors such as slope morphometry, incompetent slope material, and structural discontinuities, prolonged intensive rainfall, and construction activities are the potential factor responsible for slope instability and landslide activities (Jemal, 2011). Similarly, Sameul (2011) conducted a deterministic method of slope stability analyses along the road Gohatsion to Dejen town. The analyses investigated that, the slope was unstable under all anticipated conditions except during static dry conditions.

Landslides are the most common and widespread types of geo-hazard in Ethiopia where over 700 landslide sites were recorded which mostly affect rural communities, infrastructures, farmlands, dwelling houses, and around 54 sites along road sections Woldearegay (2013). Slope instability problems in the form of rockfall, rotational failure of colluvial material, and debris slides are the common events that can happen along the road section. Most of the time presence of loose unconsolidated materials (colluvial materials), highly weathered rock, steep natural slopes, poor drainage conditions, and the occurrence of high seasonal rains created favorable conditions for the occurrence of slope instability (Woldearegay, 2013).

Also, Kasahun (2014) analyzed the stability of the slope along the Mana Begna to Lemlem Bereha road using slope stability probability classification, stereographic projection, limit equilibrium, and probabilistic analysis methods. The analysis result identified that both critical rock and soil slope was unstable mainly during dynamic saturated conditions.

During the sunny and dry days, the slope face becomes desiccated and shrunken especially the newly cut slopes. The extent and depth depend mainly on the plasticity of the soil and type of slope protection. During a rainstorm, water percolates into cracks or other exposed surfaces, causing the slope mass to swell and saturated with the corresponding reduction in shear strength gradually through seepage, migration of soil particles, and gradually increase in void ratio in the soil mass. Initially, water percolates down into the slope mainly through the desiccation cracks and in response to the suction pressure of the highest stratum of dried soil. Because the outer face of the slope swells and saturated, the permeability parallel to the slope face increase with continued rainfall, seepage develops parallel to the slope face. Reduction in shear strength due to saturation and swelling including the condition of seepage, failure eventually occurs if the shearing resistance is adequate to or but the shearing force (Neoh, 2001).

2.3. Slope Stability Governing Factors

Several factors govern the stability of the slope in which some of them act as driving force whereas the other factor contributes as a resistive force. The governing factors are generally divided into internal factors such as the geometry of the slope, potential failure planes, surface drainage, groundwater conditions, mineral composition, and shear strength parameters of material which compose the slope and external factors which are seismicity, rainfall, and human activities (Hoek and Bray, 1981; Raghuvanshi, 2017). Each type of governing factor is discussed as follow:

2.3.1. Internal Factors

2.3.1.1. Geometry of the Slope

Parameters which are considered as the geometry of the slope, especially for rock slope are; dip and direction of the slope and failure plane, slope height, upper slope dip, tension crack Hoek and Bray, 1981; Raghuvanshi (2017). Each of the parameters has its effect on the stability of the slope either individually or collectively. Most of the time, the steeper slope causes the slope to be unstable (Willy and Mah, 2004). Similarly, Gadaawin Lamessa (2019) the input parameter within the given interval having the steepest curve has a large impact on slope stability and if gentle the slope less the effect on the slope stability.

2.3.1.2. Potential Failing Planes

One of the factors which determine the stability of the rock and soil slope is the potential failure plane. In rock slope failure, the persistence of discontinuities such as joint, fault, and shear plane act as failure plane along which the slope will fail. Sometimes, hard strata on which weak layer of the soil rest may serve as a failure plane of soil slope. For a specific mode of rock slope failure to occur, a dip of the potential failure plane should be less than the dip of the slope face but greater than the friction angle along the failure plane (Hoek and Bray, 1981; Willy and Mah, 2004).

2.3.1.3. Surface Water Drainage and Groundwater Conditions

Surface water drainage and groundwater conditions are the main slopes destabilizing factors by decreasing shear strength and increasing the shear stress applied to the failure plane. Surface water which infiltrates into the slope mainly through tension cracks will produce water force, increasing weight over the slope face and lubricate the failure plane which later enhances slope instability (Hoek and Bray, 1981; Robert, 2002; Raghuvanshi, 2017).

2.3.1.4. Shear Strength Parameter of Materials Composing the Slope

Shear strength parameters of materials that compose the slope are the main factors that define resisting force acting normal to the failure plane (Barton and Bandis, 1990; Raghuvanshi, 2017). The parameters in turn depend on the conditions of discontinuities such as roughness, continuity, aperture, and filling (Johnson and Degraff, 1991). Specifically, Barton and Bandis (1990) determine shear strength along failure plane or natural joints using empirical law of basic friction angle first proposed by (Barton, 1973).

2.3.2. External Factors

2.3.2.1. Rainfall

Most of the time, the main reason for slope failure to occur is the influence of rainfall which is one of the external and triggering factors of slope instability (Ayalew et al., 2004; Pantelidis, 2009; Woldearegay, 2013). The rainfall, which infiltrates into the slope will increase the instability of the potential failure plane by reducing shear strength (Pantelidis, 2009; Raghuvanshi, 2017). One of the impacts of rainfall is it increases the level of the groundwater table. Groundwater in turn affects the stability of the rock slope for the following reason (Wyllie and Mah, 2004).

Water pressure affects the stability of the rock slope by decreasing resisting force along the failure plane.

- Change in the moisture content of the rock accelerates weathering and then decreases the shear strength of the rock.
- Freezing of groundwater and surface water in tension cracks cause a buildup of water pressure, which in turn decreases the stability of the slope.
- Increase the degree of weathering in the rock that undermines the toe of the slope.
- The flow of groundwater into the slope face.

2.3.2.2. Seismicity

Seismic activity is another triggering factor of slope stability especially in the active seismic zone (Hoek and Bray, 1981). The minimum magnitude of an earthquake to cause slope failure is approximately 4-5mm (Pantelidis, 2009). From the safety point of view, it is recommendable that seismicity be concerned for critical structures like steep slopes (Dahle et al., 1992). Since horizontal seismic acceleration adds to driving force along the failure

plane, the planar model of rock slope failures will be easily destabilized under seismic loading conditions (Raghuvanshi, 2017).

2.3.2.3. Human Activities

Human activities like improper modifications and excavations of the slope can trigger the stability of the slope. Most of the time human activities that can cause the slope to fail are cutting the slope in an unplanned manner, steepening the slope gradient, improper excavation on the toe of the slope, adding an extra load (Raghuvanshi, 2017).

2.4. Types of Slope Failure

The typical slope failures that are expected to occur in soil slope are; translational, planar or wedge, circular, non-circular, and combination of both circular and non-circular (Abramson et al., 2002). Planar slope failure occurs in soil layer or relict joint with relatively low strength which influences the failure surface while the translational type of failure occurs where shallow soil overly relatively strong material (Hoek and Bray, 1981, Chowdhury, 2010). Similarly, circular mode of failure occurs in slope with homogeneous materials mainly soil slope and sometimes in highly fractured rock (Abramson et al.,2002). The non-circular mode of failure mostly occurs in a slope that has heterogeneous composition.

According to Goodman (1989), there are three different types of rock slope failures such as a planar, wedge, and toppling mode of failure. Planar rock slope failure occurs under gravity when rock blocks rest on an inclined failure like a joint that daylight into free space (Sharma et al., 1999).

A wedge mode of rock slope failure occurs where containing discontinuities striking obliquely into the slope face and then slide of wedges take place along the line of intersection of the two planes. A wedge mode of rock slope failures occurs over a wider range of geologic and geometric conditions than the planar mode of failure (Goodman, 1989; Wyllie and Mah, 2004). The toppling mode of rock slope occurs due to overturning of rock layers or discontinuities that are dipping steeply into the slope face Goodman (1989) and it involves rotation of columns or blocks of rocks about a fixed base (Wyllie and Mah, 2004). The circular model of slope failure occurs in weak material such as highly weathered or closely fractured rock and soils where failure occurs along surface having an approximately circular shape (Wyllie and Mah, 2004).

Cruden and Varnes (1996) classified the slope failures into the following five major categories.

a) Fall:- is detachment of soil and/or rock fragments that fall down a slope.
b) Topple:- is a forward rotation of soil and/or rock mass about an axis below the center of gravity of mass being displaced.
c) Slide:- is the downward movement of a soil mass occurring on a surface of rupture.
d) Spread:- is a form of the slide by translation. It occurs by "sudden movement of water-bearing seams of sands or silts overlain by clays or loaded by fills."
e) Flow:- is a downward movement of soil mass similar to a viscous fluid

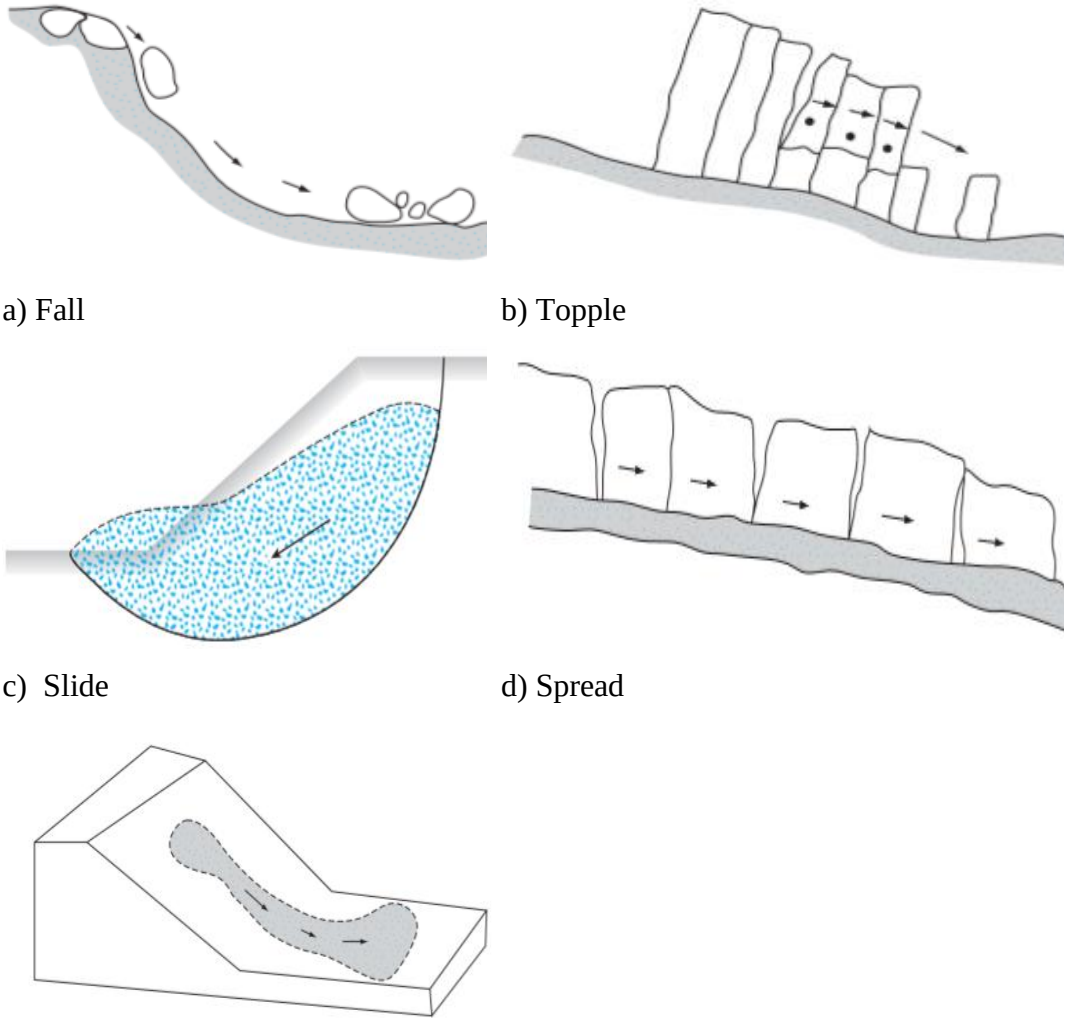

a) Fall b) Topple

c) Slide d) Spread

e) Flow

Figure 2. 1: Classification of the slope failure as per Cruden and Varnes (1996)

2.5. Stabilization Methods of Rock and Soil Slopes

Various development project such as highway, railway, tunnel, dams, mines, residential and industries found in rugged topography and mountainous terrain needs stable slopes and control of rockfalls (Hoek and Bray, 1981; Wyllie and Mah, 2004; Cheng and Lau, 2014). The slope becomes stable by performing a stabilization method for rock and soil slopes.

The slope stabilization method generally increases the factor of safety through reducing driving force by excavating material from the unstable ground, installing appropriate drainage methods, and increasing resistive force by building retaining structure or support, chemical treatment to harden the soil (Abramson et al., 2002). Before the best methods of stabilization are selected, the potential mode of failure and the actual cause of slope instability should be determined (Sharma et al., 1999; Park and West, 2001; Abramson et al., 2002; Wyllie and Mah, 2004). There are different techniques to stabilize the unstable rock slope to make it stable Abramson et al. (2002; Wyllie and Mah (2004) and each of the methods is stated below.

2.6. Slope Stability Analyses Approaches

Slope stability analysis can be carried out by employing different techniques such as Rock mass rating, slope mass rating, kinematic, deterministic, probabilistic, and numerical methods (Abramson, et al., 2002; Raghuvanshi, 2017).

2.6.1. Deterministic Method Stability Analyses of Soil Slope Failure

In a soil slope failure, there is no longer defined failure surface, failure surface is free to find the line with least resistance to failure, and it has a circular shape (Hoek and bray, 1981; Hoek, 2000, Wyllie and Mah, 2004). Soil that consists, sand, smaller rock fragment, and silt exhibit circular mode of failure even in slope with small height (Wyllie and Mah, 2004). Similarly, Chen and Lau,(2011) stated that in sandy soil pore water pressure rapidly increases when the slope was approached to failure and permeable sand fail in sliding mode while less permeable silty sand failure was initiated by erosion at shallow depth. However, due to the permeability of sandy soils, the generated pore water pressure will quickly dissipate after the failure of the slope (Wang and Sassa, 2003).

In circular slope stability analyses, failure surfaces with a minimum factor of safety considered as critical slip surface. The stability of soil slope, done by dividing a series of slides that are usually vertical, and the base of the slice is inclined at angle ψb the failure

plane. According to Wyllie and Mah (2004) factor of safety for a circular mode of failure based on deterministic limit, equilibrium is:

$$FOS = \frac{\text{Shear strength available to resist sliding}(c+\sigma\tan\varphi)}{\text{Shear stress driving the failure }(\tau c)} \quad \ldots\ldots\ldots\ldots\ldots\ldots\ldots\ldots\ldots\ldots\ldots\ldots\ldots\ldots\ldots\ldots(2.1)$$

Where c is cohesion and ϕ is friction angle along failure plane respectively while σ is normal stress applied onto failure plane.

The deterministic method analyzes the stability of the slope based on limit equilibrium concepts, which determine the factor of safety from the ratio of available shear strength to mobilized shear stress (Duncan, 2000; Abramson et al., 2002). It also uses Mohr-Coulomb failure criteria to determine the shear strength parameter along the failure plane. Especially for soil slope failure, the limit equilibrium method analyses the stability of the slope by dividing the soil mass into a different slice from which normal and shear inter-slice force and equilibrium conditions can be estimated (Abramson et al., 2002).

As cited in Abramson et al. (2002) various analyses methods of the slice that depends on the limit equilibrium principles are: (Fellenius, 1936) ordinary method, (Janbu, 1954) simplified and corrected method, Bishop (1956), Morgenstern-Price (1965), Spencer (1967) and Sharma (1973) method. Each of the methods was described as follows.

Ordinary or Fellenius method: It is the oldest technique developed by Fellenius (1936) and introduced the concept of limit equilibrium by dividing the failing soil mass into a different slice. It satisfies moment equilibrium for a circular slip surface. However, it neglects both normal and shear force applied to the failure plane which leads to the inconsistent calculation of safety factors (Abramson et al., 2002).

Janbu simplified method: It is another technique developed by Janbu (1954) which considers force equilibrium. However, the method fails to satisfy moment equilibrium and it considers zero normal and shear interslice force.

Janbu corrected method: It is another method, which depends on the dimensionless parameter and different stability charts (Janbu, 1996). It determines safety factors by considering different conditions such as surcharge, groundwater, and stress analysis and it is applicable for non-circular slip surfaces.

Bishop method: It is the technique developed by Bishop (1956) and it was the most common stability analysis for circular failure plane. This method satisfies moment equilibrium and considers interslice normal force. However, it fails to satisfy force equilibrium and it did not consider interslice shear force.

Morgenstern-Price method: It is another technique developed by Morgenstern and Price (1965) which considers both force and moment equilibrium. Besides, it considers both interslice normal and shear force with inclination at different angles to determine safety factors and it applies to the slip surface of different shapes.

Spencer method: It is a method developed by Spencer (1967) which is applicable to slip surface shape with different shapes. It satisfies both force and moment equilibrium. Also, it considers both interslice normal and shear force. However, it assumes constant inclination for both interslice normal and shear force.

Sharma method: It is another technique developed by Sharma (1973) which applies to both force and moment equilibrium and slip surface of any shape. It uses the method of the slice to calculate the magnitude of the horizontal seismic coefficient need to bring soil mass into a state of horizontal equilibrium. Under this study, the factor of safety for the identified slope failure was determined using Finite Element software (PLAXIS 2D) based on the strength reduction approach.

2.6.2. Strength Reduction FEM

Generally, there are two approaches to analyze slope stability using the finite element method. One approach is to increase the gravity load and the second approach is to reduce the strength characteristics of the soil mass (Halder et al., 2017). According to Farshidfar and Nayeri, (2015) in this method shear strength is considered to be reduced as less as failure occurs. It uses the PLAXIS, which is capable of calculating deformations rates and safety factors by gaining geometry data of a problem and soil specifications and using the finite element method (FEM). The analysis is performed at both static and pseudo-static modes.

As per Duncan, (1996) the safety factor of a slope can be defined as the reduction degree on shear strength of soil when the slope is at the critical failure state. If c and φ are divided by reduction coefficient FOS, new parameters of shear strength c′, φ′ can be gotten. Calculating by using Shen and Ohnishi, (2004) repeatedly until the critical failure state, the reduction coefficient is safety factor:

$$c' = \frac{c}{FOS} \quad \text{.....(2.2)}$$

$$\varphi' = \arctan\frac{\tan\varphi}{FOS} \quad \text{.....(2.3)}$$

The study of strength reduction FEM and its application to soil slope stability was introduced by (Song, 1997). Theoretical and applied researches Yingren et al.,(2002) have

continued with improved accuracy. In some of earlier works Yingren et al.,(2002) advanced the basic theory of strength reduction FEM and played a leading role in its application to the design of anti-slide piles. That earlier works also involved an intensive study of the ultimate bearing capacity of foundations by step-loading FEM and its applications (Weixue, 2005).

2.6.3. Sensitivity Analysis

Sensitivity analysis in slope stability is examined in the existing slope in the coal mining area. According to Surjandari et al.,*(*2019) the most sensitive of soil parameter to safety factor is soil cohesion. Another study on the sensitivity of soil parameters was carried out on the slopes in Kuala Lumpur. The analysis parameters in the form of a range of cohesion values, friction angle, unit weight, and groundwater levels are made with three conditions (maximum, mean, and minimum). Sensitivity analysis is done by two methods, namely Spencer and General Limit Equilibrium. The most sensitive parameter sequence is groundwater level, friction angle, cohesion, and unit weight. The difference in sensitivity analysis methods has a relatively small effect, which is between 0.1571% to 0.1720% for all parameters (Surjandari *et al.*,2019).

2.6.4. Numerical Method

Conventional types of slope stability analyses are limited to the simplistic problem in their scope of application encompassing simple slope geometries and basic loading conditions and provide limited analyses regarding the mechanism of slope failure. To address such a limitation numerical modeling approach has been forwarded to provide an approximate solution to problems that otherwise would have not been solved by the conventional method (Abramson et al., 2002). It is typical of the slope stability analysis approach, which solves slope stability in the form of mathematical calculation by considering deformation.

2.6.4.1. Plaxis Software

The development of the PLAXIS began in 1987 at Delft University of Technology as an initiative of the Dutch Ministry of Public Works and Water Management (Rijkswaterstaat). The initial purpose was to develop an easy-to-use 2D finite element code for the analysis of river embankments on the soft soils of the lowlands of Holland.

In subsequent years, PLAXIS was extended to cover most other areas of geotechnical engineering. Because of continuously growing activities, the PLAXIS company (PLAXIS bv) was formed in 1993. In 1998, the primary PLAXIS 2D deformation and stress analysis

program for Windows was released. The finite element is a technique for solving differential equations problems in engineering and science. PLAXIS 2D is used to investigate stability in geotechnical design. The software can break down issues in manmade and natural inclines. The factor of safety is determined by the Ø/c reduction approach where the strength parameters and cohesion of soil are successively reduced until failure of the structure occurs.

In PLAXIS 2D analysis, additional displacements were generated during a Safety calculation. The total incremental displacements in the final step (at failure) indicate the likely failure mechanism.

According to Endalkachew and Tibebu, (2019) PLAXIS software is based on stress compatibility, the soil parameters were modified to generate comparable output with the limit equilibrium program Talren-4. A minimum factor of safety was obtained from the PLAXIS 2D analysis, which is compatible with the observed field condition. Most of the failure surfaces obtained from PLAXIS 2D analysis are circular, except for a few sections, and encompass all the rail tracks.

Unlike the limit equilibrium method where a circular slip surface is adopted, the shape and location of the failure surface are not determined before analysis. According to Talren-4 outputs, the improvement measures showed an insignificant influence on the shape and size of the critical slip circle. However, the PLAXIS 2D outputs show some improvement in the shape and size of the critical slip circle. For the analysis considering the new rail alignment, both methods show a minimum factor of safety of more than 1.3, which confirms the stability of the slope under the new alignment.

Besides, PLAXIS 2D generates a slip surface, which is smaller and passes far away from the rail tracks. As per Maula and Zhang, (2011) for simple homogenous soil slopes, it was found that the results from Geo Studio software 2007 and PLAXIS 2D Program are generally in good agreement. Investigated the effect of embankment height and its slopes (geometry) on stability and liquefaction due to the earthquake. Increasing embankment height and flattering can enhance stability and reduced the liquefaction zone.

According to Wen et al., (2011) using the FLAC3D program, a 3D plane strain model was proposed and the stability analysis was implemented, placing the results in context with 2D methods. The results show that safety factors got from the 3D plane strain model were closest to the Simplified Bishop method, and the average deviation of 2D and 3D methods is 1.6%, the largest deviation is 3.2%. With the refinement of FE mesh or improvement of the element type, the deviation could be smaller.

According to Abbas, (2015) soil types largely affect slope stability issues. Also, a high factor of safety is obtained in case of stable soil type. Using 2D finite element with Mohr-Columb soil model.

Chakrabarti and Shivananda, (2017) conclude that the higher the cohesion and angle of friction value higher the stability apparently in preliminary aspects. Different stresses values are increasing with the increase of angle of friction value or some time decreasing also. But another important thing we can conclude here from this slope stability analysis by PLAXIS-2D that is without giving a minimum value of cohesion this set of programs cannot run and doesn't give the experimental results.

For further details, readers are referred to the work of Clough and Woodward, (1967), Strang and Fix, (1973), Hughes (1987), Zienkiewicz and Taylor, (1989). PLAXIS Version 8 Brinkgreve, (2002) is a finite element package intended for the two-dimensional analysis of deformation and stability in geotechnical engineering. The program can analyze problems in manmade or natural slopes. The safety factor is determined using the strength reduction approach where the strength parameters (Ø) and (c) of the soil is successively reduced until failure of the structure occurs.

2.7. Factor of Safety Obtained from Finite Element Limit Analysis

In geotechnical engineering, no generally accepted definition of the factor of safety (FOS) exists. For many bearing capacity problems, the FOS is usually defined based on the ultimate load-bearing capacity. However, for slope stability analyses, it is more common that the FOS is related to the characteristic strength parameters of the soil. The instability of a slope is an ongoing concern in most construction and infrastructure projects, as slope failures can result in significant repair and maintenance costs and can endanger both the workers and the public (Chen, 2007).

According to Benda, (2014) for general slope stability analysis of permanent fills and landslide repairs that do not support structures, a minimum safety factor of 1.3 shall be used. A minimum factor of safety of 1.5 shall be used for cut slopes. For temporary or staged construction a minimum factor of safety of 1.2 may be used. For extreme events such as a rapid drawdown or earthquake event, the minimum factor of safety is equal to 1.1. Larger safety factors should be used if there is significant uncertainty in the analysis input parameters.

During the stability analyses of the failure slope area, sensitivity analyses were performed to determine the failure conditions for each landslide. Since the triggering factor of the landslides was heavy rainfall in the study area, the analyses mainly focused on pore pressure conditions that eventually caused the failure. Besides, to investigate the present topography to determine the current stability conditions of the area (Springer, 2019).

Smoothed particle hydrodynamics is a mesh-free numerical method that can directly simulate the large displacement of soils that occurs during landslides (An et al. 2016; He et al., 2017). Gordon and Griffiths, (2005) stated that the failure prediction of a soil and rock slope has been long-standing geotechnical problems, which attracted a wide variety of solutions.

To apply slope stability principles properly, geology, hydrology, soil, and rock properties has should be understood. Site conditions should be applied precisely to the model for analysis. Engineering judgments are made based on assessing the results of analyses considering acceptable risk or safety factors (Abramson et al., 2001). Geology is one of the important factors considered in slope stability analysis (Varnes, 1996). Depending on the type of regolith, there is a strong relationship between the geology of the material and slope instability in a specific area.

According to Carson and Petley, (1970), the slope gradient is taken as the main driving force of mass movement, especially for shallow landslides. In most cases of landslide assessment, the slope gradient is taken as the main causative factor (Swanston and Dryness, 1973).

In a finite element approach, the slope failure occurs through zones that cannot resist the shear stresses applied. Hence, the results obtained from this analysis are considered to be more realistic compared to the limit equilibrium method (Griffiths and Lane, 1999).

According to Abramson, (2001) the stability of any slope will be improved if certain actions are carried out. To be effective, the first one must identify the most important controlling process that is affecting the stability of the slope; second, one must determine the appropriate technique to be sufficiently applied to reduce the influence of that process. The mitigate prescription must be designed to fit the condition of the specific slope under study. The analysis of these alternative remedial measures for soil slope problems requires experience and sound decision on the part of the experts.

This method is very advantageous as it can be used for any shape of the slip surfaces. Spencer, (1967) established a method similar to the Morgenstern and Price method which

can be used for any shape of the slip surface. The method assumed the interslice forces to be parallel i.e. they are having the same inclination.

Fredlund and Krahn, (1977) developed a factor of safety (FOS) equations for solving a composite failure surface, partial submergence, line loading, and earthquake loading conditions by comparing the varied 2D slope stability methods. One of the earliest FE methods of slope stability was introduced by Smith and Hobbs, (1974) and the method was used only for $\varphi u = 0$ soil. Zienkiewicz et al., (1975) used FEM to find the FOS for a c-φ soil slope and the results obtained were very satisfactory with slip circle solutions.

As per Griffiths, (1980) FEM used to point out consistent slope stability results for an in-depth range of soil types and geometric conditions as compared with the charts of Bishop and Morgenstern.

Griffiths and Lane, (1999) again used the FEM in combination with the Mohr-Coulomb stress-strain method to examine the stability of slopes and failure was measured as the situation when no convergence occurs within the specified number of iterations.

According to Rabie, (2014), a comparative study between the LE methods and FE methods of calculating the FOS under the effect of heavy rainfall carried out, and finally, it is concluded that the classical LE methods are highly conservative compared to the FE approach.

The stability of slopes can also be defined based on the concept of probability of failure. To take into account the various uncertainties the probability concept is very reliable to use. Probability analysis of slopes is gaining popularity in recent years. In the last few decades, some remarkable work has been published in the field of the probabilistic approach of slope stability. It was Tobutt (1982) who first demonstrated the Monte-Carlo simulation (MCS) technique for slope stability analysis.

Further, Christian et al., (1994) used the first-order method and the application of the probability concept for analyzing and accounting for the uncertainties present in the slope stability. The probability of failure is calculated based on the critical slip surface obtained from the deterministic method by the initial researchers. After that, it was Hassan and Wolff, (1999) who stated that the critical slip surface having minimum FOS may or may not be the critical surface of the maximum probability of failure. Thereafter, Chowdhury and Xu, (1995), Liang et al., (1999), and Bhattacharya et al., (2003) continued on their research work by considering the critical slip surface to be the surface with a minimum reliability index.

When assessing the stability of slopes, engineers are often faced with the challenge of selecting appropriate soil parameters and models. Only a limited number of laboratory test results are available from which such parameters could be extracted. Causes for failure of these slopes identified and remedial measures suggested to failed slopes and stability check for existing stable slope also conducted on Mohr-Coulomb failure criterion with a frictional and a cohesive component as chosen strength model for describing the shear resistance. Further, Nordal and Glaamen, (2004) say, "By lowering the strength incrementally, a soil body is identified to fail after a certain strength reduction". In this way, Plaxis computes the FOS as the ratio of the available shear strength to the strength at the failure by summing up the incremental multiplier (Msf).

2.8. Permeability and Elastic Properties of Soil

2.8.1. Permeability

The flow of soil water for nonturbulent conditions has been expressed by Darcy as

$V = ki$……(2.4)

where i = hydraulic gradient h/L, as previously defined

k = coefficient of permeability (or hydraulic conductivity) as proposed by Darcy, length/time

Table 2-3 lists typical order-of-magnitude (exponent of 10) values for various soils. The quantity of flow q through a cross-section of area A is

$q = kiA$……..…(2.5)

Table 2.1: values for permeability k, (based on the description of soil and by the USCS, m/s)

$10°$	10^{-2}	10^{-5}	10^{-9}	10^{-11}
Clean gravel GW, GP	Clean gravel and sand mixtures GW, GP SW, SP GM	Sand-silt mixtures SM, SL, SC	Clays	

The correlation equations obtained for determining the coefficient of permeability (k) for fine-grained soil by Chitra et al., 2018 are as follows:- $k=0.0005e^{-0.15LL}$, where LL= Liquid limit.

Hazen Equation;

$K = C(D_{10})^2$……...…(2.6)

where: k= coefficient of permeability (cm/sec)

C= constant ranging from 0.4 to 1.2, typically assumed to be 1.0.

D_{10} = grain size corresponding to 10% by weight passing, also referred to as the effective size(mm).

The advantage of Hazen's formula is that D_{10} from a large number of samples at a given site can be quickly and easily determined to compute permeability. This helps evaluate the variability of permeability at a given site quickly and cost-effectively.

2.8.2. Elastic Properties of Soil

Hooke's generalized stress-strain law is usually utilized in solving geotechnical problems of stress and settlement. Poisson's ratio μ is used in both pressure and settlement studies and is defined as the ratio of axial compression Ev to lateral expansion EL strains.

The μ ratio has a (+) sign in this equation if Eev is compressive strain and the lateral strain EL causes the lateral dimension to increase. In a tension test, the sign is (+) if the sample Ev produces elongation while the lateral dimension(s) decreases. The shearing strain is defined as the change in the right angle of any corner of an element in compression.

Table 2.2: Values of Poisson's ratio μ (Bowles,1997)

Type of soil	μ
Clay, saturated	0.4-0.5
Clay, unsaturated	0.1-0.3
Sandy clay	0.2-0.3
Silt	0.3-0.35
Sand, gravelly sand commonly used	-0.1-1.00 0.3-0.4
Rock	0.1-0.4 (depends somewhat on the type of rock)
Loess	0.1-0.3
Ice	0.36
Concrete	0.15
Steel	0.33

The stress-strain modulus Es, Poisson's ratio μ is one of the elastic properties of most interest. These values are commonly used in computing estimates of foundation settlements. The stress-strain modulus can be obtained from the slope (tangent or secant) of stress-strain curves from triaxial. Typical value ranges for several soils are given in Table 2-3.

Elastic Young's Modulus. Young's elastic modulus is commonly used for the estimation of settlement from static loads. Suitable values of the elastic modulus Es as a function of depth may be estimated from empirical correlations, results of laboratory tests on undisturbed specimens, and results of field tests.

Table 2.3: Values for the elastic modulus (U.S. Army Corps of Engineers, 1990)

Typical Elastic Moduli			
Soil		Es, tsf	Es, kN/m^2
Clay	Very soft clay	5 - 50	536 - 5365
	Soft clay	50 - 200	5365 - 21460
	Medium clay	200 - 500	21460 - 53650
	Stiff clay, silty clay	500 - 1000	53650 - 107300
	Sandy clay	250 -2000	26825 - 214600
	Clay shale	1000 - 2000	107300 - 214600
Sand	Loose sand	100 - 250	10730 - 26825
	Dense sand	250 - 1000	26825 - 107300
	Dense sand and gravel	1000 - 2000	107300 - 214600
	silty sand	250 - 2000	26825 - 214600

2.9. Side Slopes and Back Slopes

Side slopes should be designed to ensure the stability of the roadway and to supply an inexpensive opportunity for recovery of an out-of-control vehicle. Three regions of the roadside are important when evaluating the safety aspects: the highest of the slope (hinge point), the side slope, and therefore the toe of the slope (intersection of the fore slope with the level ground or with a back slope, forming a ditch). Research has found that rounding at the hinge point can significantly reduce the hazard potential. Similarly, rounding at the toe of the slope is additionally beneficial (ERA Geometric Design Manual-2002).

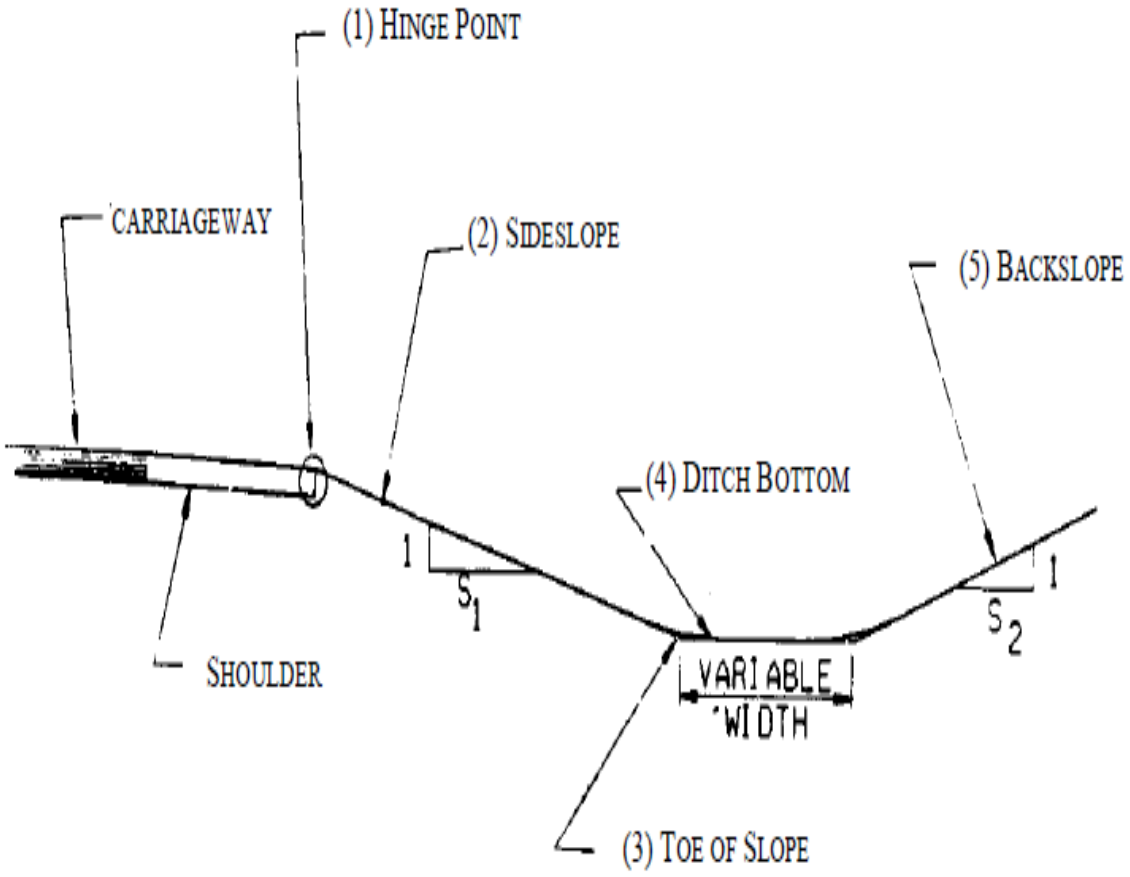

Figure 2.2: Designation of Roadside Regions (ERA Geometric Design Manual-2002)

Embankment or fill slopes parallel to the flow of traffic could also be defined as recoverable, nonrecoverable, or critical. Recoverable slopes include all embankment slopes 1:4 or flatter. Motorists who encroach on recoverable slopes can generally stop their vehicles or slow them enough to return to the roadway safely. Fixed obstacles like culvert headwalls should not extend above the embankment within the clear zone distance. A non-recoverable slope is defined together which is traversable, but from which most motorists are going to be unable to prevent or to return to the roadway easily. Typically, vehicles on such slopes are often expected to succeed at the bottom. Embankments between 1:3 and 1:4 generally fall under this category. Since a high percentage of encroaching vehicles will reach the toe of these slopes, the clear zone distance extends beyond the slope, and a clear runout area at the base is desirable. A critical slope is one on which a vehicle is probably going to overturn. Slopes steeper than 1:3 generally fall under this category (ERA Geometric Design Manual-2002).

The selection of a side slope and back slope depends on safety considerations, the height of cut or fill, and economic considerations.

Table 2.4 indicates the side slope ratios recommended for use in the design according to the height of fill and cut and the material.

Table 2.4: Slope Ratio (V: H) (ERA Geometric Design Manual-2002)

Material	Height of Slope	Side slope		Back slope	Zone Description
		Cut	Fill		
Earth or soil	0.0-1.0m	1:4	1:4	1:3	Recoverable
	1.0-2.0m	1:3	1:3	1:2	Non-recoverable
	Over 2.0m	1:2	1:2	1:1.5	Critical
Rock	Any height	See Standard Details			Critical
Black Cotton Soil	0.0-2.0m	1:6			Recoverable
	Over 2.0m	1:4			

3. MATERIALS AND METHODS

3.1. Description of the study area

3.1.1. General

The Federal Democratic Republic of Ethiopia (FDRE), represented by the Ethiopian Roads Authority as the owner of Arba Minch – Kemba - Sawla Road Project (~138 km). The consultancy service for the Detailed Engineering Design, Tender Document Preparation of the project has been undertaken by MH Engineering PLC. The construction work is done by FAL Trading General Contractor and notices to commence the services was issued on the 8th of September 2011 to construct Otolo-Sawla(~50.8 km), which is a part of Arba Minch – Sawla Road Project: Lot 3: Otolo(KM87+000) - Sawla(KM138+175). The scope of the contract is the construction of 50.8 km Road to DS5 Double Surfaced dressing standard with an initial project amount of ETB: 453,990,619.00. The construction period for this contract was 1095 calendar days (Three years), running between September 8, 2011, and February 7, 2014.

3.1.2. The Road Project Location

The Arba Minch-Sawla project road is located in the southern part of the country in Southern Nations and Nationalities People Regional State. The project starts at a village called Otolo, which is located some 87km away from Shele Mazoria, which itself, is 20km from Arba Minch on the Arba Minch-Jinka road and terminates at station 138+300 outskirts of Sawla town and the route connects Arba Minch to Sawla via Kemba. The project road, Otolo-Sawla, forms the end lot of the Arba Minch – Sawla road project stretching between Otolo and Sawla towns. The Control points of the project are Otolo village, Galma Town, and Geltsa Village. The geographic positions of the total road fall between 7º 18′ N latitude to 38º 05′ E longitude and 6º 02′ N latitude 37º 33′ E longitude. The project road will shorten the additional 270km trip from Arbaminch to Sawla, through Arbaminch -Sodo- Sawla, by nearly half-length and will also connect the towns and many villages of the two ethnic groups, Gamo and Gofa zones with a total estimated length of 138.3kms but the road faces slope stability problem.

Figure 3. 1: The road project (study area) general location

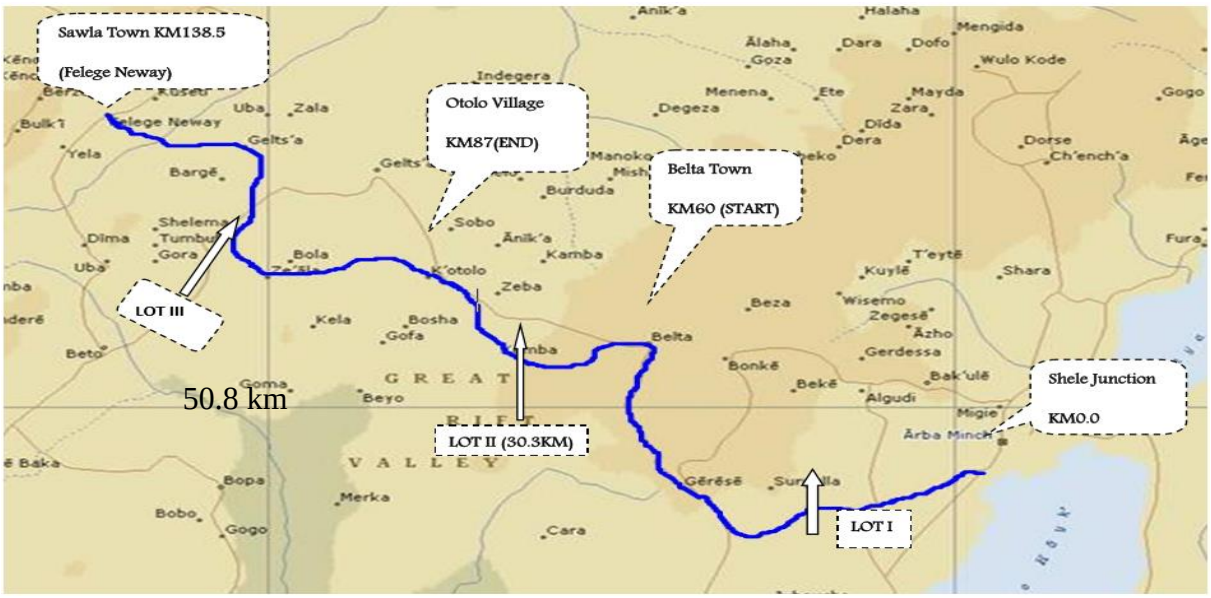

Figure 3.2: The project road location (Robust Consulting and Engineering Services PLC, 2014)

3.1.3. Topography and Climate

3.1.3.1. Topography and Terrain of the Project Area

One of the main determinants of the alignment design parameters of the road is the terrain through which the road traverses. According to the Geometric Design Manual, 2002 of Ethiopian Roads Authority, the terrain is classified by the general scope of the area through which the existing road passes.

The terrain of the project alignment is described as flat/rolling over 54% of the project length and the rest sections characterized by mountainous and escarpment physiographic features. Accordingly, the terrain classification is made for the road alignment tabulated below under table 3.1. according to ERA Geometric Design Manual, 2002.

Table 3.1: Summary of Terrain classification of the project (Robust Consulting and Engineering Services PLC, 2014)

Sr. No	Terrain Type	Slope	Length (km)	Coverage (%)
1	Flat	Up to 5%	18.92	37.24
2	Rolling	5-25%	8.74	17.20
3	Mountainous	25-50%	16.40	32.28
4	Escarpment	Over 50%	6.74	13.27
Total			50.8	100

3.1.3.2. Climate of the Project Area

Rainfall: According to ERA, (2002) drainage design, manual the project road is located in rainfall regime B2. The rainfall in the project area is bimodal - the first rainy season is from March-May and the second is from September-November. The annual rainfall of the project area varies between 900 mm/year to 1400 mm/year.

Temperature: Under normal conditions, air temperature decreases with increasing altitude. The Mean maximum and minimum temperatures in the project are 30 ℃ and 16.5℃ respectively.

3.1.4. Geology of the Project Area

According to the geological map of Ethiopia at a scale of 1:2,000,000, the 1:500,000 scale geological map of Omo River Project Area, and field observation, the project route corridor, is comprised of Jimma Volcanic (Pjb), and Alluvial, Lacustrine Deposits (Q) and (Peqf).

The Jimma basalts are pre-lift tertiary volcanic rocks with thick basaltic base rock and thin Salic rocks. They form the dominant formation in hilly and mountainous terrains. The weathered and fractured parts are used as natural gravel wearing sources and the fresh ones used for aggregate crushing.

The Alluvial and Lacustrine deposit formed in the flat terrains of the project route with reddish silty clay soil formations and brownish sand and silts around the rivers. The reddish clay soils are suitable materials for the construction of embankments.

3.2. Materials

The required samples were collected from the potential slope section having test pits dug through the embankment of the road cut slope section. Disturbed samples are generally obtained to determine the soil type, gradation, consistency, and specific gravity of the soil. The methods for obtaining disturbed samples vary from hand excavating of materials with picks and shovels to using truck-mounted augers and other rotary drilling techniques. These samples are considered disturbed since the sampling process modifies their natural structure. In this thesis, disturbed samples were taken from a test pit dug in the slope section by hand excavation. Undisturbed samples are used to determine the in-place strength, compressibility (settlement), natural moisture content, unit weight, permeability, discontinuities, fractures, and fissures of subsurface formations.

Even though such samples are designated as undisturbed, in reality, they are disturbed to vary degrees. The degree of disturbance depends on the type of subsurface materials, type and condition of the sampling equipment used, the skill of the drillers, and the storage and transportation methods used. In this thesis work is true about field tests such as field density test and unit weight tests with natural moisture content determination from those seven selected slope locations. Remolded soil is usually substituted for undisturbed soil in shear tests to measure the strength of natural soil.

Disturbed samples were taken from seven slope locations to conduct laboratory tests. From seven samples four samples were taken from each failed slope location and three were from existing slopes. In the study area, there were four failed slopes during the site survey, and sample from each slope section collected. In the case of existing slope locations, three samples were taken based on the slope angle and the material forming the slope through field observations. A field density test was conducted to remold the sample for shear strength

tests. Bulk density of the slope material from field density test is used to determine the mass used for shear strength test using direct shear test having a shear box with volume 90 centimeter cubic preserving the natural moisture content by proper handling of the sample.

To achieve the described objective of this thesis, different field and laboratory materials are used. These materials were: - Sampling tool for disturbed samples collection and unit weight determination mold; Geometry and elevation of the selected slope sections: GPS, rope, meter, and water level; Field density test apparatus: sand replacement method with complete accessories; For particle size distribution: set of Sieves, hydrometer, balance, shaker, sample splitter and can; For specific gravity test: Pycnometer, water dropper, thermometer, vacuum pump, digital balance, oven and can; For Atterberg's limit test: Casagrande apparatus, mixing dish, flat glass, water dropper, can, balance, spatula, and oven-dry; The direct shear test equipment; For writing the thesis and analyzing, the data computer is used.

3.3. Study Methodology

The overall workflow diagram of the study has been presented below in figure 3.2.

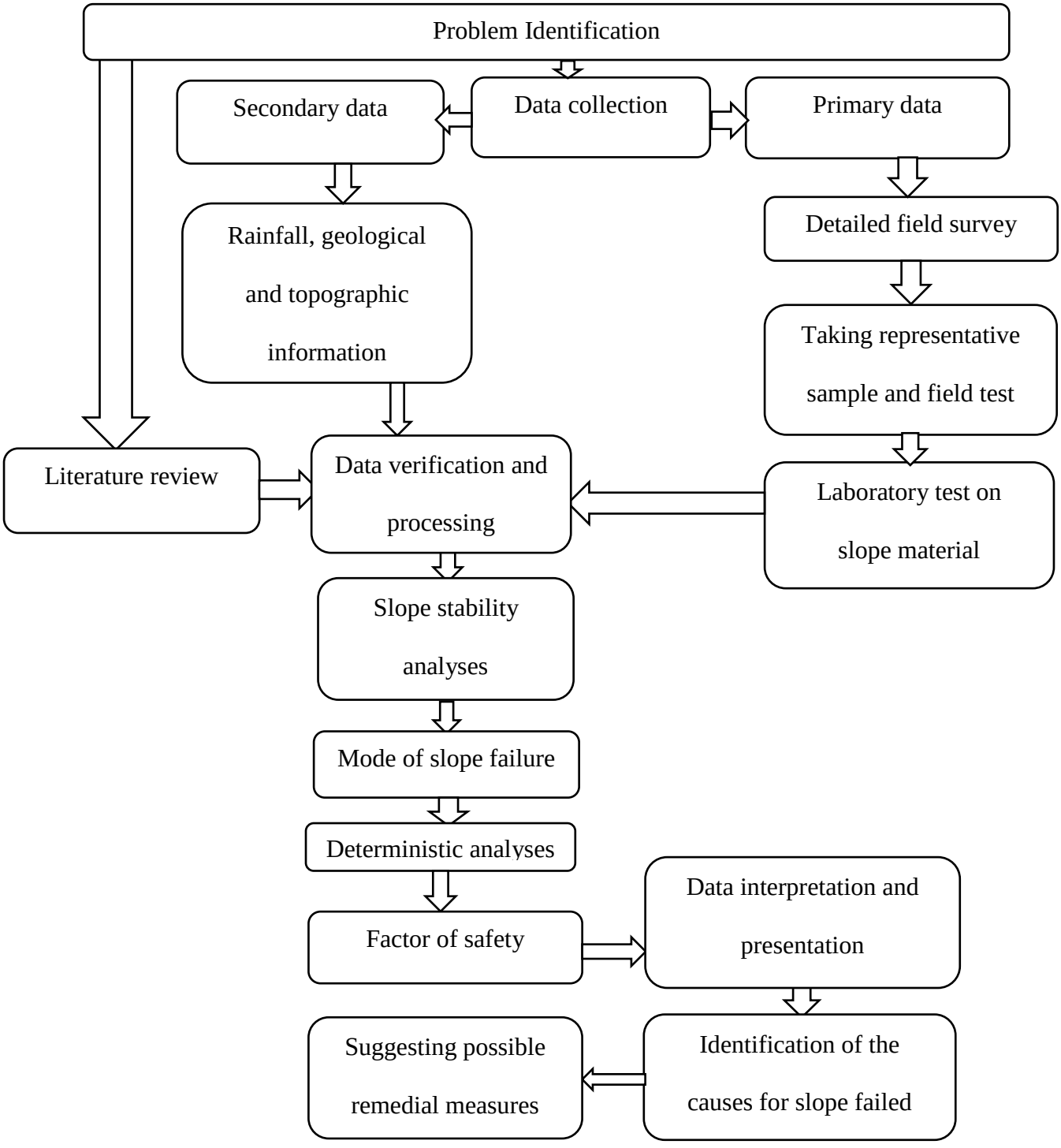

Figure 3.3: Conceptual framework of the study

3.3.2. Area of Study

These sites were listed below in Table 3.3 with their geographical location and elevation. The aerial photograph from Google Earth for the selected site are presented in Appendix H.

Table 3.2: Location of the selected sites

S. No	Location	Station	Northing	Easting	Elevation	Slope condition
1	FS1	107+930 to 107+980(RHS)	687879	286959	1621	Failed
2	FS2	108+340 to 109+120(RHS)	688162	286218	1581	Failed
3	ES1	109+680 to 109+740(LHS)	688373	284906	1435	Existing
4	ES2	121+240 to 121+290(RHS)	693122	275843	1668	Existing
5	FS3	126+060 to 126+140(LHS)	693597	275946	1749	Failed
6	ES3	126+420 to 126+460(RHS)	693772	275887	1737	Existing
7	FS4	129+380 to 129+440(LHS)	694262	274099	1483	Failed

3.4. Soil Sampling

Sampling is conducted to characterize the soil material and carry out laboratory testing to derive its physical and mechanical properties. A major assumption of this methodology is that the soil sample is representative of the ground from which it was retrieved. The geotechnical investigations that we must run will eventually dictate the type of sample collection method. In this study, seven disturbed soil samples were collected from a selected road section of 50.8 km total length based on the slope condition survey at the site. Along the selected road, section failed slope observed at four sections with different potential and those selected (FS1, FS2, FS3, and FS4) for analysis. Three existing slopes (ES1, ES2, and ES3) were selected based on slope height and exposure to erosion as per field observation. In both cases, samples were taken from pit excavated up to 1.5m depth at these selected slope sections. Disturbed soil samples were collected for soil type and specific gravity and moisture content analysis, among other evaluations.

3.5. Testing Methods

3.5.1. Field Test

3.5.1.1. Visual Identification of Soils in the Field

The fundamental step under the visual-manual method accustomed is describing whether the soil is fine-grained or coarse-grained by using visually looking at the soil and checking its texture through our fingers of the sample to be taken. The sample has been viewed to be representative of the stratum from which it was obtained by using an appropriate, accepted, or standard procedure. The descriptive information of the soil accustomed to being viewed and beside color could be an important property in distinctive soils. According to ASTM D-2488, the standard procedure has been carried out for visual field identification of soils in the study area.

3.5.1.2. Field Density Test

Density and Unit Weight of Soil in Place by the Sand-Cone Method used to determine the in-place density and unit weight of soils using a sand cone apparatus as per the ASTM D 1556 standard. By exposing a flat area, approximately 450mm square, of the soil to be tested and trim it down to a level surface, preferably with the aid of the scraper tool. Brush away any loose extraneous material. Lay the metal tray on the prepared surface with the hole over the portion of the soil to be tested. Using this hole as a pattern, excavate a round hole, approximately 100mm in diameter and the depth of the layer tested up to a maximum of 150mm deep. Collect all the excavated soil from the hole and determine its mass. Lastly, by replacing the sand with known density to the hole in place of soil removed and computation of moisture content and density of soil made.

3.5.1.3. Geometry of Road Cut Slope

In measurement over difficult terrain, we can use a measuring line made from a rope(chain with a rope). Depending on the distances we need to measure, we can make a measuring rope 10, 20, 30, 50, or 100m long. In this thesis work rope of 100m, 50m steel tape, and sprit level to check horizontality of the measuring line were used to measure the slope length and height of the embankment. After having those measurements then other slope geometry parameters were determined from measured dimensions such as horizontal distance and slope angle to have full slope geometric information for analysis.

3.5.1.4. Sample Preservation and Method of Transportation

The disturbed samples have been preserved to prevent contamination by using foreign material and to make sure that the in-situ soil conditions are preserved. An effort has been created to collect samples that have to be representative of the selected slope sections. The protective and transporting of the samples have been performed according to the ASTM D-4220-14 standard.

The origin of the sample was recognized by the method of marking all the samples. The identity of the sampling area, the sample place, the depth of the sampling, and therefore, the sampling date are written on every sampling bag with a waterproof permanent marker.

Disturbed samples do not need distinctive transport precautions. However, the sample bags are lined from breakage and exposure to excessive wetness, which can cause deterioration of the labels, and also the sampling bags. Related to transportation, the simplest approach of sample transportation was a car that it can be loaded at the exploration site after the sample collection was completed and driven on to the test laboratory.

3.5.2. Laboratory Test

3.5.2.1. Moisture Content

Seven test specimens have been prepared for moisture content determinations and conducted oven-dried at 105ºC until successive weighing show that no loss of mass. Again, from those samples have been conducted air-dried almost successive weighing shows that no loss of mass. Then, the two moisture content results were compared. According to ASTM D 2216, 7 moisture content tests were conducted within the laboratory.

3.5.2.2. Atterberg's Limit

Atterberg's limit test was conducted in keeping with ASTM D 4318–10 of methodology "A" that is, multipoint liquid limit. Getting ready fine-grained soils of the sample to determine the fine content of the soil, the testing soil sample to be tested was first oven-dried at 105ºC. Then the sample was completely pulverized with fingers and a wooden hammer. A Representative sample of 200gm oven-dried at 105ºC samples was taken that pass No 40(0.425 mm) and before beginning the blending to soften the material has been soaked in for 24hrs for LL and PL tests.

3.5.2.3. Specific Gravity

Specific gravity result is used to calculate parameters like void ratio, porosity, soil particle size distribution by means that of the measuring device and degree of saturation. The specific gravity of the soil samples has been conducted by using ASTM D 854–14 of methodology 'B', which is for oven-dry soil sample.

3.5.2.4. Particle-Size Analysis

Particle-size distribution analysis has been conducted by using ASTM D 422–63 procedures. Grain size analyses of the soil that constitute the slope sections were done to determine the type of soil which composes the slope and the type of soil found along the road sections. The analyses were done on seven different soil samples taken from the field by digging test pits. Later mechanical analyses were used for particle size larger than 0.075mm diameter (No. 200 Sieve) and hydrometer analyses (for particle size smaller than 0.075mm diameter, No. 200 Sieve) was done for all soil sample taken from the seven test pit at slope section to determine soil with particle diameter less than 0.075mm. In step with this procedure dry sieve, wet sieve, and hydrometer analysis on disturbed samples have been performed and the graph was plotted using soil particle size in millimeter on a semi-log scale against the percentage finer. From this curve, the proportion and type of soil particles were determined.

3.5.2.5. Classification of Soils

Commonly based on grain size and soil consistency several classification systems exist. In this study Unified Soil Classification System (USCS) (ASTM D2487-11) and American Association of State Highway and Transportation Officials (AASHTO) (ASTM D3282-09) methods were applied. Coarse-grained soils are classification based upon the grain size distribution and fine-grained soils are classified based upon the water content and plasticity index.

3.5.2.6. Direct Shear Test

Direct Shear Test of Soils has been conducted by using ASTM D 3080 procedure. A direct shear device will be used to determine the shear strength parameters of soil (i.e. angle of internal friction (φ)) and cohesion (c). Three specimens using a shear box with dimensions 60mm by 60mm are prepared and tested; each under a different normal load (50, 100, 200, and 400 KPa) to determine the effects upon shear resistance and displacement, and strength properties such as Mohr strength envelopes. From the plot of the maximum shear stresses

versus the vertical (normal) confining stresses for each of the tests, a straight-line approximation of the Mohr-Coulomb failure envelop curve can be drawn, and then the shear strength parameters can be determined.

3.6. Data Management and Analysis

3.6.1. General

This thesis work has been broadly divided into two phases. The initial phase was the experimental part in which soil samples from selected sites were collected. Seven different slopes were analyzed. Tests were conducted to determine the engineering properties of the soil such as cohesion, angle of internal friction, and Young's modulus. Other input parameters for numerical analysis such as slope angle and geometry of the area were found out by direct field measurement. The second phase was the numerical analysis part, which was done by using FEM based software, PLAXIS (2D). The slip circle and factor of safety of existing slopes were obtained. In the case of failed slopes, reanalysis by changing slope angle, water level, and using geogrids were done.

3.6.2. Slope Stability Analysis

The analysis and design of failing slopes require an in-depth understanding of the failure mechanism to choose the right slope stability analysis method. The present study made it possible to compare on a real geometrical model the computation result that the behavior law stress-strain which is lacking to the limit equilibrium methods is integrated into the finite element methods. For a different set of slope stability, and analysis of Mohr's-Coulomb material model is followed here especially. The importance of the various parameters and their applicability under several special cases are considered in the analysis. The input parameters from field tests and observations, laboratory tests, and published data the analysis of slope stability carried out by using finite element program PLAXIS 2D. Slope stability analyses of the selected road section using field and laboratory test results to be carried out and cause for slope failure and existing slope stability to be checked. Under the discussions of the obtained results the causes for fail slope and stability of existing slope to be evaluated.

3.6.3. Description of FEM Analysis

3.6.3.1. Strength Reduction FEM

Generally, there are two approaches to analyze slope stability using the finite element method. One approach is to increase the gravity load and the second approach is to reduce

the strength characteristics of the soil mass. The second approach is adopted in this study by using a powerful software finite element program PLAXIS. The strength reduction method using FEM can be used to simulate the failure limit states of slopes and thus to determine their sliding surfaces and factors of safety. Strength reduction means reducing the parameters of shear strength (cohesion and internal friction angle) of soil (or rock) slopes in the finite element calculation, within a theoretical framework of perfect elastoplasticity, until the limit failure state is reached. In the strength reduction method, the strength characteristics of the soil materials are reduced by a factor until the loss of stability or failure of the structure occurs. The reciprocal of this reduction factor is identified as the factor of safety associated with the soil model under investigation. Then, the sliding surface of the slope can be automatically obtained from the results of the elastoplastic FEM, and the factor of safety of strength reserve can be calculated.

In this approach the cohesion and the tangent of the friction angle are reduced in the same proportion:

$$\frac{c}{cr} = \frac{\tan\varphi}{\tan\varphi r} = \sum Msf \quad \text{.....(3.1)}$$

The reduction of strength parameters is controlled by the total multiplier ∑Msf. This parameter is increased in a step-by-step procedure until failure occurs. The safety factor is then defined as the value of ∑MSF at failure, provided that at failure a more or less constant value is obtained for many successive load steps.

FEM enables a realistic simulation of excavation and construction stages by activating and deactivating of construction parts, application of loads, and boundary conditions. The strength reduction method (phi/c reduction) used in a Safety calculation gives a factor of safety comparable to other methods (e.g. Bishop method) FEM allows for complicated geometry that is possible using exact methods. Conventional Methods; Finite Elements; Safety Factor; Slopes Stability Introduction anchoring are not influenced by Phi-C reduction. You can do this by the strength reduction technique (marked as phi/c reduction) where the PLAXIS reduces the friction angle and the cohesion of the soil mass until a collapse mechanism is identified and the PLAXIS determines a Safety Factor.

3.6.3.3. Deterministic Method of Slope Stability Analyses

The deterministic method which determines the stability of the slope in terms of safety factors was followed to determine the stability of the seven identified soil slope. The analyses

were done by using PLAXIS 2D software which calculates the safety factor of a slope by the deterministic method. Plaxis software determines the factor of safety under the finite element method. The analyses were done under different anticipated conditions such as static saturated, static dry conditions, and varying the slope height. For the selected existing slope reanalysis using geogrids was conducted in addition to evaluating the influence of variation in water table elevation. The input parameters used in the analysis methods were; shear strength parameters, Elastic modulus, poison's ratio, permeability, and unit weight of the soil which were determined in the laboratory.

Usually, many researchers recommend using the finite element method for any reason. This useful and easy method can help the researchers and professionals to evaluate all expected issues that can be developed during studying the problems of slope stability. Therefore, this thesis includes 2D finite element simulation and analysis of slope stability problems.

3.6.3.4. Application of Geogrids

Geogrids' functions and applications are the major concern for soil reinforcement below roads, understructures, and behind retaining walls. Are the major geosynthetic material, geogrid has unique properties, functions, and applications geogrid compared with other geosynthetics. Geogrid is engineered with large openings or apertures which is made from polymers such as polypropylene, polyethylene, or polyester. The geogrids are manufactured high strength reinforcement grid that comes in rolls of various sizes and strengths. The soil can strike through the apertures and the two materials interlock together to give composite behavior. The geogrid provides high strength and longevity to your wall to help prevent wall failure; resistant to biological degradation and naturally encountered chemicals, alkalis, and acids. BPM innovative, high-quality geogrid products include plastic biaxial geogrid, fiberglass geogrid, plastic uniaxial geogrid, warp knitting polyester geogrid, and steel plastic georgic mesh, etc. Geogrid can maintain the tensile reinforcement load and efficiently transfer that tensile load into the surrounding soil. Biaxial geogrid slope stabilization is often the ideal solution in roadbed, subbase, or dam construction projects and applied in this study for existing slopes to study the effect of its application on stability.

3.6.3.5. Side Slopes for a Road Cut

The selection of a side slope and back slope is dependent on safety considerations, height of cut or fill, and economic considerations. On maintenance and rehabilitation projects, the

primary emphasis is placed on the roadway itself. According to ERA Geometric Design Manual-2002 side slope ratios recommended for use in the design according to the height of cut is 1:2(Vertical to Horizontal). In this study, the recommended slope was applied and the stability condition was compared with the applied slope angle at the selected sites.

3.6.3.6. Sensitivity Analysis

The sensitivity analysis is used to analyze the influence of individual parameter variations on the results with the purpose to evaluate the relative influence of those parameters.

The relative influence (sensitivity) is evaluated based on a user-defined criterion; for example, the horizontal displacement of a particular node. Please note that nodes or stress points used in these criteria can only be taken from the set of nodes and stress points that have been selected for load-displacement curves or stress-strain curves. In a sensitivity analysis, the upper and lower bound values of parameters are varied individually. The result of a sensitivity analysis is an overview of the relative influence (sensitivity) of the parameter variations. This sensitivity is evaluated based on user-defined criteria. Criteria can be based on nodal displacements, stress, or strain components. The points used for these criteria can be selected from the set of points as defined for load-displacement curves or stress-strain curves. These points have to be predefined for the original project before the sensitivity analysis is started. The results of the sensitivity analysis project are used as reference values for the calculation of the parameter sensitivity. In this thesis, the influence of the individual input parameter on the analysis result was evaluated using a different value for each input parameter based on test results. While changing the value of individual parameter other parameters kept constant.

The sensitivity analysis is used to determine the effect of various input parameters on slope stability. The effect of uncertainty or variability in the values of soil parameters can be explored. The most effect of soil parameters on the stability of a slope can be determined. Changes that may occur on the safety factor of slopes can be known and anticipated by conducting a sensitivity analysis. Sensitivity analysis will provide an overview of the extent to which a system will be consistent even though changes in parameters affect it. Sensitivity analysis is done by changing the value of a parameter at a time, then be seen how it affects a system. Soil parameters that can affect the safety factor of slopes are unit weight, cohesion, friction angle, slope height, permeability coefficient, Young’s modulus, and Poisson's ratio.

A comparison of the sensitivity of different parameters, need to define the sensitivity factor and eliminate dimension influence to the calculation result. The sensitivity analysis outputs on each input parameter were included under appendix G.

Because the slope morphology cannot be described as specific data, its sensitivity cannot be calculated through the derivation. The sensitivity can be calculated as (Jixun et al., 2006):

$$S(xi) = \max\{(\frac{Axmax.-A*}{A*}), (\frac{A*-Axmin}{A*})\} \quad \text{(3.2)}$$

Where S(xi) is the sensitivity factor of xi,

A* is system response relative to the basic parameters,

Axmax, Axmin is the maximum value and minimum value of system response in xi range, respectively.

4. RESULTS AND DISCUSSION

4.1. Field Characterization of Failed Slope Materials

Four potential slopes were identified during a field survey along with the Otolo-Sawla Asphalt Road Project, the southern part of Ethiopia. Field data appropriate to slope stability were carefully collected by considering the geological and geotechnical complexities of the slope failure along mountainous terrain. From field inspection, four failed slopes were identified based on failed slope section, crack observed on the ground, and tilting of trees. Saturation conditions of the slope were also visually estimated in which some of the slopes such as slope section FS2, FS3, and FS4 were damp except FS1 that was identified as dry. Also, there were three intermittent springs originated in a different part of the road sections. Springs, which originate at a different part of the slope revealed that; groundwater may act as threatening.

Table 4.1: Location and descriptions of selected failed slopes

Slope sections	Northing	Easting	Characteristic of the slope sections based on the field manifestations
FS1	687879	286959	Slope, which was found within brown soil- rock mix.
FS2	688162	286218	Steeply slope, Soil with gray-color where large slide observed.
FS3	693597	275946	Medium weathered rock with gray soil slope where large slide observed next to Woyde slope.
FS4	694262	274099	Steeply, highly weathered rock with nearly deep gray soil and existence of groundwater at the road level.

Moreover, the soil of the study area that was visually classified on the field according to ASTM D 2488 became reddish soil formations and brownish. Groundwater condition of the study area was indirectly determined from field conditions, which mean observing at tints of water and spring over the slope surface (Figure.4.1).

a) FS2 Slope

b) FS4 Slope

c) FS3 Slope

Figure 4.1: Groundwater exposed to slope sections

4.2. Engineering Characterization of Slope Material

4.2.1. Grain Size Analyses Failed slopes

From the analysis result, particle size diameter versus percent finer (particle size distribution curve) was plotted for soil samples taken from four failed slope sections (Figure.4.2). Grain size analyses result of soil following the road sections indicated that the maximum

percentage of soil, which pass 75µm, was 49.27% and the minimum percent of soil, which pass 75 µm, was 20.04 %. This revealed that soil type along the road sections were nearly coarse-grained soils which means fine grain soils like silt and clay soils were less in percent than gravel and sand. However, most of the samples contain coarser size particles in larger percent than finer particles as per AASHTO soil classification all soils along with the road section fall in between fair to poor. Therefore, the probability that material combination contributes to the failure of the selected failed soil slope sections was high. Besides, these materials were friable and collapsible so that they can easily move or slide when subjected to heavy rainfall.

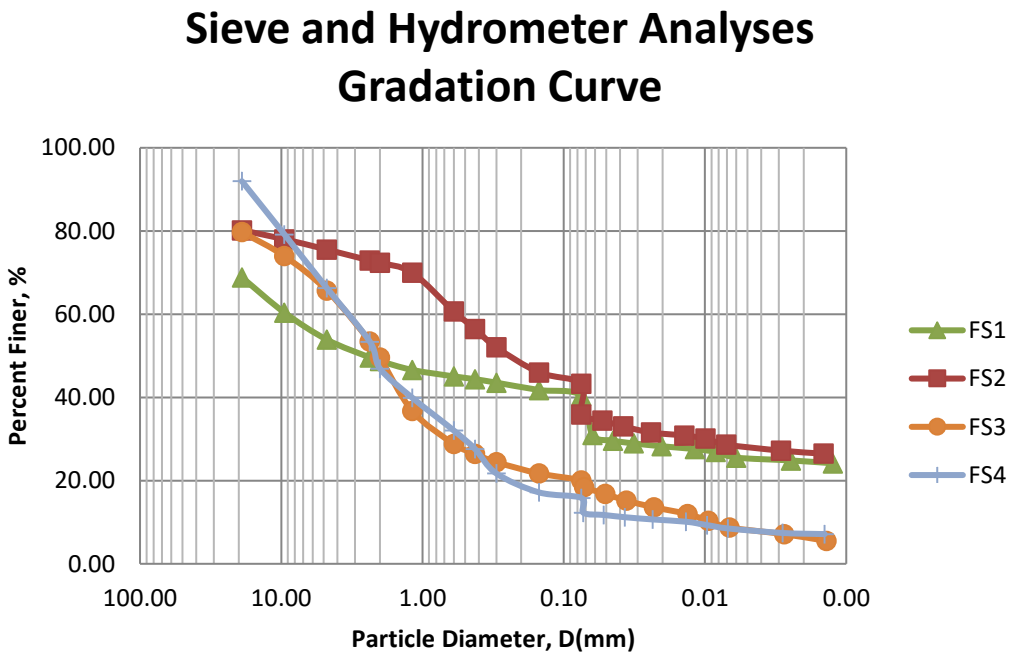

Figure 4.2: Graph of the particle size distribution for selected failed slopes

4.2.2 Atterberg's Limit for Failed Slopes

After sieve analyses were conducted, Atterberg's limit like liquid limit, plastic limit, and plasticity index was determined in the laboratory and the final analysis result was shown in (Table.4.2).

Table 4.2: Atterberg's limit of the soil in the selected failed slopes

Slope sections	Depth (m)	Liquid limit at 25 drops (%)	Plastic limit (%)	Plasticity index (%)
FS1	1.5	55	31	24
FS2	1.5	49	25	24
FS3	1.5	40	28	12
FS4	1.5	51	28	23

Based on this, the soil at selected failed slope sections above, the liquid limit of FS1 slope is larger than the other with little value difference except for the FS3 slope. The result from the plasticity chart (Figure.4.3) indicated that the fine-grain fraction of soil at all identified test pit location fall in medium plasticity clay.

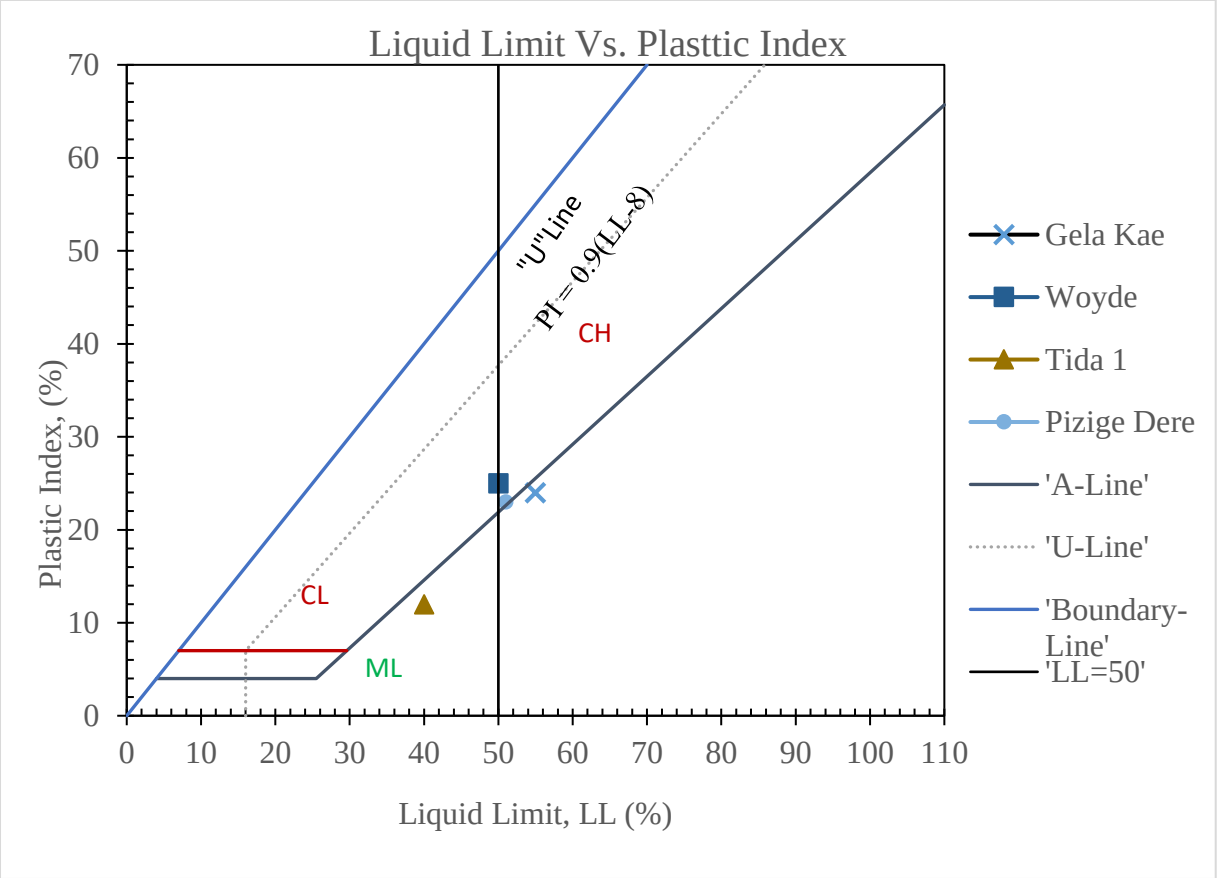

Figure 4.3: Plasticity chart of the study area according to USCS

4.2.3. Classification of Failed Slope Soils

From gradation analyses and Atterberg limit test results, the soil of the failed slope along the road section was classified as shown in (Table 4.3). From sieve analyses result, percent retained on No.200 sieve size ranges from 50.73-79.96% and percent passing No.200 sieve size ranges from 20.04-49.27% for material along selected failed road slope section. Furthermore, based on the Atterberg limit and particle size analysis, the type of soil was found to be A-7 according to the AASHTO classification system except for soil at slope section Tida1, which is A-6. Soil found in-group A-7 and A-6 consists of dominantly coarse grain soil with a high fraction of fine-grained soil. Based on the AASTHTO classification system, soils of the study area were classified as coarse-grained soils and fair to poor subgrade material. Similarly, based on 50% of the soil pass or retained on No.200 sieve size, percent of gravel, sand, and fines, the soil of the study area was also classified according to USCS to further determine fine-grained soils. According to USCS, the soil at FS1 was classified as GM and the soil at FS2, FS3, and FS4 were classified as SC, SM, and GC respectively. This implies that the percent of silt and clay soil in the study area was significant and also the coarse-grained soil fraction. Therefore, failure of soil slope at FS1, FS2, FS3, and FS4 may be due to poor material property along the road sections.

Table 4.3: Types of soil classified according to AASHTO and USCS

Slope location	Gravel (%)	Sand (%)	Fine (%)	Atterberg's limit		Soil type	
				LL(%)	PI(%)	AASHTO	USCS
FS1	46.13	13.48	40.39	55	24	A-7	GM
FS2	24.48	32.25	43.28	49	24	A-7	SC
FS3	34.3	45.66	20.04	40	12	A-6	SM
FS4	28.17	22.56	49.27	51	23	A-7	GC

4.2.4. Shear Strength of Failed slope Soils.

Shear strength parameters such as cohesion and friction angle and unit weight of the soil which compose the critical soil slope sections are major input parameters to calculate the factor of safety and failure probability of the soil slope. The internal angle of friction and cohesion were measured from direct shear tests. From the laboratory test result, the soil at slope sections as shown in the table below (Table 4.4). Similarly, the soil at failed slope section FS1 had shown on the graph as a sample(Figure. 4.4) and the rest included under Appendix E. Angle of friction, φ varies from 5º to 25º. The cohesive strength of all soil samples varies from 1 kN/m^2 to 43 kN/m^2.

Table 4.4: Shear strength parameters of soil at failed slope section

Slope location	Material type	Shear strength parameters		Unit weight, kN/m^3	Optimum moisture content, %
		Cohesion, kN/m^2	Friction angle, (º)		
FS1	Silty Gravel	31	11	18.3	22.5
FS2	Clayey Sand with gravel	43	5	18.7	24
FS3	Silty sand with gravel	1	25	18.5	15.5
FS4	Clayey gravel with sand	10	21	18.9	17.5

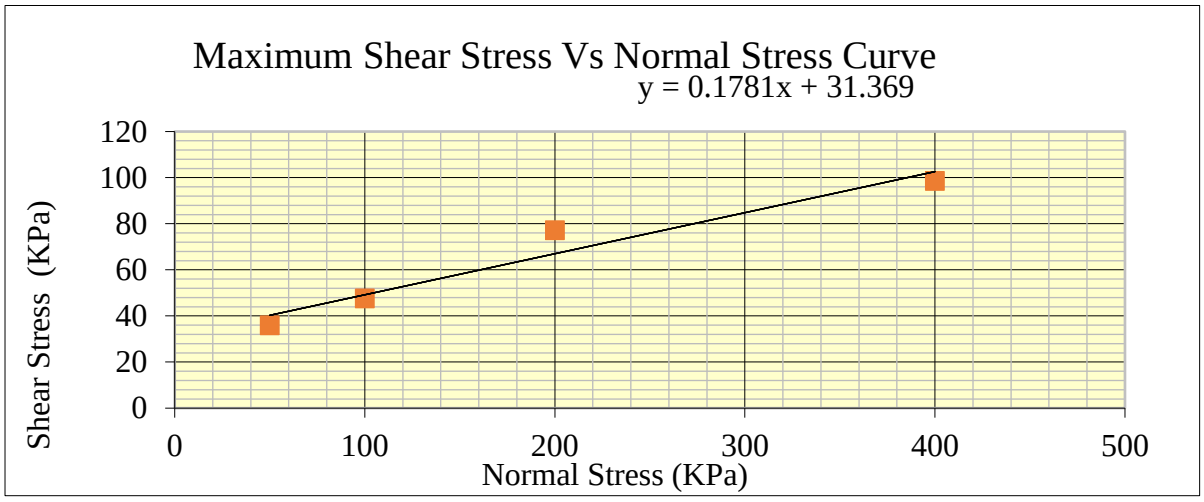

Figure 4.4: Normal stress vs maximum shear stress graph for FS1 slope

4.3. Stability Analyses of Selected Slope Sections

4.3.1. Deterministic Method of Failed Slope Stability Analyses

As stated in chapter three of this study, based on the field manifestations four failed and three stable slopes were identified for stability analyses. The analyses were conducted by determining the safety factor of the seven selected slope sections. The slope height and angle of the selected slope sections were summarized under Table 4.5. According to field identification based on physical properties and laboratory classifications systems such as gradation and Atterberg limit test result, the selected slope section was composed of different material properties as shown in table 4.3. Therefore, the stability of the soil slope was determined by considering the selected failed slope sections separately. In addition to that, one of the input parameters used to determine the factor of safety was shear strength parameters (cohesion and friction angle), unit weight of soil, coefficient of permeability, Young's modulus, and Poisson's ratio. Therefore, shear strength parameters determined from the direct shear test, unit weight of the soil, coefficient of permeability, Young's modulus, and Poisson's ratio were used as the input parameters for stability analyses (Table. 4.5). The permeability and elastic properties for selected slope sections on identified slope material properties were put under table 4.5 referring to foundation analysis and design (5^{th} Edition), by Bowles,(1996) and from developed correlations.

Besides, stability analyses were done under different slope height, saturated, and dry conditions as stated below.

Table 4.5: Deterministic input parameters to PLAXIS 2D software for failed slopes

Parameter	Symbol	Selected slope section				Unit
		FS1	FS2	FS3	FS4	
Type of behavior	Type	Undrained	Undrained	Undrained	Undrained	
Bulk unit weight	γ_{unsat}	18.3	18.7	18.5	18.9	kN/m^3
Saturated unit weight	γ_{sat}	18.8	19	19.8	19.3	kN/m^3
Permeability	k	$1.31*10^{-4}$	$1.31*10^{-4}$	$1.07*10^{-3}$	$2.06*10^{-4}$	m/day
Young's modulus, MPa	E	50	50	25	65	MPa
Poisson's ratio	ν	0.3	0.3	0.3	0.3	-
Cohesion	c	31	43	1	10	kN/m^2
Friction angle	φ	11	5	25	21	(^{0})
Slope height	H	3	15	4	5	m
Slope angle	α	1:1.5	1:1.5	1:1.7	1:1.1	(^{0})

Using the soil properties obtained from laboratory tests, numerical analysis of failed and existing slopes was performed in PLAXIS 2D by the phi-c reduction method. For the analysis, the slopes were assumed as homogenous soil slope and the dimensions of the slopes were assumed as uniform. Mesh generation output with having model, plain strain, and elements, 15-noded is shown in figure4.5 and mesh information in table 4.6 for failed slopes.

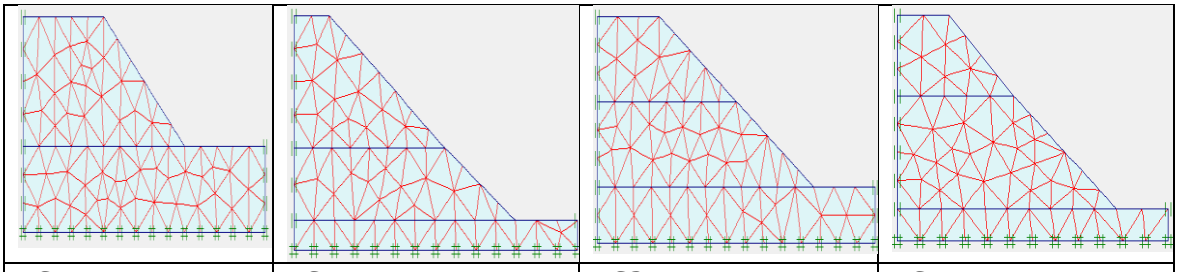

FS1	FS2	FS3	FS4

Figure 4.5: Connectivity plot for failed slopes

Table 4.6: Mesh Information for Failed Slopes

Mesh information	FS1	FS2	FS3	FS4
Number of elements	149	114	131	105
Number of nodes	1275	989	1131	911
Number of stress points	1788	1368	1572	1260
Average element size,m	0.63457	2.12	1.05	1.67

The incremental displacement profile and factor of safety are obtained from software analysis. From the field manifestations, the most critical conditions in which severe slope failure occurred was found to be when heavy rainfall took place. First, the stability analysis in terms of safety factor was done for actual investigated site conditions and then safety factor analyzed for varying site conditions for selected slope sections were summarized under (Table 4.7) and (Figure.4.6) and all the rest outputs on different site conditions were included under appendix F.

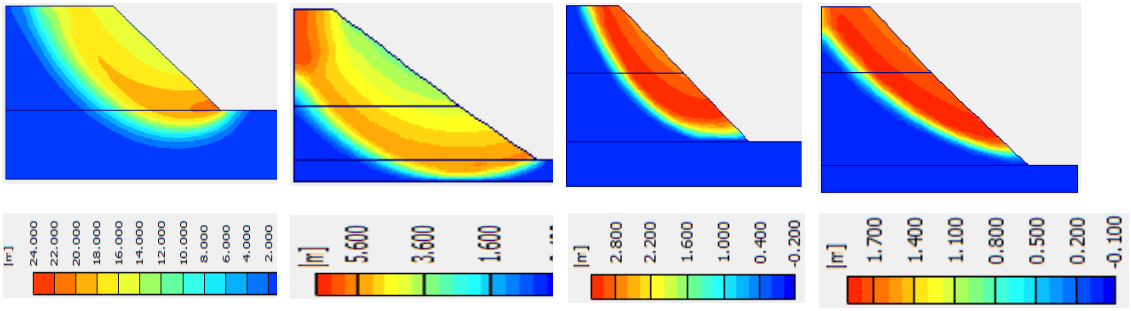

a) FS1 analysis FOS=3.929 | b) FS2 analysis FOS=1.231 | c) FS3 analysis FOS=0.875 | d) FS4 analysis FOS=0.887

Figure 4.6: Incremental displacement profile and FOS with actual site condition

Stability analyses in terms of safety factors were done under saturated conditions which means when the slope was assumed to be saturated (during heavy rainfall or groundwater level rise to the surface); stability of the slope under a dry condition which means when the slope was assumed to be dry. Similarly, the effect of groundwater on the failed slope stability was analyzed using PLAXIS 2D software with different height of the groundwater table, and FOS's obtained were summarized under the table 4.7.

Table 4.7: FOS values for failed slopes under different site conditions

Slope location	FOS for actual site condition	FOS for saturated condition	FOS for dry condition
FS1	3.929	3.842	3.929
FS2	1.231	1.198	1.231
FS3	0.875	0.848	0.877
FS4	0.887	0.747	0.887

Based on this, the groundwater or high rainfall that results in saturation of slope material caused the slope to fail with a considerable contribution since the FOS decreases with an

increase in height of the groundwater level. One of the slope failure factors is saturation and pore water pressure building up in the subsoil. In the case of FS2 slope blasting operation held at the time of construction to extract the rocks was also contribute to failure.

The factor of safety represents the main key for the analysis of slope stability problems. For every selected slope section, the factor of safety increased when decreased slope height. Based on this, the slope height has greatly influenced the stability of slope since the FOS of the selected failed slope sections decreases with an increase in slope height and vice versa. This indicates that the slowing or lowering the slope height with critical consideration of space limitation has a direct contribution to the stability of slope that is similar to Gadaawin, (2019) studied; a result of the literature Kedir et al.,(2018) confirms that, flattening the slope with lowering the groundwater table stabilizes the cut slope. The FOS for different slope height and the groundwater table is summarized in table 4.8.

Table 4. 8: FOS values for failed slopes varying slope height and groundwater level.

Slope location	Slope height in m	FOS for groundwater level		
		Actual	Saturated	Dry
FS2	14	1.231	1.198	1.231
	11	1.635	1.607	1.635
	8	2.432	2.431	2.434
	5	4.401	3.395	4.409
FS3	6	0.875	0.848	0.877
	4	1.42	1.416	1.442
	2	3.578	3.578	3.728
FS4	12	0.887	0.747	0.887
	9	1.121	1.003	1.123
	6	1.557	1.464	1.561
	3	2.806	2.742	2.822

To study the effect of the slope angle on the slope stability this study compares the initial *ERA* Geometric Design Manual-2002 recommendation of slope angle for different slope material with actual site slope angle and FOS's compared table 4.9

Table 4.9: FOS for failed slopes with ERA recommendation slope profile

Slope location	FOS for ERA recommendation V: H(1:2)	FOS for actual site slope profile
FS1	4.255	3.929
FS2	1.477	1.231
FS3	1.692	0.875
FS4	1.851	0.887

This indicates the slope angle at the site was higher than the design manual requirement and effect less FOS values and caused the failure of slope specially FS4 and little on FS3 in addition to other causing parameters.

4.4. Field Characterization of Existing Slope Materials

From field inspection, three existing slopes were identified based on slope height, slope forming material, and exposure to erosion. Slopes such as ES1, ES2, and ES3 were identified as stable and dry through field surveys.

Table 4.10: Location and descriptions of selected existing slopes

Slope sections	Northing	Easting	Characteristic of the slope sections based on the field manifestations
ES1	688373	284906	Steeply, stable deep brown soil.
ES2	693122	275843	Stable, Light brown soil slope.
ES3	693772	275887	Steeply, stable reddish soil.

4.5.1. Grain Size Analyses for Existing slopes

From the analysis result, particle size diameter versus percent finer (particle size distribution curve) was plotted for soil samples taken from three existing slope sections (Figure.4.7). Grain size analyses result of soil following the road sections indicated that the maximum percentage of soil, which pass 75μm, was 90.07% and the minimum percent of soil, which pass 75 μm, was 71.94%. This revealed that soil type along the selected existing slope sections was fine-grained. As per AASHTO soil classification, all soils along the road section falls in between Fair to poor. Therefore, the probability that material combination contributes to the failure of the selected failed soil slope sections was high again.

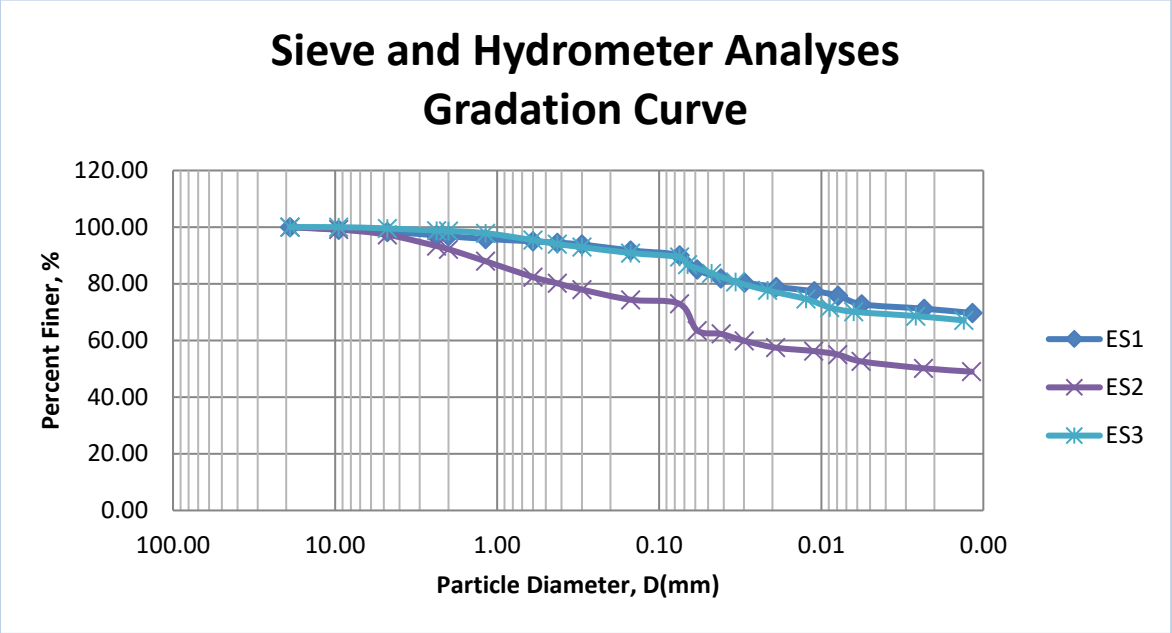

Figure 4.7: Graph of the particle size distribution for selected existing slopes

4.5.2. Atterberg's Limit for Existing Slopes

Atterberg's limit test result for selected existing slope sections through laboratory test are summarized in table 4.11.

Table 4.11: Atterberg's limit of the soil in the selected existing slope sections

Slope sections	Depth (m)	Liquid limit at 25 drops (%)	Plastic limit (%)	Plasticity index (%)
ES1	1.5	64	37	27
ES2	1.5	34	22	12
ES3	1.5	51	26	25

The values of the liquid limit indicate ES1 and ES3 slope locations larger than Basa slope. The result from the plasticity chart (Figure.4.8) indicated that all identified test pit locations fall in medium plasticity clay at both sample locations except the ES2 sample.

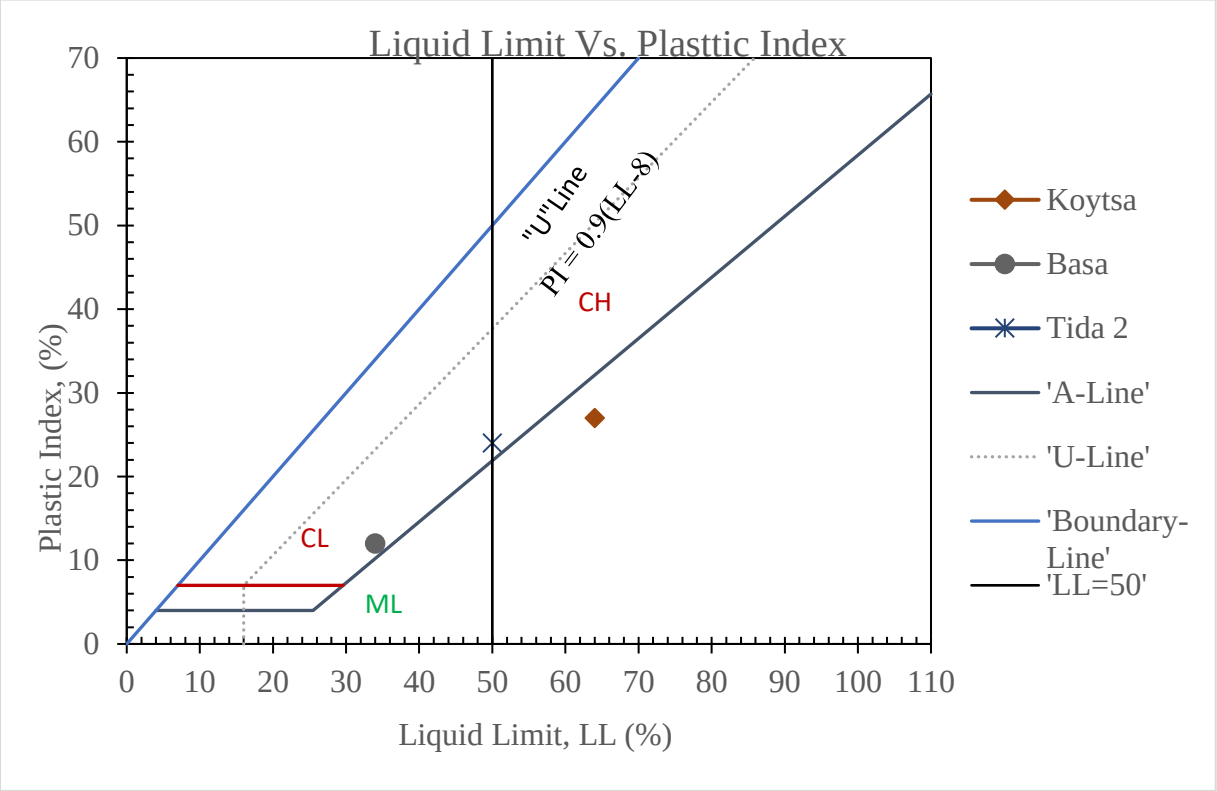

Figure 4.8: Plasticity chart of the study area according to USCS

4.5.3. Classification of Existing Slope Soils

From gradation analyses and Atterberg limit test results, the soil of the existing slope along the road section was classified as shown in (Table 4.6). From sieve analyses result, percent retained on No.200 sieve size ranges from 9.93-28.06 %, and percent passing No.200 sieve size ranges from 71.94-90.07% for material along selected existing road slope section. Furthermore, based on the Atterberg limit and particle size analysis, the type of soil was found to be A-7 for ES1 and ES3 slopes according to the AASHTO classification system and for soil at the slope section, ES2 is A-6. Soil found in group A-7 and A-6 consists of dominantly fine-grain soil with some fraction of coarse-grained soil. Based on the AASTHTO classification system, soils of the study area were classified as fine-grained soils and fair to poor subgrade material.

According to USCS, the soil at ES1 was classified as MH; the soil at ES2 and ES3 were classified as CL and CH respectively. Therefore, slopes at ES1, ES2, and ES3 may have a chance to fail due to poor material property.

Table 4.12: Types of soil classified according to AASHTO and USCS for existing slope

Slope location	Gravel (%)	Sand (%)	Fine (%)	Atterberg' limit		Soil type	
				LL	PI	AASHTO	USCS
ES1	1.66	8.27	90.07	64	27	A-7	MH
ES2	2.69	24.37	72.94	34	12	A-6	CL
ES3	0.46	10.1	89.44	51	25	A-7	CH

4.5.4. Shear Strength of Existing Slope Soils.

From the laboratory test result, the soil at existing slope sections as shown in the table (Table 4.13). Angle of friction, φ varies from 3º to 19º. Cohesive strength of all soil samples varies from 22 kN/m2 to 37 kN/m2. The soil at the existing slope section ES1 had shown on the graph as a sample(Figure. 4.9) and the rest included under appendix E.

Table 4.13: Shear strength parameters of soil at existing slope section

Slope location	Material type	Shear strength parameters		Unit weight, kN/m^3	Optimum moisture content, %
		Cohesion, kN/m^2	Friction angle, (º)		
ES1	Elastic silt	32	3	18.9	27
ES2	Lean clay with sand	22	19	18.2	24.5
ES3	Fat clayey	37	3	19.3	23.14

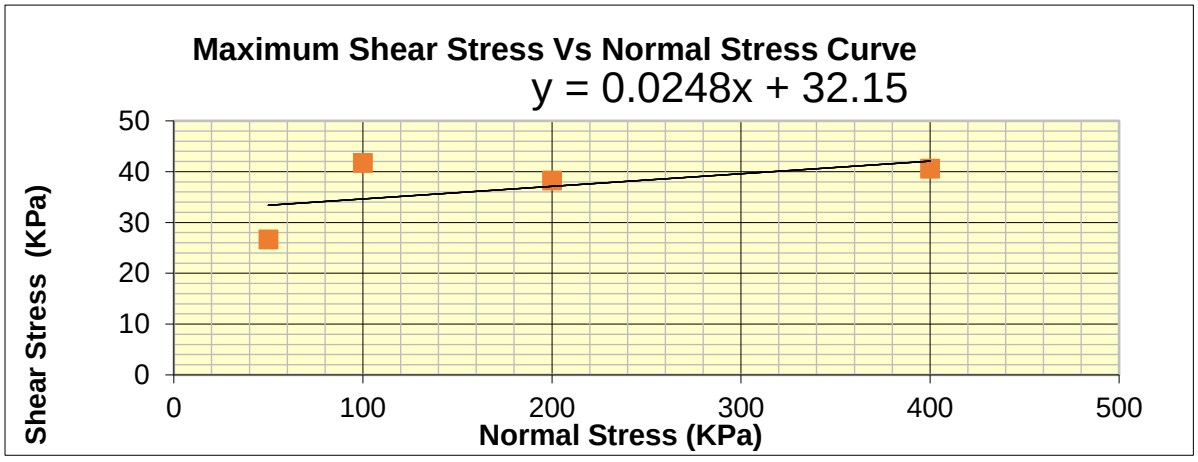

Figure 4.9: Normal stress vs maximum shear stress graph for ES1 slope

Table 4.14: Deterministic input parameters to PLAXIS 2D software for existing slopes

Parameter	Symbol	Selected slope section			Unit
		ES1	ES2	ES3	
Type of behavior	Type	Undrained	Undrained	Undrained	
Bulk unit weight	γ_{unsat}	18.9	18.2	19.3	kN/m^3
Saturated unit weight	γ_{sat}	19.1	18.7	19.7	kN/m^3
Permeability	K	$2.93*10^{-5}$	$2.63*10^{-3}$	$2.4*10^{-4}$	m/day
Young's modulus, MPa	E	10	27	22	MPa
Poisson's ratio	ν	0.3	0.3	0.3	-
Cohesion	C	32	22	37	kN/m^2
Friction angle	ϕ	3	19	3	(^{0})
Slope height	H	9	7	6	m
Slope angle	S	1:2.1	1:1.43	1:1.73	(^{0})

The contribution of groundwater on the existing slope to fail was studied and the FOS with different groundwater table height have summarized in table 4.15.

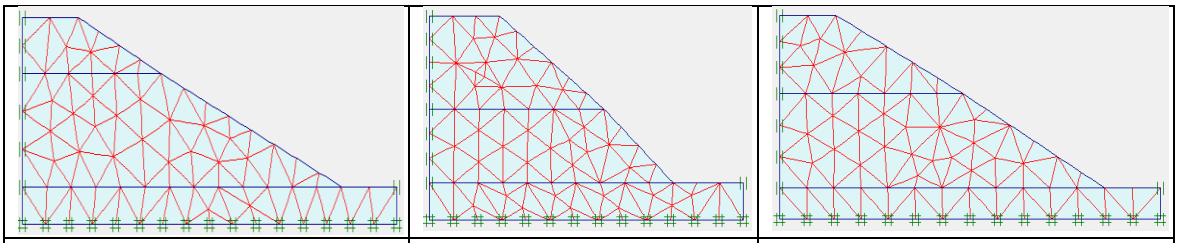

ES1 ES2 ES3

Figure 4.10:Connectivity plot for Existing Slopes

Table 4.15: Mesh information for Existing slopes

Mesh information	ES1	ES2	ES3
Number of elements	115	134	117
Number of nodes	999	1149	1011
Number of stress points	1380	1608	1404
Average element size,m	1.61	1.22	1.73

Table 4.16: FOS values for existing slopes under different site conditions

Slope location	FOS for actual site condition	FOS for saturated condition
ES1	1.455	1.414
ES2	1.479	1.407
ES3	1.243	1.236

Based on the analysis result, the existing slope stability has also be affected by the rise of the groundwater level, since the FOS decreases with increasing the height of the groundwater level.

In addition to other measures like providing adequate drainage, decreasing the exposure to erosion; it is also better to apply geogrids to existing slopes to keep them stable since the FOS improved by applying the geogrids as compared to slope without geogrids as shown in the table 4.17

Table 4.17: FOS values for selected existing slopes without and with geogrids.

Slope location	FOS for saturated slope without geogrids	FOS for the saturated slope with geogrids
ES1	1.414	2.84
ES2	1.407	2.343
ES3	1.236	3.066

Based on this, FOS increases with the application of geogrids with a considerable contribution to slope stability. The existing research results on the application of geosynthetic material reinforcement are the same. For example, the analysis result of literature Salahudeen and Sadeeq, (2016) is that the slopes with geosynthetic material reinforcement are safer and yielded better results of settlement and shear strains than the slope of embankments without geosynthetic material reinforcements.

For the selected existing slopes there is also deviation of slope angle applied with that of *ERA* Geometric Design Manual, (2002) except Koytsa slope.

Table 4.18: FOS for selected existing slopes with ERA recommendation slope profile

Slope location	FOS for ERA recommendation V: H(1:2)	FOS for actual site slope profile
ES1	1.417	1.455
ES2	2.375	1.479
ES3	1.565	1.243

Based on this, the slope angle applied to the actual road cut slope higher than *ERA* Geometric Design Manual, (2002) may contribute the slope to fail.

4.3.2. Sensitivity Analysis for Slope Failure

Sensitivity analyses of critical slope failure were done for input parameters like shear strength parameter and unit of the soil and considering elastic modulus, poison's ration, and permeability coefficient concerning factor of safety. A comparison of the sensitivity of different parameters, need to define the sensitivity factor and eliminate dimension influence to the calculation result. The sensitivity analysis outputs on each input parameter were included under appendix G.

Table 4.19: Range analysis table

Parameter	C	φ	γ	H	k	E	μ
Sensitivity Factor	1.87	2.52	0.18	2.2	0.0247	0.0004	0.0004
The order of sensitivity	3	1	4	2	5	6	7

The above analysis results show that the internal friction angle, cohesion, and slope height are all sensitive factors affecting the stability of the slope, and the sensitivity of the other four input parameters are not much different. It can be seen that the shear strength parameters and slope height are the most sensitive to the slope stability, and the unit weight of the soil effect is secondary, while the remaining factors have little effect for all selected slope sections.

From design and construction, it is of great significance to stabilize the slopes by slowing slopes, avoiding deep cuts of slopes, and strengthening drainage. In this paper the order of sensitivity of factors affecting the slope stability obtained as φ>H>c>γ >k >E>μ.

5. SUMMARY AND CONCLUSION

5.1. Summary

This part summarizes the study with the main findings from the assessment of slope stability performance. The main purpose of this thesis is to gain more information about the effect of slope forming material, water table, application of geogrids, and slope angle on slope stability.

The study can be summarized as follows:

- Seven potential slopes were identified during a field survey along with the Otolo-Sawla Asphalt Road Project, the southern part of Ethiopia. Field data appropriate to slope stability were carefully collected by considering the geological and geotechnical complexities of the slope failure along mountainous terrain.
- On collected samples, laboratory tests were conducted to determine the soil type, gradation, consistency, specific gravity, and engineering properties of the slope material.
- From grain size analysis result the soil type along failed slope sections were nearly coarse-grained soils with fines 20.04-49.27% and under existing slope sections were nearly fine-grained with coarser fraction 9.93-27.06%
- The result from the plasticity chart indicated that the fine-grain fraction of soil at all identified test pit location fall in medium plasticity clay.
- The slope forming materials are classified as per AASHTO A-6 to A-7 that is fair to the poor material category.
- From shear strength test result angle of friction, φ varies from 3º to 25º and cohesive strength of all soil samples varies from 1 kN/m2 to 43 kN/m2.
- The water table was assumed to be above the road level for finite element analysis of FS2, FS3, and FS4 slopes in line with the observations made at the field.
- The factor of safety increased when decreased slope angle or H.
- The slope performance is mainly influenced by the angle of slope, poor drainage, and types of slope forming materials.
- The computed FOS on the actual site slope angle was less than that of FOS on the recommended slope angle by ERA Geometric Design manual, 2002 so, the deviation contributed a part to slope failure.

- In the case of failed slopes, poor slope material, excessive slope height, and high groundwater levels could be a potential reason for the failure.
- A stability check for the existing slopes was carried out and was found stable with a factor of safety slightly more than one.
- It can be predicted that the slopes near the failed slopes are prone to failure because of similar soil properties and groundwater influence.
- Methods like geogrids adopted in the analysis and improved the stability for the existing slopes near the failed slopes.

5.2. Conclusion

- The slope forming materials are classified as per AASHTO A-6 to A-7 that is fair to the poor material category.
- In the case of failed slopes, poor slope material, excessive slope height, and high groundwater levels could be a potential reason for the failure.
- It can be predicted that the slopes near the failed slopes are prone to failure because of similar soil properties and groundwater influence.
- On the results from the analysis, the failed slope sections require reconstruction of a slope with an angle of less than 50%, and an adequate drainage system should be provided.
- Incorporating benches in the selected failed slopes is required to transform the behavior of one high slope into several lower ones.
- Methods like geogrids could be adopted to avoid failure of the existing slopes near the failed slopes.
- The provision of geosynthetic for adequate drainage has been recommended as a remedial solution to avoid failure of the existing slopes near the failed slopes.

REFERENCES

Abbas, J. M. (2015, June). 2D-FEM for assessment of slope stability. *Diyala Journal of Engineering Sciences, 08*, 84-98.

Abramson. (2002). *Assay for the measurement of DNA synthesis rates.*

Abramson LW, L. T. (2002). *Slope stability and stabilization methods.* New York, USA: John Wiley & Sons.

Abramson, F. P. U.S. Patent No. 6,355,416. Washington, DC: U.S. Patent and Trademark Office. (Abramson, F. P. (2002). U.S. Patent No. 6,355,416. Washington, DC: U.S. Patent and Trademark Office.). *Assay for the measurement of DNA synthesis rates.*

Ayalew, L. (1999). The effect of seasonal rainfall on landslides in the highlands of Ethiopia. *Bulletin of Engineering Geology and the Environment*, 58(1), 9-19.

Ayalew, L., Yamagishi, H., & Ugawa, N. (2004). Landslide susceptibility mapping using GIS-based weighted linear combination, the case in Tsugawa area of Agano River, Niigata Prefecture, Japan. *Landslides, 1(1)*, 73-81.

BARNHART, T. (2018). *Disturbed Vs. Undisturbed Soil Sampling.*

Barton N. and Bandis S. (1990). Review of predictive capabilities of the JRC-JCS model in engineering practice. *In: Balkema, A.A, (Ed), Proceedings of International Conference on Rock Joints, Leon*, 603-610.

Barton, N. (1973). Review of a new shear strength criterion for rock joints. *Engng Geol*, 287-332.

Bidisha Chakrabarti, Dr. P. Shivananda. (2017). Two-Dimensional Slope Stability Analysis by Plaxis-2d. *International Journal for Research in Applied Science & Engineering Technology (IJRASET)*, 871-877.

Bishop, A. W. (1956). The use of slip circles instability analysis of slopes. *Geotechnique, 5(1)*, 7-17.

Bowles, J. E. (1997). *FOUNDATION ANALYSIS AND DESIGN* (Fifth Edition ed.). Singapore: McGraw-Hill Companies, Inc.

Chen, R. H., Kuo, K. J., & Chang, C. M. (2011). Experiment on the stability of granular soil slopes by rainfall infiltration. *In 5th International Conference on Debris-Flow Hazards Mitigation, Mechanics, Prediction and Assessment*, 303-311.

Cheng, Y. M., & Lau, C. K. (2014). Slope stability analysis and stabilization: new methods and insight. *CRC Press.*

Chowdhury, R. F. P. & Bhattacharya G.,. (2010). Geotechnical Slope Analysis.

Clough RW, W. R. (1967). Analysis of embankment stress and deformations. *Journal of Soil Mechanics and Foundation Division, ASCE*, 529–549.

Dahle A, Bungum, H & Alsaker, A . (1992). Earthquake hazard at strait crossings. *In: Norwegian subsea tunneling, 8. Norwegian Soil and Rock Engineering Association, Tapir, Trondheim*, 43–46.

Davis, E. (1968). Theories of plasticity and failure of soil masses. (L. IK, Ed.) *Soil mechanics*, 341-54.

Donald IB, C. Z. (1997). Slope stability analysis by the upper bound approach: Fundamentals and methods. *Canadian Geotechnical Journal 34*, 853-862.

Duncan, J. (2000). Factors of Safety and Reliability in Geotechnical Engineering. *Journal of Geotechnical and Geoenvironmental Engineering, ASCE, 126, No. 4*, 307–316.

Endalkachew Mergia Anbese and Tibebu Tsegaye Zigale. (2019). Numerical Analysis of Earth Slopes Using Finite Element Program. *Global scientific journal*.

ERA. (2002). *Geometric Design Manual.*

Fellenius, W. (1936). Calculation of the stability of earth dams. Proceedings of the Second Congress on Large Dams. *4*, pp.445.

GADAAWIN, L. (2019). Slope Stability Analysis Along with Selected Road Section From Gutane Migiru Town to Fincha Sugar Factory, Western Ethiopia.

GETINET, T. G. (2016). *A Thesis in Analysis and Remedial Measures for Slope Instability Related Problems of Selected Sections of LOT II: Belta (KM60+000) – Otolo (KM 87+000) Asphalt Road Project, Southern Part of Ethiopia.* ADDIS ABABA.

Giam P S K; Donald I B. (1989). *Example problems for testing soil slope stability programs.* Monash University.

Goodman, R. E. (1989). Introduction to rock mechanics. (Wiley, Ed.) *Vol. 2*.

Hamed Niroumand, Khairul Anuar Kassim, and Amin Ghafooripour. (2012). Investigation of Slope Failures in Soil. *Electronic Journal of Geotechnical Engineering, 17*, 2703 - 2720.

Hamed Niroumand, Khairul Anuar Kassim, Amin Ghafooripour, Ramli Nazir, Sayyed Yaghoub Zolfeghari Far. (2012). Investigation of Slope Failures in Soil Mechanics. *EJGE*, 2704-2720.

JM, D. (1996). State of the Art: Limit equilibrium and finite element analysis of slopes. *Journal of Geotechnical Engineering*, 577- 596.

Johnson, R.B., and Degraff, J.V. (1991). Principles of Engineering Geology. 497.

Kasahun, M. (2014). Slope Stability Assessment for Selected Sections along Mana Begna-Lemlem Bereha Road, Northwestern Ethiopia. *Unpublished MSc Thesis, Addis Ababa University, Ethiopia.*

M.Das, B. (2010). *Principles of Geotechnical Engineering.* USA: Cengage Learning.

Matthews C, F. Z. (2014). Slope stability analysis–limit equilibrium or the. *Ground Engineering*, 22-8.

ML, R. (1995). Slope stability analysis: A Kinematical approach. *Geotechniques*, 283-93.

Morgenstern, N., & Price, V. (1965). The Analysis of the Stability of General Slip Surfaces. *Geotechnique, 15 (No. 1)*, pp. 77-93.

N, A. (2006). Slope stability analysis using 2D and 3D methods. *The University of Akron*.

Nima Farshidfar, Arash Nayeri. (2015). Slope Stability Analysis by Shear Strength Reduction Method. *Journal of Civil Engineering and Urbanism, 5*(1), 35-37.

Nordal, S. and Glaamen, M.G. . (2004). “Some examples of slope stability evaluations from Norwegian geotechnical practice”. *Geotechnical innovations*, 347-63.

Park, H., and West, T. (2001). Development of a probabilistic approach for rock wedge failure. *Eng Geol, 59*, 233–251.

Rahman, M. Z. (2012). Slope stability analysis and Road safety Evaluation - A case on two roads located close to the Pitea river-in Silkrors AND Nystrand. 1-111.

RN, C. (1981). Discussion of stability analysis of embankment and slope. *Journal of the Geotechnical Engineering Division, ASCE*, 691–693.

Robust Consulting Engineers, P. (2014). *Draft Design Review Report of Arbaminch-Kemba-Sawla Road project Lot III: Km87+000-Km138+438.*

S. Halder, M. O. Imam & M. S. Basir. (2017). A Detailed Analysis of Slope Stability Using Finite Element Method (FEM). *Proceedings of 3rd International Conference on Advances in Civil Engineering.* Chittagong, Bangladesh.

Samuel, M. (2011). Slope Stability Analysis on a Selected Slope Section along the Road Gohatsion-Dejen. *Unpublished MSc Thesis, Addis Ababa University, Ethiopia*.

Sarma, S. (1973). Stability Analysis of Embankment and Slopes. *Geotechnique, 23 (3)*, 423-33.

Sharma, S., Raghuvanshi, T., & Sahai, A. (1999). An engineering geological appraisal of the Lakhwar dam, Garhwal Himalaya, India. *Engineering Geology, 53(3-4)*, 381-398.

Singh, R., Umrao, R. K., & Singh, T. N. (2014). Stability evaluation of road-cut slopes in the Lesser Himalaya of Uttarakhand, India: conventional and numerical approaches. *Bulletin of Engineering Geology and the Environment, 73(3)*, 845-857.

Spencer, E. (1967). A method of Analysis of the Stability of Embankments, Assuming Parallel Interslice Forces. *Geotechnique, 17*, pp. 11-26.

Springer-Verlag. (2008). Stability analysis of slopes using the finite element method and limiting equilibrium approach.

U.S. Army Corps of Engineers. (1990). *Engineer Manual 1110-1-1904.* Washington: DEPARTMENT OF THE ARMY.

Wang, G., and Sassa, k. (2003). Pore-water pressure generation and movement of rainfall-induced landslides: effects of grain size and fine-particle content. *Engineering Geology, 69 (2),* 109-205.

Wen Xiang Peng, Jian Jun Mo, Yu Jun Xie. (2011, September). comparison for the result from 2D and 3D analysis for slope stability. (X. Zhou, Ed.) *Applied Mechanics and Materials, 90-93,* pp. 255-259.

Woldearegay, K. (2013). Review of the occurrences and influencing factors of landslides in the highlands of Ethiopia. *With implications for infrastructural development. Momona Ethiopian Journal of Science*, 5(1), 3-31.

Wyllie D. C., & Mah C. W. (2004). Rock Slope Engineering 4thEd. . *The Institution of Mining and Metallurgy London.*

APPENDIX

Appendix A: Analysis and Specific Gravity Test Results

Table A.1: Specific Gravity analysis for FS1 Site

	Hawassa University Institute Of Technology	Specific Gravity Test			
	Faculty of Civil Engineering and Built Environment				
	Civil Engineering Department				
	Geotechnical Engineering Laboratory				
Project:	Geotechnical Investigation Program				
Sampled by:	Natnael Bereded				
Station:	FS1				
Sample of:	Disturbed				
Location:	From Slope section				
Method used:	ASTM D 854-92				
Date tested:	15/02/2020				
Determination No.					
Pycnometer No.		1	2	3	A
Weight of pycnometer, gm		110.5	95.3	90.6	120.5
weight of pycnometer + dry soil sample, in gm		135.5	120.3	115.6	145.2
Weight of pycnometer + soil + water, W_{pws} (g)		*373.8*	*358.9*	*353.8*	383.7
Temperature, T_x(^{o}c)		21	21	21	22
Weight of pycnometer + water at T_x , W_{pw}(atT_x) (g)		*359*	*344.2*	*338.9*	368.9
Weight of dry soil, w_s (gm)		25	25	25	25
Conversion factor , K		0.9998	0.9998	0.9998	0.9998
Specific gravity of soil		2.45	2.43	2.47	2.45
The average specific gravity of soil		2.45			

Table A.2: Specific Gravity Analysis for FS2 Site

	Hawassa University Institute Of Technology	Specific Gravity Test
	Faculty of Civil Engineering and Built Environment	
	Civil Engineering Department	
	Geotechnical Engineering Laboratory	
Project:	Geotechnical Investigation Program	
Sampled by:	Natnael Bereded	
Station:	FS2	
Sample of:	Disturbed	
Location:	From Slope section	
Method used:	ASTM D 854-92	
Date tested:	15/02/2020	

Determination No.				
Pycnometer No.	1	2	3	B
Weight of pycnometer, gm	110.5	95.3	90.6	97.1
weight of pycnometer + dry soil sample, in gm	135.5	120.3	115.6	122.5
Weight of pycnometer + soil + water, W_{pws} (g)	*373.9*	*358.8*	*353.7*	360.7
Temperature, T_x(^{o}c)	21	21	21	22
Weight of pycnometer + water at T_x , W_{pw}(atT_x) (g)	*359*	*343.9*	*339*	345.7
Weight of dry soil, w_s (gm)	25	25	25	25
Conversion factor , K	0.9998	0.9998	0.9998	0.9998
Specific gravity of soil	2.47	2.47	2.43	2.50
The average specific gravity of soil	2.47			

Table A.3: Specific Gravity Analysis for ES1 Site

	Hawassa University Institute Of Technology	Specific Gravity Test			
	Faculty of Civil Engineering and Built Environment				
	Civil Engineering Department				
	Geotechnical Engineering Laboratory				
Project:	Geotechnical Investigation Program				
Sampled by:	Natnael Bereded				
Station:	ES1				
Sample of:	Disturbed				
Location:	From Slope section				
Method used:	ASTM D 854-92				
Date tested:	15/02/2020				
Determination No.					
Pycnometer No.		1	2	3	C
Weight of pycnometer, gm		110.5	95.3	90.6	90.4
weight of pycnometer + dry soil sample, in gm		135.5	120.3	115.6	115.5
Weight of pycnometer + soil + water, W_{pws} (g)		*373.7*	*358.6*	*353.6*	353.8
Temperature, $T_x(^oc)$		21	21	21	22
Weight of pycnometer + water at T_x , $W_{pw}(atT_x)$ (g)		*359.1*	*344*	*338.9*	339
Weight of dry soil, w_s (gm)		25	25	25	25
Conversion factor , K		0.9998	0.9998	0.9998	0.9998
Specific gravity of soil		2.40	2.40	2.43	2.45
The average specific gravity of soil		2.42			

Table A.4: Specific Gravity Analysis for ES2 Site

	Hawassa University Institute Of Technology	Specific Gravity Test			
	Faculty of Civil Engineering and Built Environment				
	Civil Engineering Department				
	Geotechnical Engineering Laboratory				
Project:	Geotechnical Investigation Program				
Sampled by:	Natnael Bereded				
Station:	ES2				
Sample of:	Disturbed				
Location:	From Slope section				
Method used:	ASTM D 854-92				
Date tested:	15/02/2020				
Determination No.					
Pycnometer No.		1	2	3	D
Weight of pycnometer, gm		110.5	95.3	90.6	101.5
weight of pycnometer + dry soil sample, in gm		135.5	120.3	115.6	126.4
Weight of pycnometer + soil + water, W_{pws} (g)		*374.1*	*358.9*	*353.8*	363.8
Temperature, T_x(^{o}c)		21	21	21	22
Weight of pycnometer + water at T_x , W_{pw}(atT_x) (g)		*359*	*344*	*338.7*	348.8
Weight of dry soil, w_s (gm)		25	25	25	25
Conversion factor , K		0.9998	0.9998	0.9998	0.9998
Specific gravity of soil		2.52	2.47	2.52	2.50
The average specific gravity of soil		2.51			

Table A.5: Specific Gravity Analysis for FS3 Site

	Hawassa University Institute Of Technology	Specific Gravity Test			
	Faculty of Civil Engineering and Built Environment				
	Civil Engineering Department				
	Geotechnical Engineering Laboratory				
Project:	Geotechnical Investigation Program				
Sampled by:	Natnael Bereded				
Station:	FS3				
Sample of:	Disturbed				
Location:	From Slope section				
Method used:	ASTM D 854-92				
Date tested:	15/02/2020				
Determination No.					
Pycnometer No.		1	2	3	B
Weight of pycnometer, gm		110.5	95.3	90.6	97.1
weight of pycnometer + dry soil sample, in gm		135.5	120.3	115.6	122.3
Weight of pycnometer + soil + water, W_{pws} (g)		*374.3*	*359.1*	*354.4*	361.1
Temperature, T_x(^{o}c)		21	21	21	22
Weight of pycnometer + water at T_x , W_{pw}(atT_x) (g)		*359*	*343.6*	*338.8*	345.70
Weight of dry soil, w_s (gm)		25	25	25	25
Conversion factor , K		0.9998	0.9998	0.9998	0.9998
Specific gravity of soil		2.58	2.63	2.66	2.60
The average specific gravity of soil		2.62			

Table A.6: Specific Gravity Analysis for ES3 Site

	Hawassa University Institute Of Technology	Specific Gravity Test
	Faculty of Civil Engineering and Built Environment	
	Civil Engineering Department	
	Geotechnical Engineering Laboratory	
Project:	Geotechnical Investigation Program	
Sampled by:	Natnael Bereded	
Station:	ES3	
Sample of:	Disturbed	
Location:	From Slope section	
Method used:	ASTM D 854-92	
Date tested:	15/02/2020	

Determination No.				
Pycnometer No.	1	2	3	C
Weight of pycnometer, gm	110.5	95.3	90.6	90.4
weight of pycnometer + dry soil sample, in gm	135.5	120.3	115.6	115.6
Weight of pycnometer + soil + water, W_{pws} (g)	*373.8*	*358.7*	*353.6*	354.1
Temperature, $T_x(^oc)$	21	21	21	22
Weight of pycnometer + water at T_x , $W_{pw}(atT_x)$ (g)	*359.1*	*343.9*	*339.1*	339.00
Weight of dry soil, w_s (gm)	25	25	25	25
Conversion factor , K	0.9998	0.9998	0.9998	0.9998
Specific gravity of soil	2.43	2.45	2.38	2.52
The average specific gravity of soil	2.45			

Table A.7: Specific Gravity Analysis for FS4 Site

	Hawassa University Institute Of Technology	Specific Gravity Test			
	Faculty of Civil Engineering and Built Environment				
	Civil Engineering Department				
	Geotechnical Engineering Laboratory				
Project:	Geotechnical Investigation Program				
Sampled by:	Natnael Bereded				
Station:	FS4				
Sample of:	Disturbed				
Location:	From Slope section				
Method used:	ASTM D 854-92				
Date tested:	15/02/2020				
Determination No.					
Pycnometer No.		1	2	3	A
Weight of pycnometer, gm		110.5	95.3	90.6	120.5
weight of pycnometer + dry soil sample, in gm		135.5	120.3	115.6	145.8
Weight of pycnometer + soil + water, W_{pws} (g)		*373.8*	*358.6*	*353.3*	383.3
Temperature, T_x(^{o}c)		21	21	21	22
Weight of pycnometer + water at T_x , W_{pw}(atT_x) (g)		*358.8*	*343.8*	*339*	368.90
Weight of dry soil, w_s (gm)		25	25	25	25
Conversion factor , K		0.9998	0.9998	0.9998	0.9998
Specific gravity of soil		2.50	2.45	2.34	2.36
The average specific gravity of soil		2.41			

Appendix B: Analysis and Laboratory Test Results of Particle-size Distribution

Table B.1: Particle-size Distribution Analysis for FS1

	Hawassa University Institute Of Technology Faculty of Civil Engineering and Built Environment Civil Engineering Department Geotechnical Engineering Laboratory	Seive + hydrometer analysis

Project:	Geotechnical Investigation Program
Sampled by:	Natnael Bereded
Station:	FS1
Sample of:	Disturbed
Location:	From Slope section
Method used:	AASHTO T-88
Date tested:	16/01/2020

Seive size, mm	% Passing
19	68.85
9.5	60.39
4.75	53.87
2.36	49.60
2	48.74
1.18	46.59
0.6	45.05
0.425	44.38
0.3	43.54
0.15	41.78
0.075	40.39
0.070	30.98
0.050	29.62
0.035	28.94
0.023	28.25
0.013	27.57
0.010	26.89
0.007	25.52
0.003	24.84
0.001	24.16

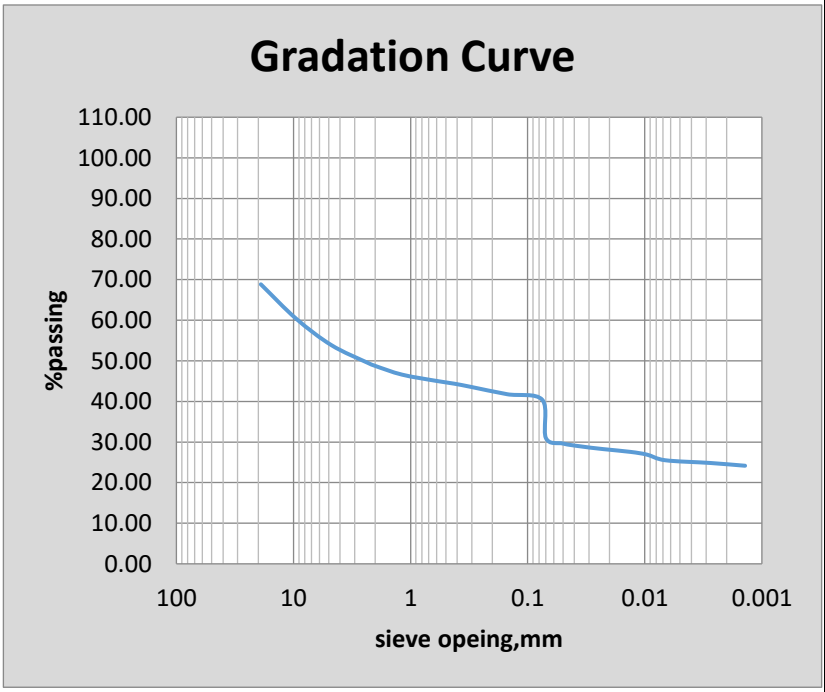

Gravel, %	46.13
Sand, %	13.48
Silt, %	15.55
Clay, %	24.84

Table B.2: Particle-size Distribution Analysis for FS2

	Hawassa University Institute Of Technology Faculty of Civil Engineering and Built Environment Civil Engineering Department Geotechnical Engineering Laboratory	Seive + hydrometer analysis

Project:	Geotechnical Investigation Program
Sampled by:	Natnael Bereded
Station:	FS2
Sample of:	Disturbed
Location:	From Slope section
Method used:	AASHTO T-88
Date tested:	16/01/2020

Seive size, mm	% Passing
19	80.18
9.5	78.02
4.75	75.53
2.36	72.91
2	72.35
1.18	69.95
0.6	60.68
0.425	56.47
0.3	52.04
0.15	46.01
0.075	43.28
0.075	35.92
0.053	34.47
0.038	33.02
0.024	31.56
0.014	30.83
0.010	30.11
0.007	28.65
0.003	27.20
0.001	26.47

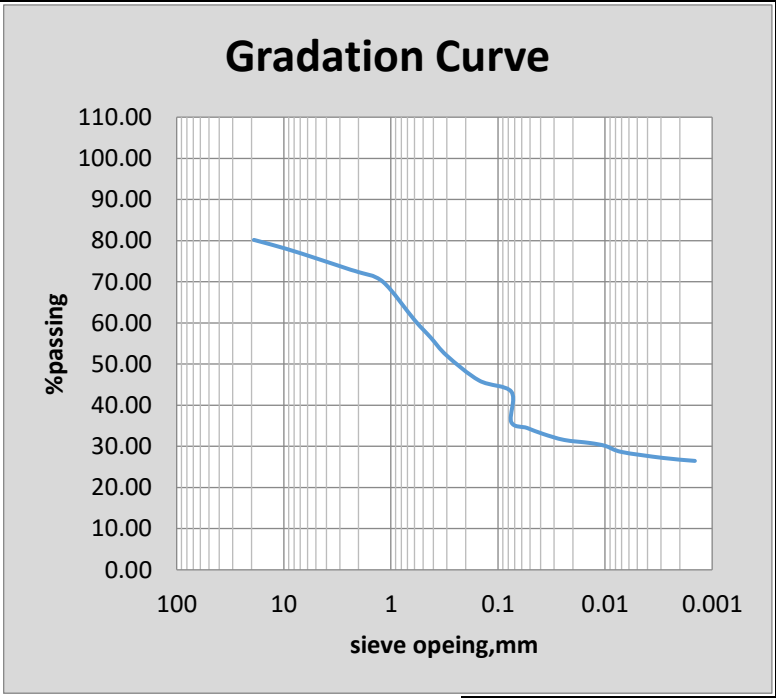

Gravel, %	24.48
Sand, %	32.25
Silt, %	16.08
Clay, %	27.20

Table B.3: Particle-size Distribution Analysis for ES1

	Hawassa University Institute Of Technology Faculty of Civil Engineering and Built Environment Civil Engineering Department Geotechnical Engineering Laboratory	Seive + hydrometer analysis

Project:	Geotechnical Investigation Program
Sampled by:	Natnael Bereded
Station:	ES1
Sample of:	Disturbed
Location:	From Slope section
Method used:	AASHTO T-88
Date tested:	16/01/2020

Seive size, mm	% Passing
19	100.00
9.5	99.10
4.75	98.34
2.36	97.12
2	96.80
1.18	95.84
0.6	94.98
0.425	94.50
0.3	93.88
0.15	91.77
0.075	90.07
0.068	85.04
0.048	81.97
0.034	80.43
0.022	78.90
0.013	77.36
0.009	75.83
0.006	72.76
0.003	71.22
0.001	69.69

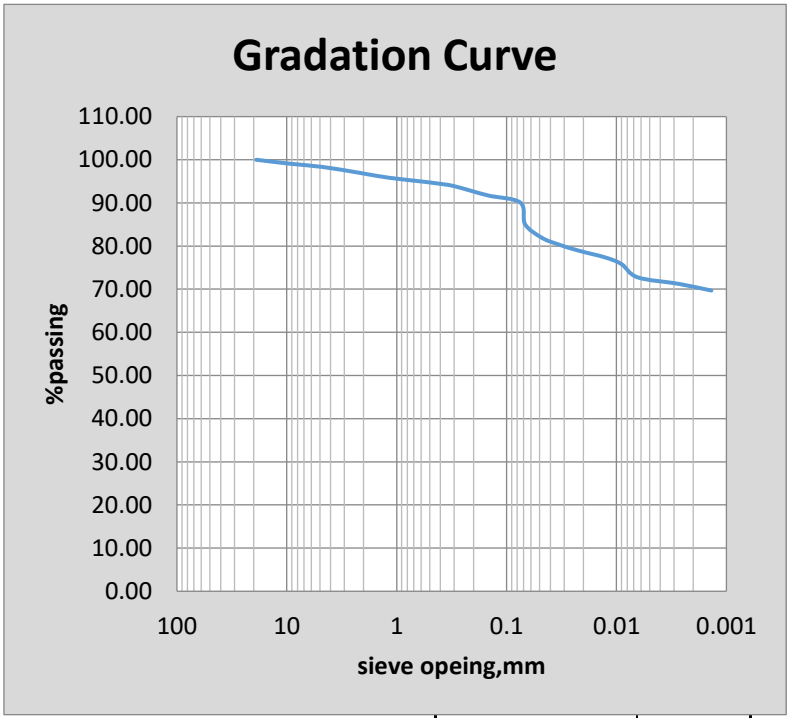

Gravel, %	1.66
Sand, %	8.27
Silt, %	18.85
Clay, %	71.22

Table B.4: Particle-size Distribution Analysis for ES2

	Hawassa University Institute Of Technology Faculty of Civil Engineering and Built Environment Civil Engineering Department Geotechnical Engineering Laboratory	Seive + hydrometer analysis

Project:	Geotechnical Investigation Program
Sampled by:	Natnael Bereded
Station:	ES2
Sample of:	Disturbed
Location:	From Slope section
Method used:	AASHTO T-88
Date tested:	16/01/2020

Seive size, mm	% Passing
19	100.00
9.5	99.18
4.75	97.31
2.36	93.31
2	92.25
1.18	87.99
0.6	82.38
0.425	80.18
0.3	77.97
0.15	74.38
0.075	72.94
0.068	63.53
0.048	62.32
0.035	59.89
0.022	57.47
0.013	56.26
0.009	55.05
0.007	52.62
0.003	50.20
0.001	48.98

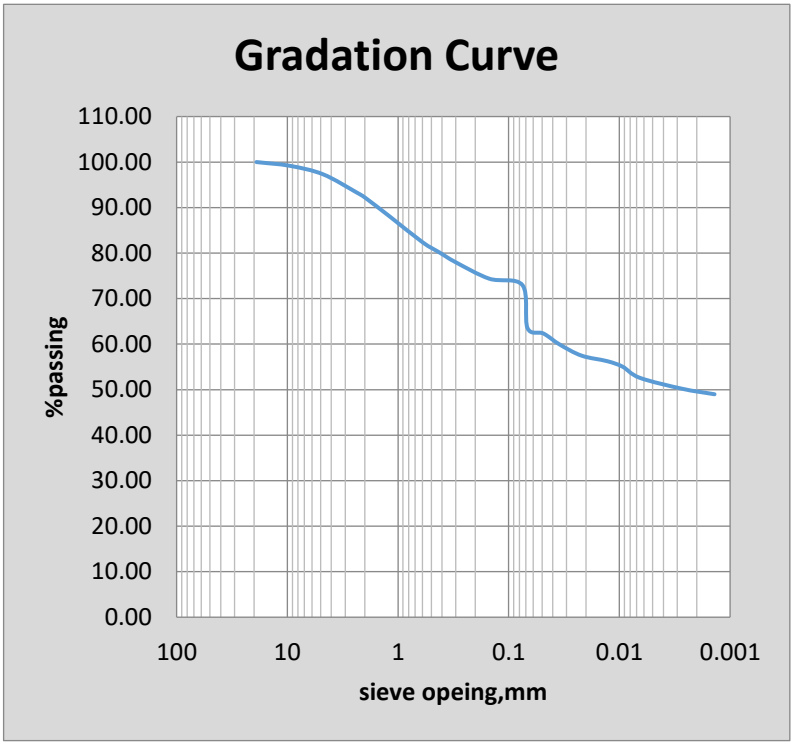

Gravel, %	2.69
Sand, %	24.37
Silt, %	22.74
Clay, %	50.20

Table B.5: Particle-size Distribution Analysis for FS3

	Hawassa University Institute Of Technology Faculty of Civil Engineering and Built Environment Civil Engineering Department Geotechnical Engineering Laboratory	Seive + hydrometer analysis

Project:	Geotechnical Investigation Program
Sampled by:	Natnael Bereded
Station:	FS3
Sample of:	Disturbed
Location:	From Slope section
Method used:	AASHTO T-88
Date tested:	16/01/2020

Seive size, mm	% Passing
19	79.74
9.5	73.95
4.75	65.68
2.36	53.45
2	49.58
1.18	36.69
0.6	28.76
0.425	26.37
0.3	24.40
0.15	21.69
0.075	20.00
0.072	18.44
0.051	16.82
0.036	15.20
0.023	13.59
0.013	11.97
0.009	10.35
0.007	8.73
0.003	7.12
0.001	5.50

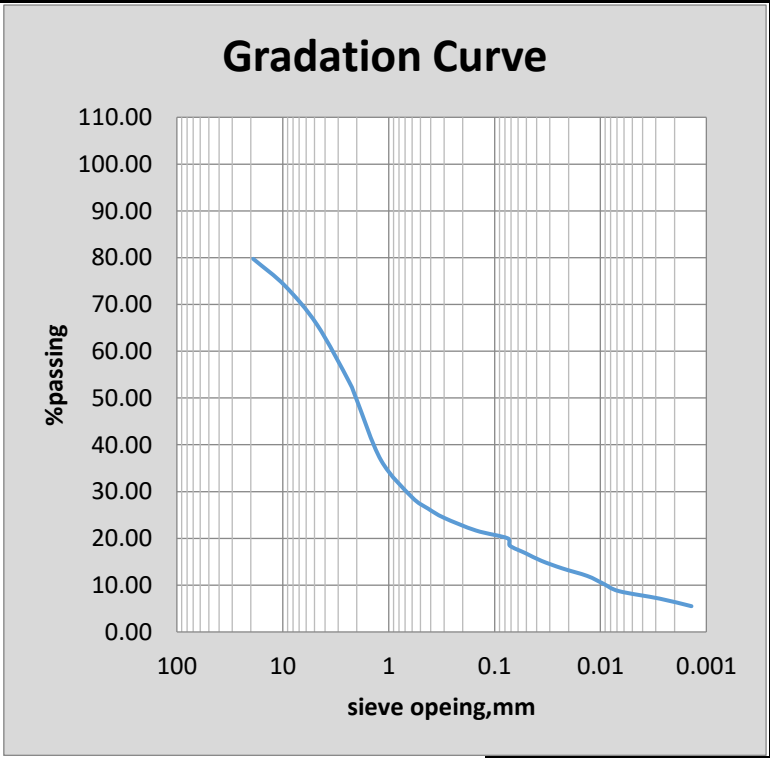

Gravel, %	34.30
Sand, %	45.66
Silt, %	18.61
Clay, %	1.43

Table B.6: Particle-size Distribution Analysis for ES3

	Hawassa University Institute Of Technology Faculty of Civil Engineering and Built Environment Civil Engineering Department Geotechnical Engineering Laboratory	Seive + hydrometer analysis

Project:	Geotechnical Investigation Program
Sampled by:	Natnael Bereded
Station:	ES3
Sample of:	Disturbed
Location:	From Slope section
Method used:	AASHTO T-88
Date tested:	16/01/2020

Seive size, mm	% Passing
19	100.00
9.5	100.00
4.75	99.54
2.36	98.78
2	98.66
1.18	97.89
0.6	95.43
0.425	94.04
0.3	92.95
0.15	90.86
0.075	89.43
0.057	86.74
0.041	83.72
0.029	80.70
0.019	77.68
0.011	74.65
0.008	71.63
0.006	70.12
0.002	68.61
0.001	67.10

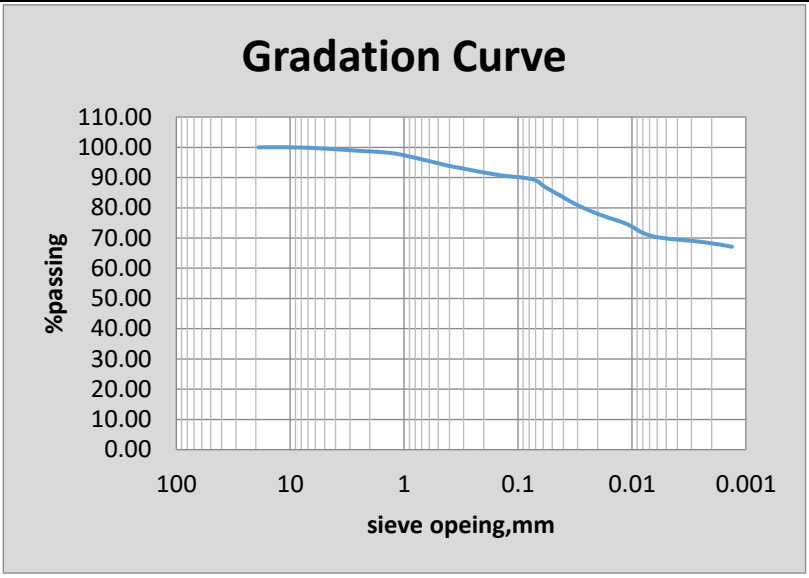

Gravel, %	0.46
Sand, %	10.10
Silt, %	20.83
Clay, %	68.61

Table B.7: Particle-size Distribution Analysis for FS4

	Hawassa University Institute Of Technology Faculty of Civil Engineering and Built Environment Civil Engineering Department Geotechnical Engineering Laboratory	Seive + hydrometer analysis

Project:	Geotechnical Investigation Program
Sampled by:	Natnael Bereded
Station:	FS4
Sample of:	Disturbed
Location:	From Slope section
Method used:	AASHTO T-88
Date tested:	16/01/2020

Seive size, mm	% Passing
19	91.98
9.5	79.18
4.75	66.27
2.36	53.40
2	46.91
1.18	39.90
0.6	32.03
0.425	27.59
0.3	21.71
0.15	17.17
0.075	15.83
0.063	12.28
0.045	11.74
0.032	11.20
0.021	10.66
0.012	10.12
0.009	9.31
0.006	8.50
0.003	7.41
0.001	7.14

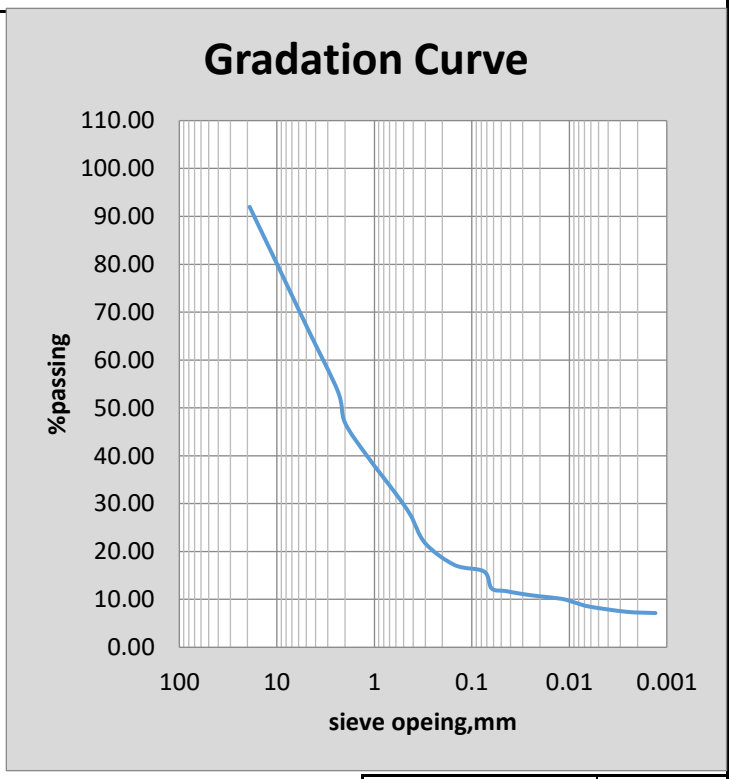

Gravel, %	33.73
Sand, %	50.44
Silt, %	8.42
Clay, %	7.41

Appendix C: Analysis and Laboratory Test Results of Atterberg's Limit

Table C.1: Atterberg's Limit Analysis for FS1

	Hawassa University Institute of Technology				Atterberg's Limit	
	Faculty of Civil Engineering and Built Environment					
	Civil Engineering Department					
	Geotechnical Laboratory					
Project:-	Geotechnical Investigation Program					
Sampled by:-	Natnael Bereded					
Station:-	FS1					
Sample of:-	Disturbed					
Depth:-	1.5m					
The method used:-	ASTM D 4318 - 10					
Date tested:-	13/02/2020					
	Liquid Limit				Plastic Limit	
	1	2	3	4	1	2
No.of Blows N	32	26	21	18		
Can n	L1	GTZ	H10	W11	Z8	WPZ8
Wt. Can + Wet Soil, g	35.00	36.10	32.30	34.90	26.40	25.90
Wt Can + Dry Soil, g	30.40	30.50	27.70	29.60	25.00	24.30
Wt. water, g	4.6	5.6	4.6	5.3	1.4	1.6
Wt. of Can, g	21.20	20.30	19.50	20.30	20.00	19.50
Wt. of Dry Soil, g	9.2	10.2	8.2	9.3	5	4.8
Moisture Content, %	50.00	54.90	56.09	56.99	28.00	33.33

Liquid Limit, LL, (%)	55	Average Plastic Limit
Plastic Limit, PL, (%)	31	31
Plasticity Index, PI, (%)	24	

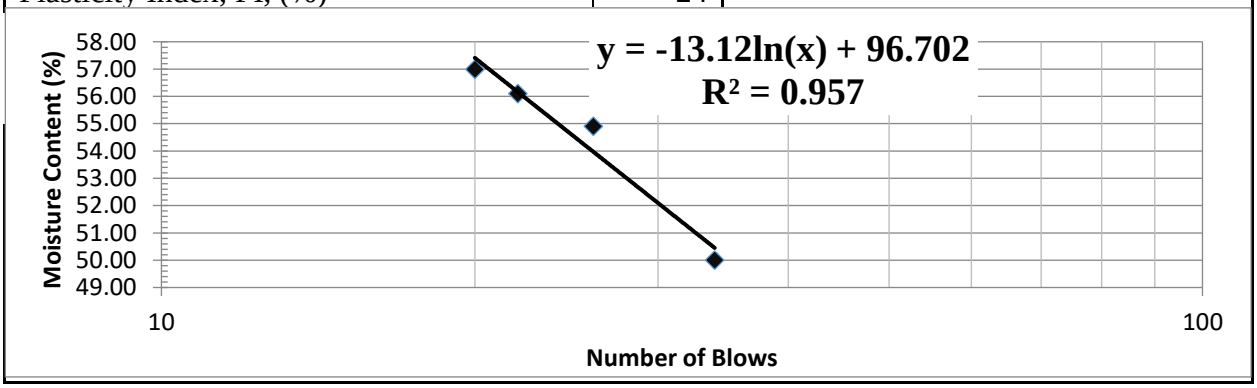

Table C.2: Atterberg's Limit Analysis for FS2

	Hawassa University Institute of Technology					Atterberg's Limit
	Faculty of Civil Engineering and Built Environment					
	Civil Engineering Department					
	Geotechnical Laboratory					
Project:-	Geotechnical Investigation Program					
Sampled by:-	Natnael Bereded					
Station:-	FS2					
Sample of:-	Disturbed					
Depth:-	1.5 m					
The method used:-	ASTM D 4318 - 10					
Date tested:-	13/02/2020					
	Liquid Limit				Plastic Limit	
	1	2	3	4	1	2
No.of Blows N	31	29	22	17		
Can n	B3	C4	A7	A3	A8	B7
Wt. Can + Wet Soil, g	31.20	33.40	29.70	32.60	26.30	27.90
Wt Can + Dry Soil, g	27.70	28.90	26.40	28.00	25.20	26.50
Wt. water, g	3.5	4.5	3.4	4.6	1.1	1.4
Wt. of Can, g	19.90	19.40	19.70	19.40	20.90	20.60
Wt. of Dry Soil, g	7.8	9.5	6.7	8.6	4.3	5.9
Moisture Content, %	44.87	47.37	50.75	53.49	25.58	23.73
Liquid Limit, LL, (%)	49				Average Plastic Limit	
Plastic Limit, PL, (%)	25				25	
Plasticity Index, PI, (%)	24					

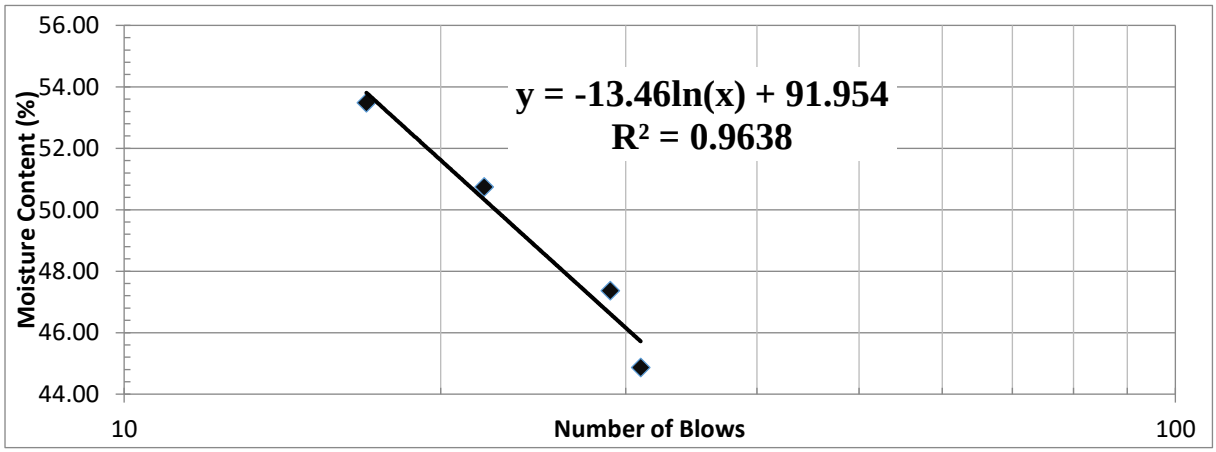

Table C.3: Atterberg's Limit Analysis for ES1

	Hawassa University Institute of Technology	Atterberg's Limit
	Faculty of Civil Engineering and Built Environment	
	Civil Engineering Department	
	Geotechnical Laboratory	

Project:-	Geotechnical Investigation Program					
Sampled by:-	Natnael Bereded					
Station:-	ES1					
Sample of:-	Disturbed					
Depth:-	1.5 m					
The method used:-	ASTM D 4318 - 10					
Date tested:-	13/02/20120					
	Liquid Limit				Plastic Limit	
	1	2	3	4	1	2
No.of Blows N	31	28	20	17		
Can n	P9	C11	A9	Z22	B4	FZ
Wt. Can + Wet Soil, g	31.10	28.80	40.30	34.10	26.60	27.30
Wt Can + Dry Soil, g	27.50	25.00	32.00	27.80	24.90	25.50
Wt. water, g	3.6	3.8	8.3	6.3	1.7	1.8
Wt. of Can, g	21.60	18.90	19.50	18.40	20.20	20.80
Wt. of Dry Soil, g	5.9	6.1	12.5	9.4	4.7	4.7
Moisture Content, %	61.02	62.30	66.40	67.02	36.17	38.30
Liquid Limit, LL, (%)	64				Average Plastic Limit	
Plastic Limit, PL, (%)	37				37	
Plasticity Index, PI, (%)	27					

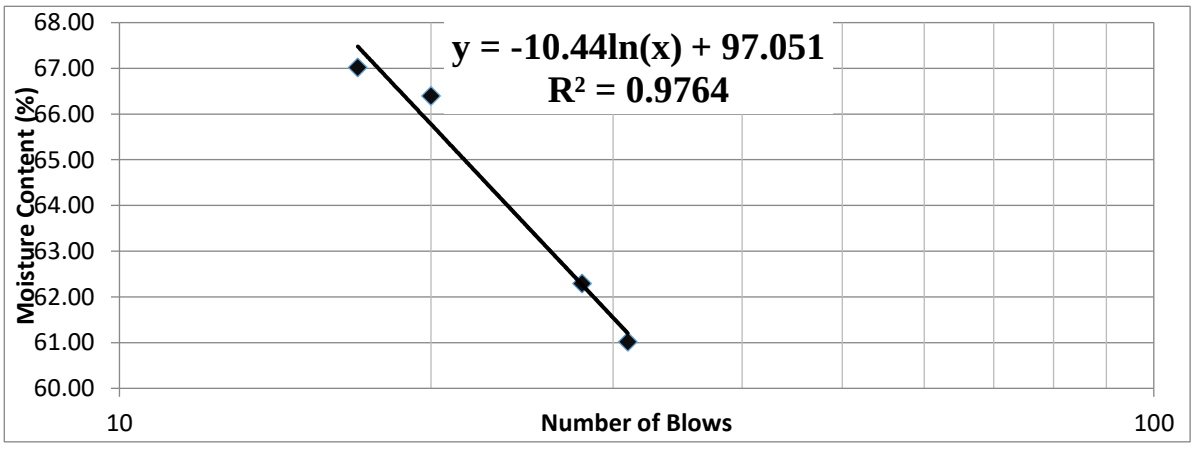

Table C.4: Atterberg's Limit Analysis for ES2

	Hawassa University Institute of Technology				Atterberg's Limit	
	Faculty of Civil Engineering and Built Environment					
	Civil Engineering Department					
	Geotechnical Laboratory					
Project:-	Geotechnical Investigation Program					
Sampled by:-	Natnael Bereded					
Station:-	ES2					
Sample of:-	Disturbed					
Depth:-	1.5 m					
The method used:-	ASTM D 4318 - 10					
Date tested:-	13/02/2020					
	Liquid Limit				Plastic Limit	
	1	2	3	4	1	2
No.of Blows N	30	26	21	20		
Can n	B22	TV-4	GA	B9	VI-10	A3
Wt. Can + Wet Soil, g	31.10	34.70	31.90	30.70	24.40	29.80
Wt Can + Dry Soil, g	28.50	31.20	29.10	27.80	23.00	28.30
Wt. water, g	2.6	3.50	2.80	2.90	1.40	1.50
Wt. of Can, g	20.50	20.70	21.20	19.70	17.10	21.00
Wt. of Dry Soil, g	8	10.5	7.9	8.1	5.9	7.3
Moisture Content, %	32.50	33.33	35.44	35.80	23.73	20.55

Liquid Limit, LL, (%)	34	Average Plastic Limit
Plastic Limit, PL, (%)	22	22
Plasticity Index, PI, (%)	12	

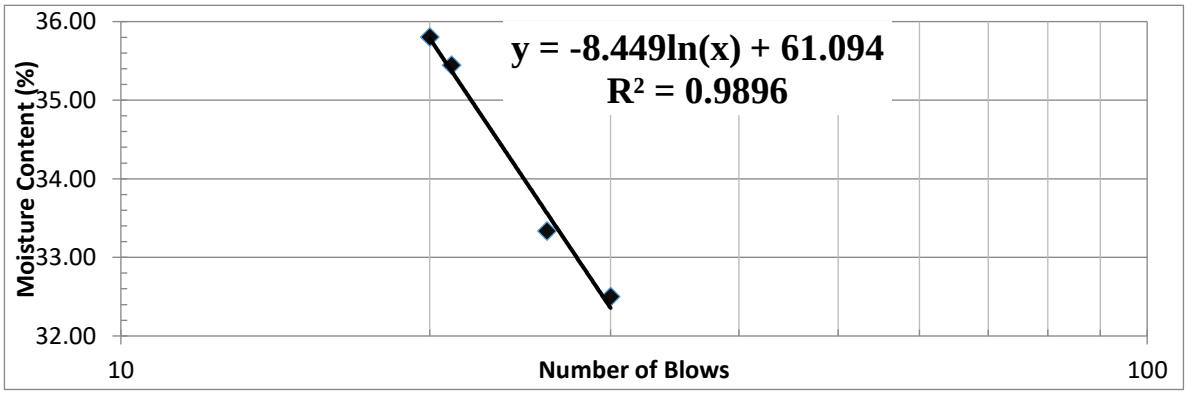

Table C.5: Atterberg's Limit Analysis for FS3

	Hawassa University Institute of Technology	Atterberg's Limit
	Faculty of Civil Engineering and Built Environment	
	Civil Engineering Department	
	Geotechnical Laboratory	

Project:-	Geotechnical Investigation Program					
Sampled by:-	Natnael Bereded					
Station:-	FS3					
Sample of:-	Disturbed					
Depth:-	1.5 m					
The method used:-	ASTM D 4318 - 10					
Date tested:-	13/02/2020					
	Liquid Limit				Plastic Limit	
	1	2	3	4	1	2
No.of Blows N	32	26	21	19		
Can n	G3	Z11	D4	B3	Z31	G2
Wt. Can + Wet Soil, g	33.80	34.70	36.60	31.50	29.60	28.30
Wt Can + Dry Soil, g	29.50	31.00	31.90	28.40	27.70	26.60
Wt. water, g	4.3	3.7	4.7	3.1	1.9	1.7
Wt. of Can, g	18.00	21.50	20.50	21.00	20.60	20.90
Wt. of Dry Soil, g	11.5	9.5	11.4	7.4	7.1	5.7
Moisture Content, %	37.39	38.95	41.23	41.89	26.76	29.82

Liquid Limit, LL, (%)	40	Average Plastic Limit
Plastic Limit, PL, (%)	28	28
Plasticity Index, PI, (%)	12	

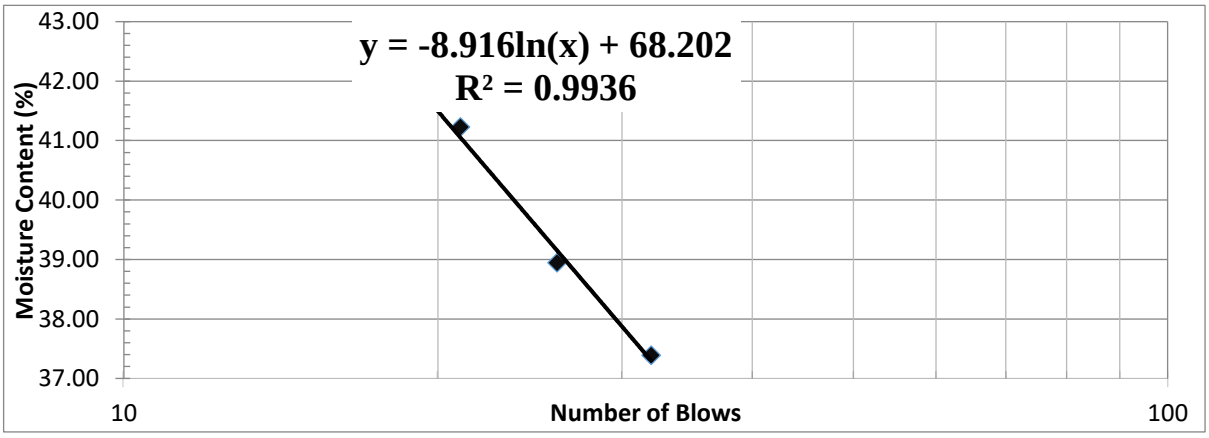

Table C.6: Atterberg's Limit Analysis for ES3

	Hawassa University Institute of Technology				Atterberg's Limit	
	Faculty of Civil Engineering and Built Environment					
	Civil Engineering Department					
	Geotechnical Laboratory					
Project:-	Geotechnical Investigation Program					
Sampled by:-	Natnael Bereded					
Station:-	ES3					
Sample of:-	Disturbed					
Depth:-	1.5 m					
The method used:-	ASTM D 4318 - 10					
Date tested:-	13/02/2020					
	Liquid Limit				Plastic Limit	
	1	2	3	4	1	2
No.of Blows N	30	26	24	20		
Can n	F32	D5	B10	FA	A9	A3
Wt. Can + Wet Soil, g	50	33.5	47	31.5	28.5	27.6
Wt Can + Dry Soil, g	40.7	28.9	37.5	27.3	26.7	25.9
Wt. water, g	9.3	4.6	9.5	4.1	1.8	1.7
Wt. of Can, g	21.5	19.6	19.1	19.5	19.5	19.6
Wt. of Dry Soil, g	19.2	9.3	18.4	7.9	7.2	6.3
Moisture Content, %	48.44	49.46	51.63	53.85	25.00	26.98
Liquid Limit, LL, (%)	51				Average Plastic Limit	
Plastic Limit, PL, (%)	26				26	
Plasticity Index, PI, (%)	25					

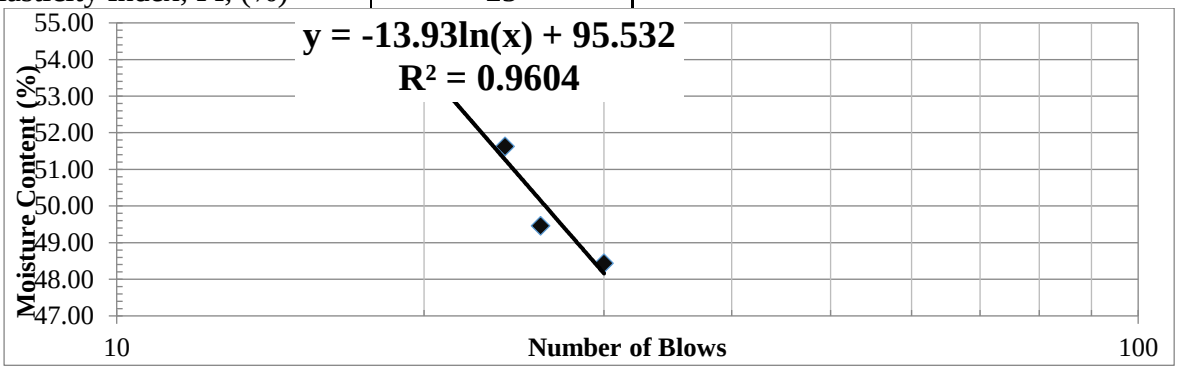

Table C.7: Atterberg's Limit Analysis for FS4

	Hawassa University Institute of Technology	Atterberg's Limit
	Faculty of Civil Engineering and Built Environment	
	Civil Engineering Department	
	Geotechnical Laboratory	

Project:-	Geotechnical Investigation Program
Sampled by:-	Natnael Bereded
Station:-	FS4
Sample of:-	Disturbed
Depth:-	1.5 m
The method used:-	ASTM D 4318 - 10
Date tested:-	13/02/2020

	Liquid Limit				Plastic Limit	
	1	2	3	4	1	2
No.of Blows N	30	28	23	19		
Can n	G8	B9	G1	DRA4	P9	ZN1
Wt. Can + Wet Soil, g	50	30.8	47	30.5	29.5	26
Wt Can + Dry Soil, g	40.6	27.1	38	26.4	27.7	24.8
Wt. water, g	9.4	3.7	9	4.1	1.8	1.2
Wt. of Can, g	20.9	19.6	21	18.9	21.6	20.4
Wt. of Dry Soil, g	19.7	7.5	17	7.5	6.1	4.4
Moisture Content, %	47.72	49.33	52.94	54.67	29.51	27.27

Liquid Limit, LL, (%)	51
Plastic Limit, PL, (%)	28
Plasticity Index, PI, (%)	23

Average Plastic Limit
28

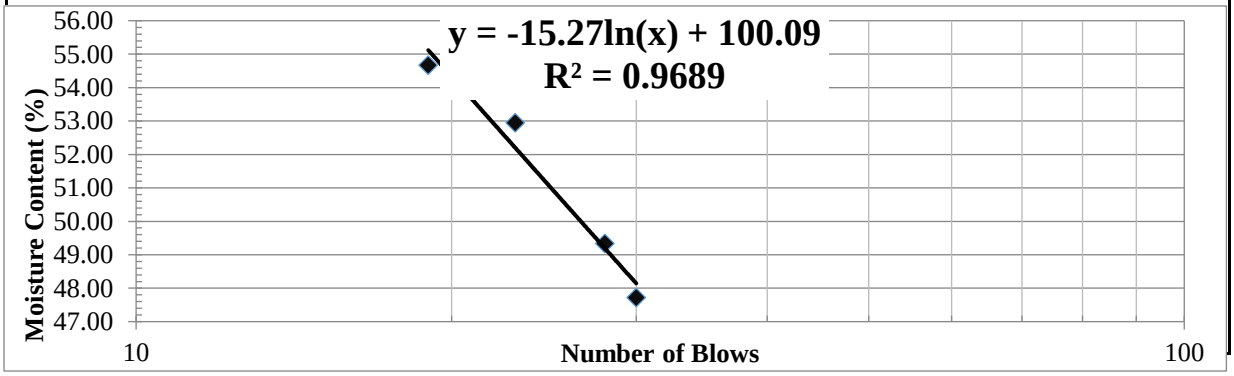

Appendix D: Analysis and Test Results of Field Density Test

Table D.1: Field Density Test Analysis for Selected Failed Slopes

	Hawassa University Institute Of Technology	Field Density Test
	Faculty of Civil Engineering and Built Environment	
	Civil Engineering Department	
	Geotechnical Engineering Laboratory	
Project:	Geotechnical Investigation Program	
Sampled by:	Natnael Bereded	
Station:	Failed Slopes	
Sample of:	Disturbed	
Location:	From Slope section	
Method used:	ASTM D 1556 - 00	
Date tested:	16/01/20	

Measurement of Soil Density				
Slope Location	FS1	FS2	FS3	FS4
Weight of sand + cylinder before pouring W_1 gm	6976	6941	7007	7021
Weight of sand + cylinder after pouring W_4 gm	3605	3394	3735	3936
Weight of wet soil from hole $W_{soil\ from\ the\ hole,}$ gm	2895	3206	2781	2556
Weight of sand in the cone W3, gm	1358	1358	1358	1358
Weight of sand in hole $W_b = (W_1-W_2-W_4)$ gm	2013	2189	1914	1727
The density of the sand used in gm/cc	1.3	1.3	1.3	1.3
The volume of the hole (Vh) in cc	1548.46	1683.85	1472.31	1328.46
Bulk density $g_b = (W_w / W_b)$, gm/cc	1.87	1.90	1.89	1.92
Water content determination				
Container number	Z8	F2	B10	SL
Weight of container Wc in gm	20	20.9	19.1	20.6
Weight of container + wet soil, Wcws, gm	83	84.9	95	99.1
Weight of container +dry soil, Wcds, gm	71.8	72.4	84.2	87
Weight of water, Ww, gm	11.2	12.5	10.8	12.1
Weight of dry soil, Wds, gm	51.8	51.5	65.1	66.4
Moisture content (%)=(Ww/ Wds)*100	21.62	24.27	16.59	18.22
Dry density $g_d = g_b / (1+w)$ gm/c	1.54	1.53	1.62	1.63
Unit weight of the wet soil	18.34	18.68	18.53	18.87
Unit weight of the dry soil	15.08	15.03	15.89	15.97

Table D. 2: Field Density Test Analysis for Selected Existing Slopes

	Hawassa University Institute Of Technology	Field Density Test
	Faculty of Civil Engineering and Built Environment	
	Civil Engineering Department	
	Geotechnical Engineering Laboratory	
Project:	Geotechnical Investigation Program	
Sampled by:	Natnael Bereded	
Station:	Existing Slopes	
Sample of:	Disturbed	
Location:	From Slope section	
Method used:	ASTM D 1556 - 00	
Date tested:	16/01/20	

Measurement of Soil Density			
Slope Location	ES1	ES2	ES3
Weight of sand + cylinder before pouring W_1 gm	6910	6990	6997
Weight of sand + cylinder after pouring W_4 gm	3650	3632	3717
Weight of wet soil from hole $W_{soil\ from\ the\ hole}$, gm	2813	2849	2912
Weight of sand in the cone W3, gm	1358	1358	1358
Weight of sand in hole $W_b = (W_1-W_2-W_4)$ gm	1902	2000	1922
The density of the sand used in gm/cc	1.3	1.3	1.3
The volume of the hole (Vh) in cc	1463.08	1538.46	1478.46
Bulk density $g_b = (W_w / W_b)$, gm/cc	1.92	1.85	1.97
Water content determination			
Container number	ZN1	W11	L1
Weight of container Wc in gm	20.6	20.3	21.2
Weight of container + wet soil, Wcws, gm	91	98	102
Weight of container +dry soil, Wcds, gm	75.9	83.7	86.3
Weight of water, Ww, gm	15.1	14.3	15.7
Weight of dry soil, Wds, gm	55.3	63.4	65.1
Moisture content (%)=(Ww/ Wds)*100	27.31	22.56	24.12
Dry density $g_d = g_b / (1+w)$ gm/c	1.51	1.51	1.59
Unit weight of the wet soil	18.86	18.17	19.32
Unit weight of the dry soil	14.82	14.82	15.57

Appendix E: Analysis and Laboratory Test results of Direct Shear Test

Table E.1: Direct Shear Test Analysis for FS1

	Hawassa University Institute Of Technology		Direct Shear Strength
	Faculty of Civil Engineering and Built Environment		
	Civil Engineering Department		
	Geotechnical Engineering Laboratory		
Project:	Geotechnical Investigation Program		
Sampled by:	Natnael Bereded		
Station:	FS1		
Sample of:	Disturbed		
Location:	From Slope section		
Method used:	ASTM D 3080		
Date tested:	21/01/2020		
Bulk Density (gm/cm^3)	1.87	Data for maximum shear stress	
Dry Density (gm/cm3)	1.54	Normal Stress,Kpa	Maximum Shear stress,Kpa
		0	36.799
		50	36
		100	48
		200	77
		400	99
		Cohesion (c),Kpa	31
		Angle of internal friction Ø	11

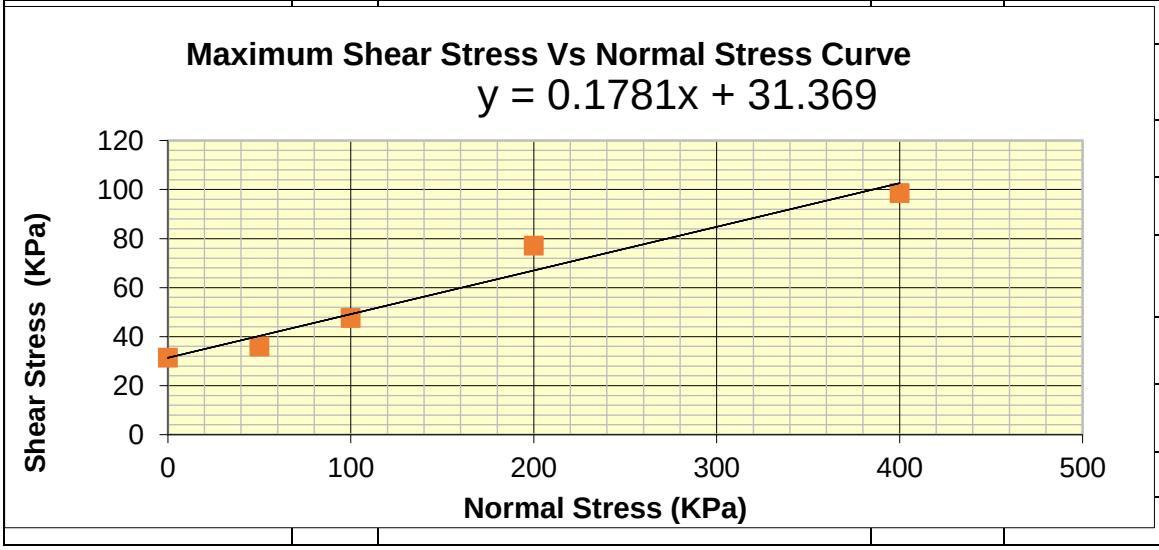

Table E.2: Direct Shear Test Analysis for FS2

	Hawassa University Institute Of Technology		Direct Shear Strength
	Faculty of Civil Engineering and Built Environment		
	Civil Engineering Department		
	Geotechnical Engineering Laboratory		
Project:	Geotechnical Investigation Program		
Sampled by:	Natnael Bereded		
Station:	FS2		
Sample of:	Disturbed		
Location:	From Slope section		
Method used:	ASTM D 3080		
Date tested:	21/01/2020		
Bulk Density (gm/cm^3)	1.90	Data for maximum shear stress	
Dry Density (gm/cm3)	1.53	Normal Stress,Kpa	Maximum Shear stress,Kpa
		0	43.086
		50	43
		100	50
		200	71
		400	73
		Cohesion (c),Kpa	43
		Angle of internal friction	5

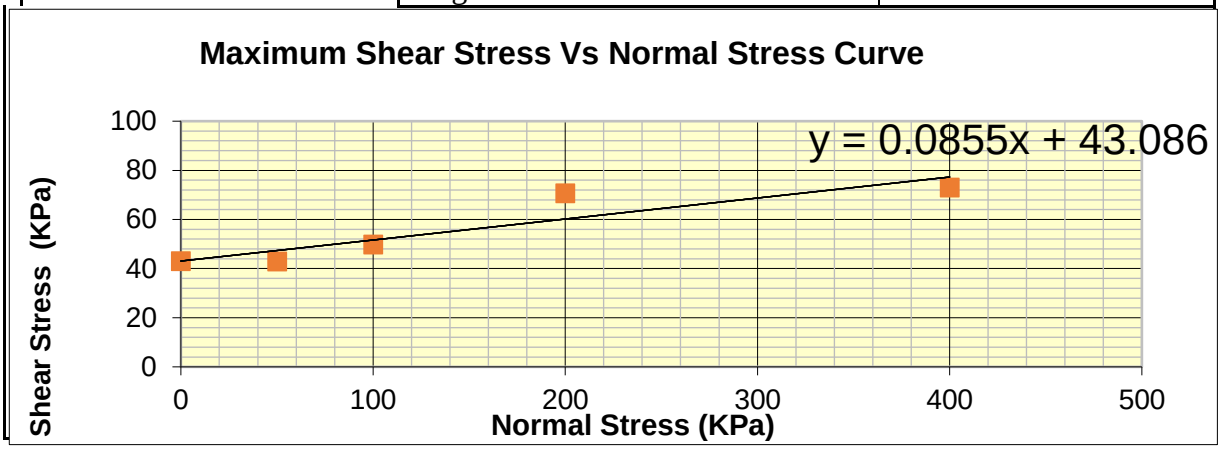

Table E.3: Direct Shear Test Analysis for ES1

	Hawassa University Institute Of Technology		Direct Shear Strength
	Faculty of Civil Engineering and Built Environment		
	Civil Engineering Department		
	Geotechnical Engineering Laboratory		
Project:	Geotechnical Investigation Program		
Sampled by:	Natnael Bereded		
Station:	ES1		
Sample of:	Disturbed		
Location:	From Slope section		
Method used:	ASTM D 3080		
Date tested:	21/01/2020		
Bulk Density (gm/cm^3)	1.92	Data for maximum shear stress	
Dry Density (gm/cm3)	1.51	Normal Stress,Kpa	Maximum Shear stress,Kpa
		0	32.15
		50	27
		100	42
		200	38
		400	41
		Cohesion (c),Kpa	32
		Angle of internal friction Ø	3

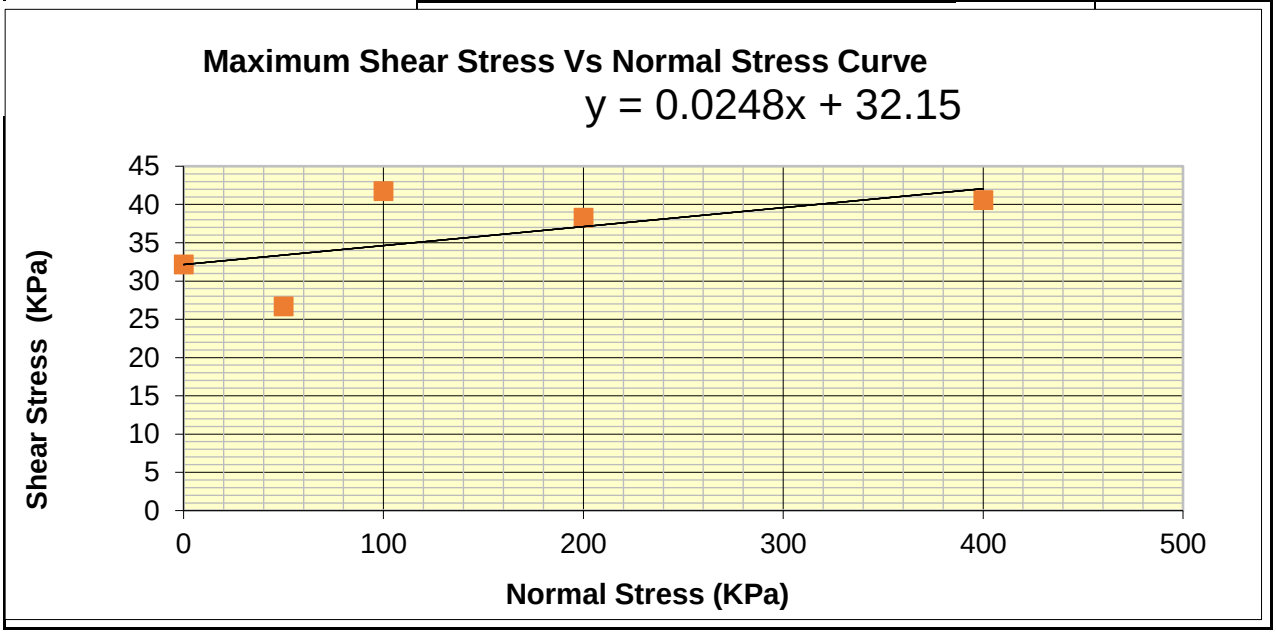

Table E.4: Direct Shear Test Analysis for ES2

	Hawassa University Institute Of Technology	
	Faculty of Civil Engineering and Built Environment	
	Civil Engineering Department	
	Geotechnical Engineering Laboratory	
Project:	Geotechnical Investigation Program	Direct Shear Strength
Sampled by:	Natnael Bereded	
Station:	ES2	
Sample of:	Disturbed	
Location:	From Slope section	
Method used:	ASTM D 3080	
Date tested:	21/01/2020	

Bulk Density (gm/cm^3)	1.85	Data for maximum shear stress	
Dry Density (gm/cm3)	1.51	Normal Stress,Kpa	Maximum Shear stress,Kpa
		0	21.568
		50	36
		100	57
		200	93
		400	156
		Cohesion (c),Kpa	22
		Angle of internal friction Ø	19

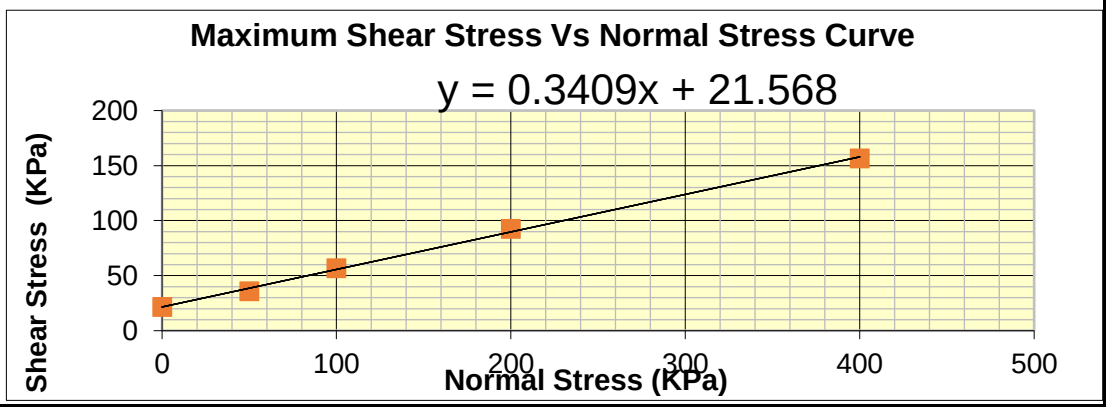

Table E.5: Direct Shear Test Analysis for FS3

	Hawassa University Institute Of Technology		Direct Shear Strength
	Faculty of Civil Engineering and Built Environment		
	Civil Engineering Department		
	Geotechnical Engineering Laboratory		
Project:	Geotechnical Investigation Program		
Sampled by:	Natnael Bereded		
Station:	FS3		
Sample of:	Disturbed		
Location:	From Slope section		
Method used:	ASTM D 3080		
Date tested:	21/01/2020		
Bulk Density (gm/cm^3)	1.89	Data for maximum shear stress	
Dry Density (gm/cm3)	1.62	Normal Stress,Kpa	Maximum Shear stress,Kpa
		0	4.2834
		50	44
		100	46
		200	72
		400	198
		Cohesion (c),Kpa	43
		Angle of internal friction Ø	5

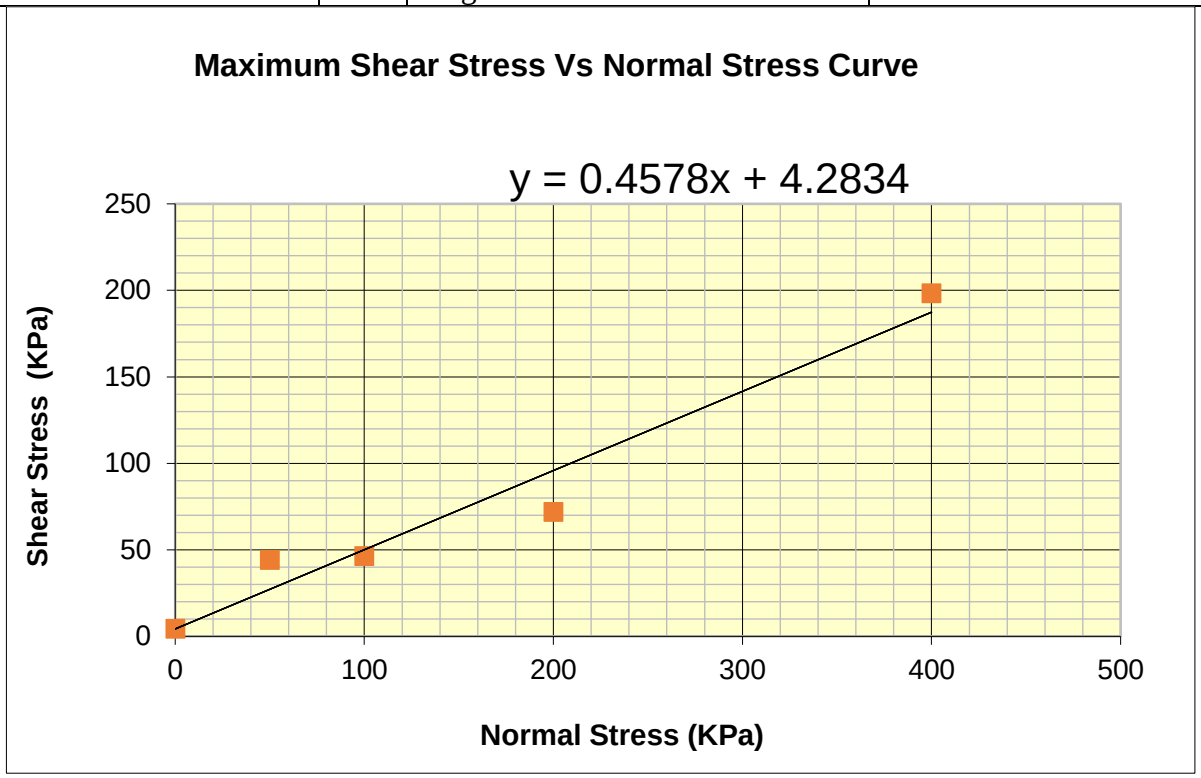

Table E.6: Direct Shear Test Analysis for ES3

	Hawassa University Institute Of Technology		Direct Shear Strength
	Faculty of Civil Engineering and Built Environment		
	Civil Engineering Department		
	Geotechnical Engineering Laboratory		
Project:	Geotechnical Investigation Program		
Sampled by:	Natnael Bereded		
Station:	ES3		
Sample of:	Disturbed		
Location:	From Slope section		
Method used:	ASTM D 3080		
Date tested:	21/01/2020		
Bulk Density (gm/cm^3)	1.97	Data for maximum shear stress	
Dry Density (gm/cm3)	1.59	Normal Stress,Kpa	Maximum Shear stress,Kpa
		0	37.064
		50	27
		100	48
		200	45
		400	39
		Cohesion (c),Kpa	37
		Angle of internal friction Ø	3

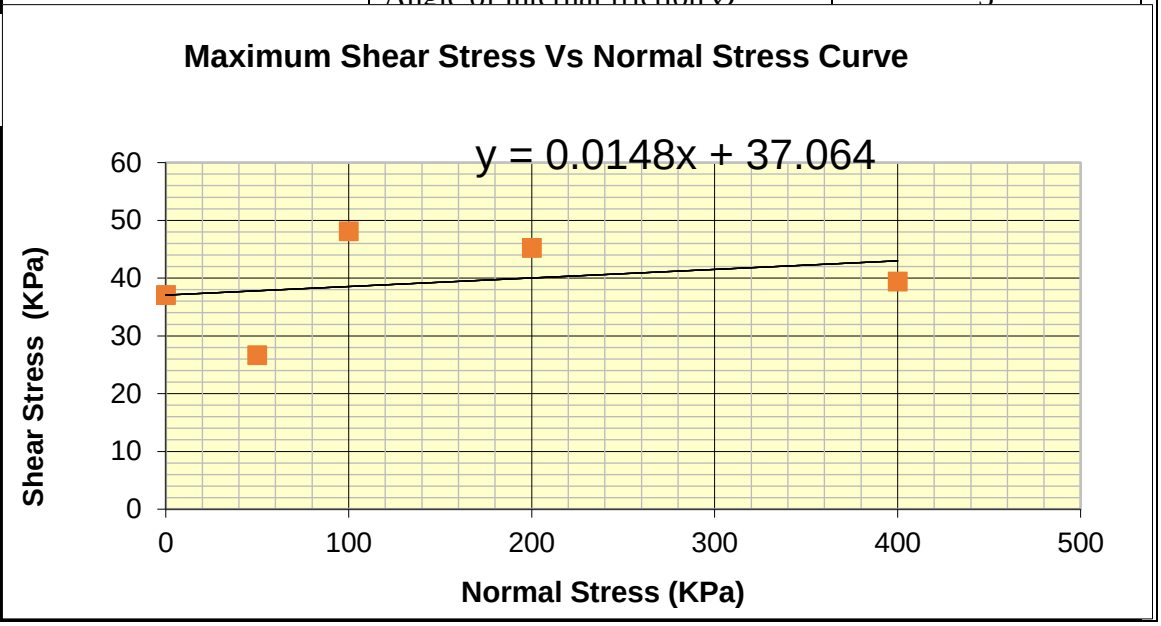

Table E.7: Direct Shear Test Analysis for FS4

	Hawassa University Institute Of Technology		Direct Shear Strength
	Faculty of Civil Engineering and Built Environment		
	Civil Engineering Department		
	Geotechnical Engineering Laboratory		
Project:	Geotechnical Investigation Program		
Sampled by:	Natnael Bereded		
Station:	FS4		
Sample of:	Disturbed		
Location:	From Slope section		
Method used:	ASTM D 3080		
Date tested:	21/01/2020		
Bulk Density (gm/cm^3)	1.92	Data for maximum shear stress	
Dry Density (gm/cm3)	1.62	Normal Stress,Kpa	Maximum Shear stress,Kpa
		0	9.7761
		50	34
		100	45
		200	92
		400	173
		Cohesion (c),Kpa	10
		Angle of internal friction Ø	21

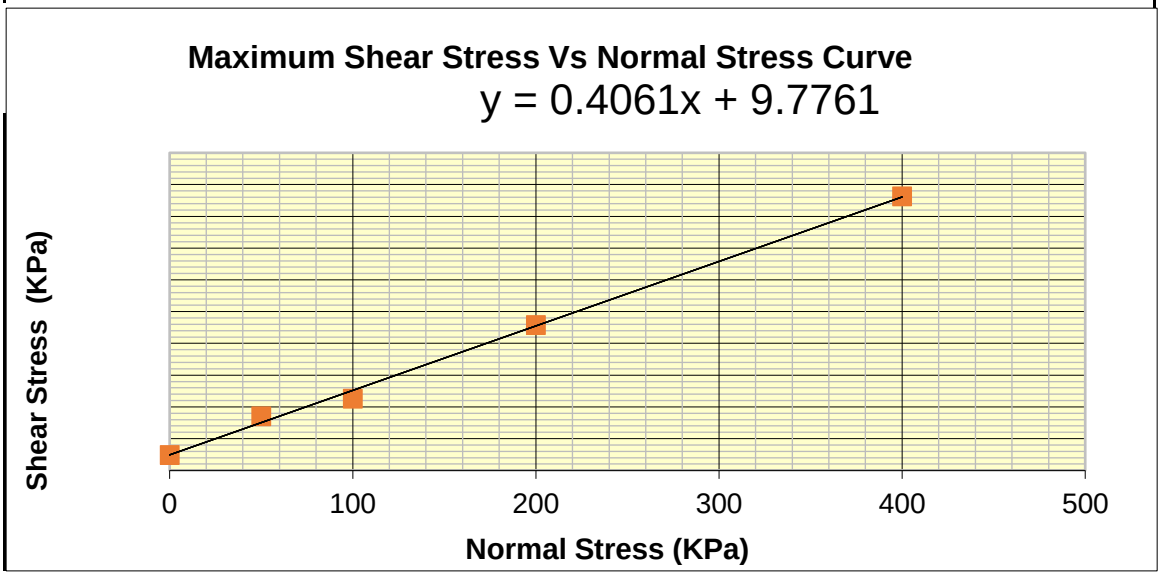

Appendix F: Summary of Data Analyzed by Plaxis

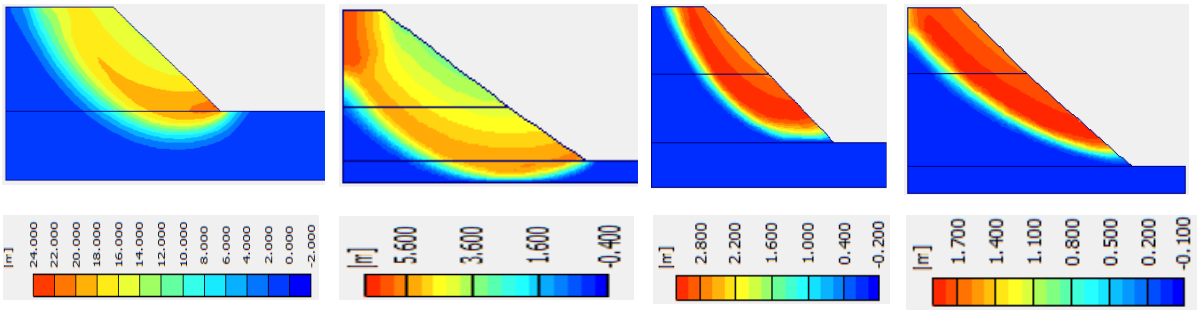

a) FS1 analysis FOS=3.929

b) FS1 analysis FOS=1.231

c) FS3 analysis FOS=1.0036

d) FS4 analysis FOS=0.887

Figure F.1: IDP and FOS under actual site condition

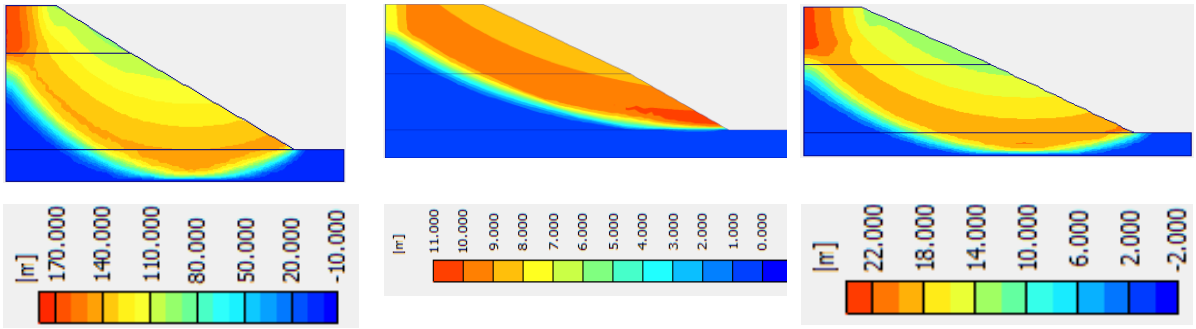

a) ES1 analysis FOS=1.455

b) ES2 analysis FOS=1.479

c) ES3 analysis FOS=1.243

Figure F.2: IDP and FOS for existing slopes with actual site condition

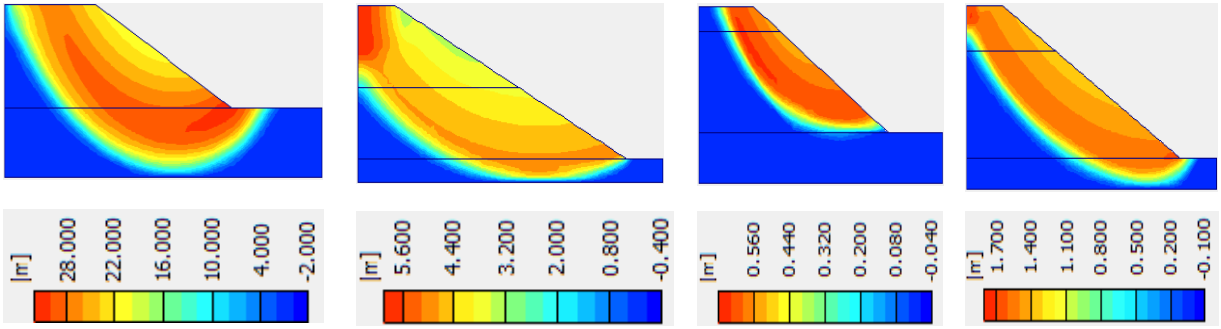

a) FS1 analysis FOS=4.255

b) FS2 analysis FOS=1.477

c) FS3 analysis FOS=1.692

d) FS4 analysis FOS=1.851

Figure F.3: IDP and FOS for failed slopes with ERA recommendation slope profile

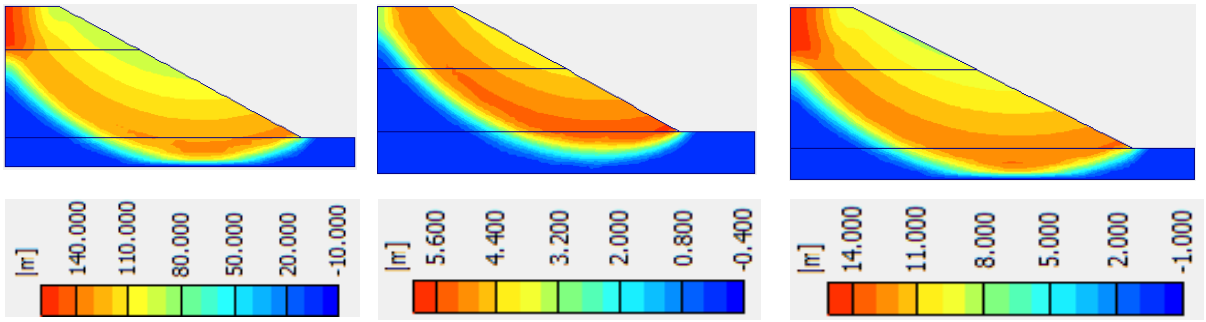

a) ES1 analysis FOS=1.417

b) ES2 analysis FOS=2.375

c) ES3 analysis FOS=1.565

Figure F.4: IDP and FOS for existing slopes with ERA recommendation slope profile

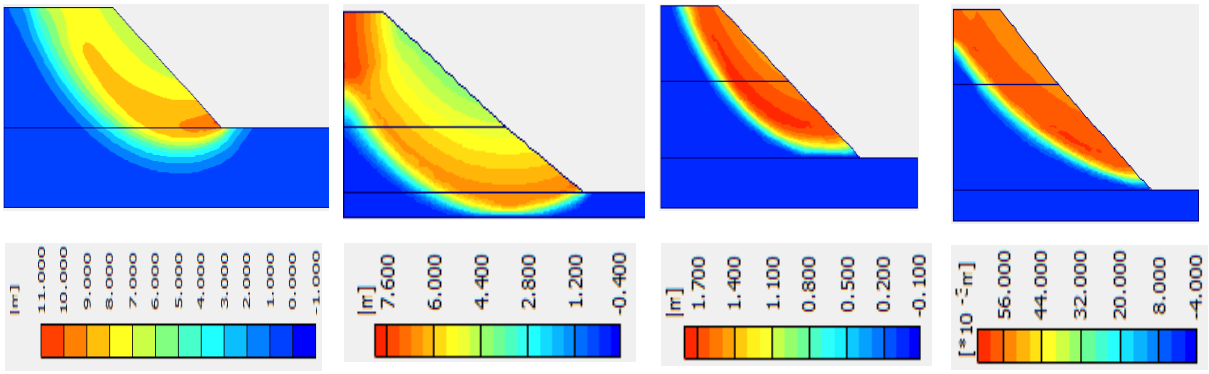

a) FS1 analysis FOS=3.842

b) FS2 analysis FOS=1.198

c) FS3 analysis FOS=0.9964

d) FS4 analysis FOS=0.747

Figure F.5: IDP and FOS for failed slopes in a saturated condition

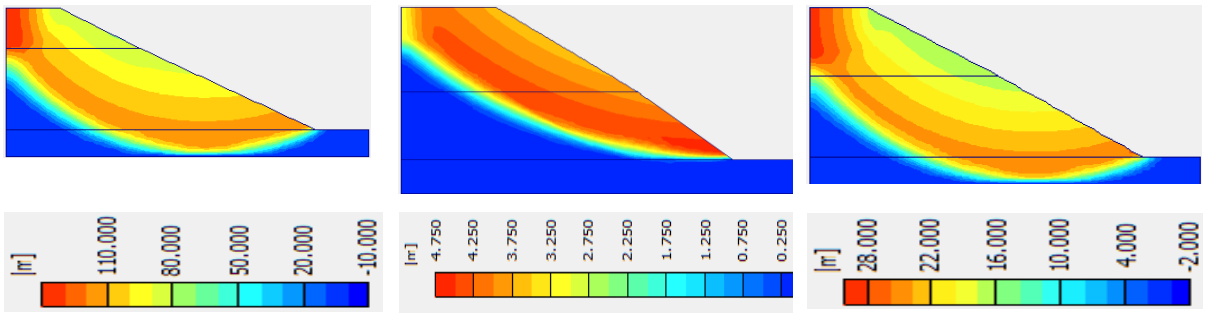

a) ES1 analysis FOS=1.414

b) ES2 analysis FOS=1.407

c) ES3 analysis FOS=1.236

Figure F.6: IDP and FOS for existing slopes with saturated condition

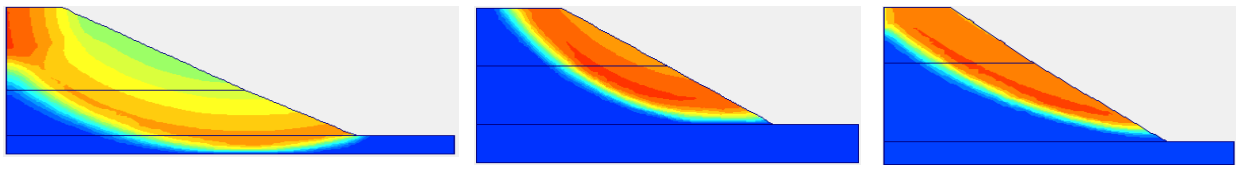

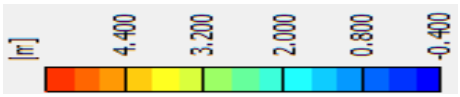

a) FS2 dry analysis

FOS=1.231

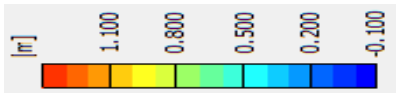

b) FS3 dry analysis

FOS=1.0064

d) FS4 dry analysis

FOS=0.887

Figure F.7: IDP and FOS for selected failed slopes with dry condition

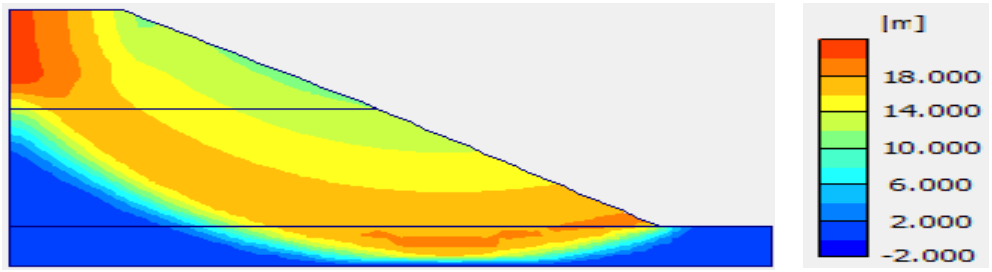

c) ES3 dry analysis

FOS=1.243

Figure F.8: IDP and FOS for existing slope(ES3) with dry condition

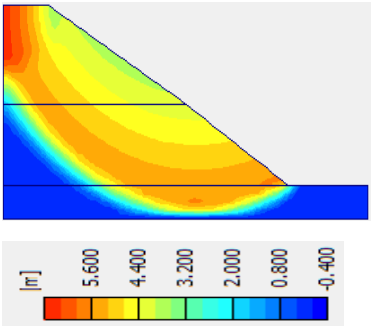

a) FS2 H=11m actual,

FOS=1.635

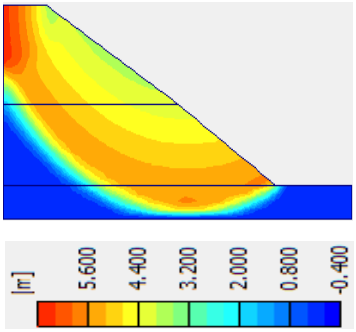

b) FS2 saturated H=11m,

FOS= 1.607

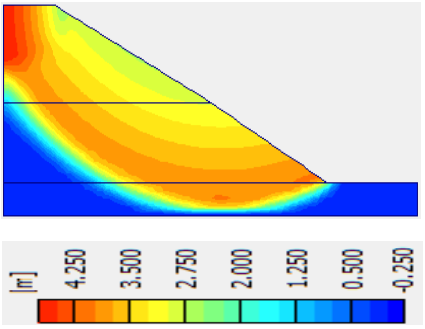

c) FS2 dry H=11m,

FOS=1.635

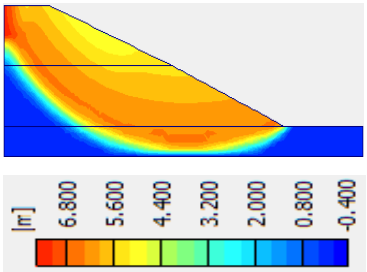

d) FS2 H=8m actual

FOS=2.432

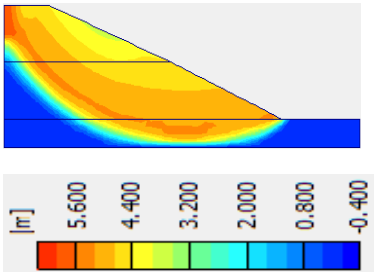

e) FS2 H=8m, saturated

FOS=2.431

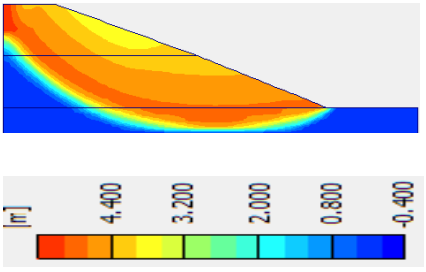

f) FS2 H=8m, dry

FOS=2.434

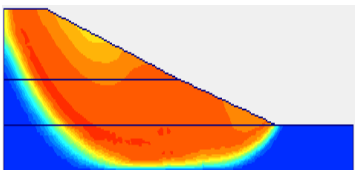

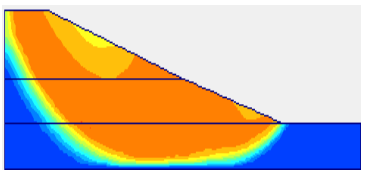

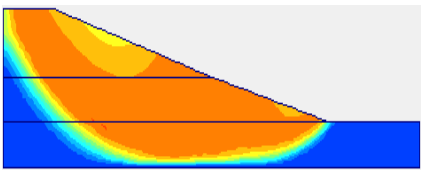

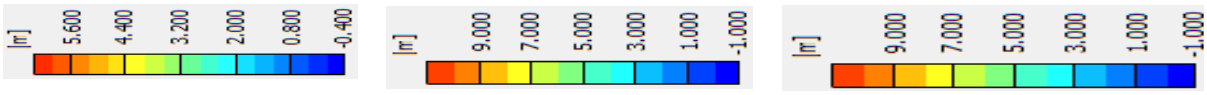

g) FS2 H=5m FOS=4.401

h) FS2 H=5m saturated FOS=3.395

i) FS2 H=5m dry FOS=4.409

Figure F.9: FOS values of FS2 slope under varying slope height and groundwater level

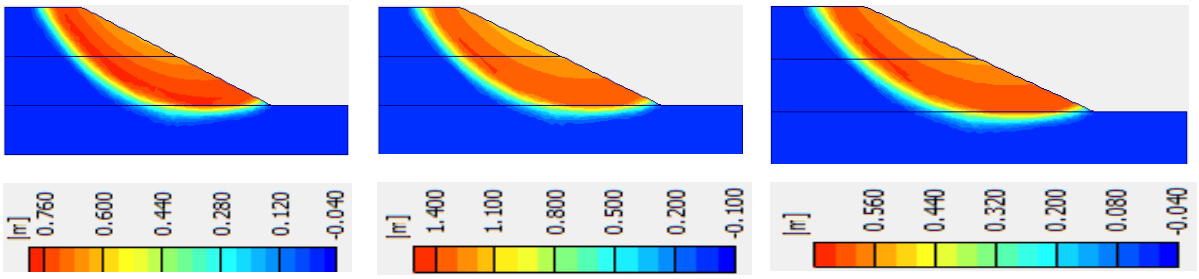

a) FS3 actual H=4m FOS=1.42

b) FS3 Saturated H=4m FOS=1.416

c) FS3 dry H=4m FOS=1.442

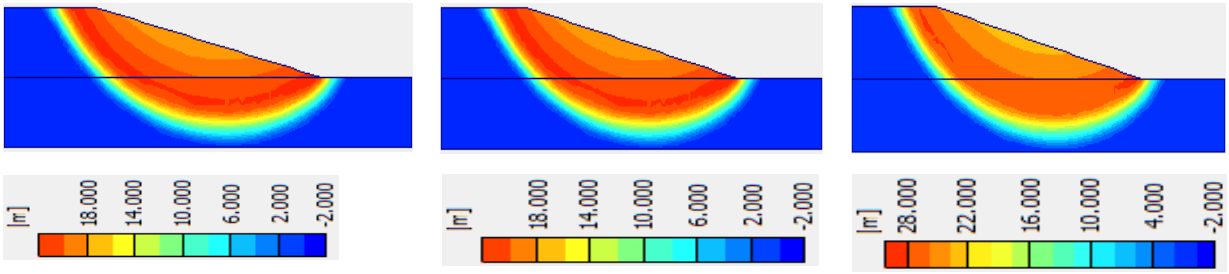

d) FS3 actual H=2m FOS=3.578

e) FS3 saturated H=2m FOS=3.578

f) FS3 dry H=2m FOS=3.728

Figure F.10: FOS values of FS3 under varying slope height and groundwater level

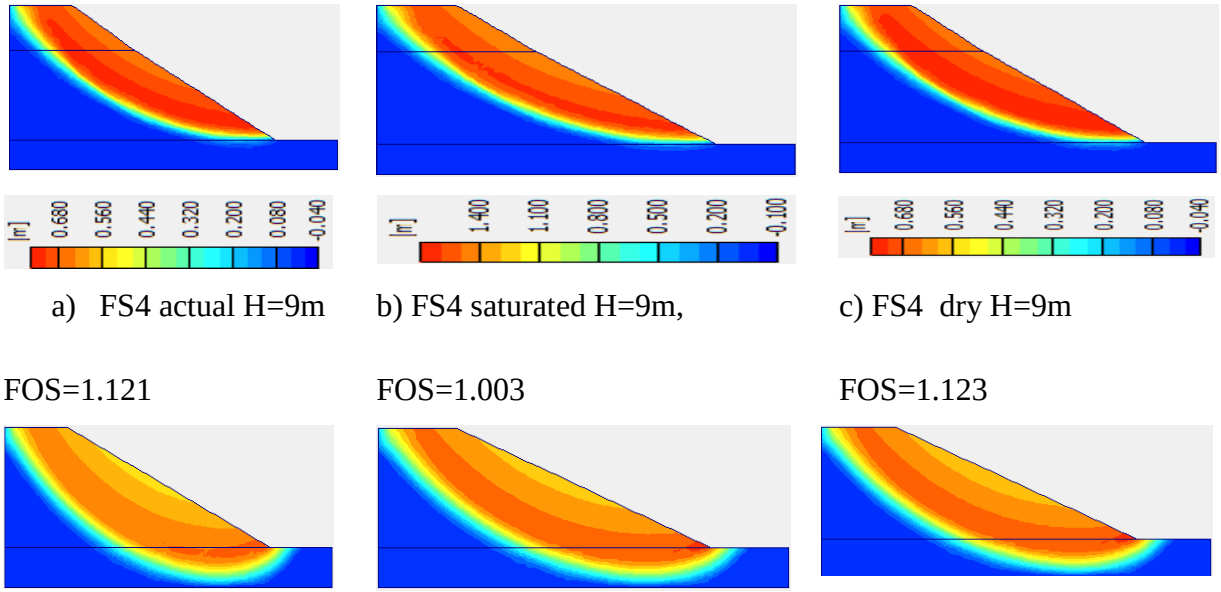

a) FS4 actual H=9m FOS=1.121

b) FS4 saturated H=9m, FOS=1.003

c) FS4 dry H=9m FOS=1.123

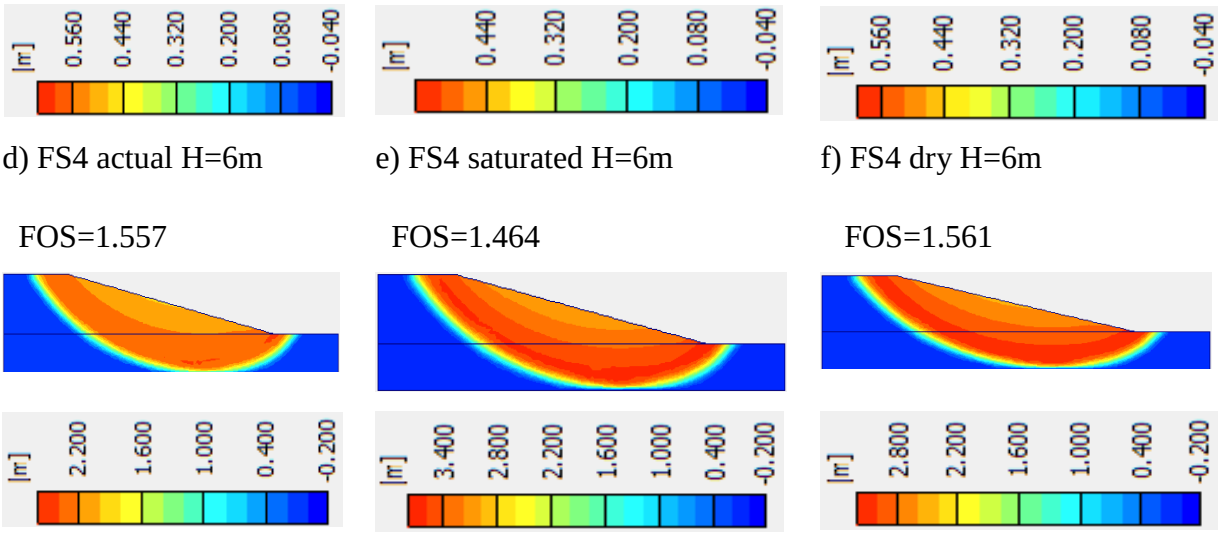

d) FS4 actual H=6m FOS=1.557

e) FS4 saturated H=6m FOS=1.464

f) FS4 dry H=6m FOS=1.561

g) FS4 actual H=3m FOS=2.806

h) FS4 saturated H=3m FOS=2.742

i) FS4 dry H=3m FOS=2.822

Figure F.11: FOS values of FS4 slope under varying slope height and groundwater level

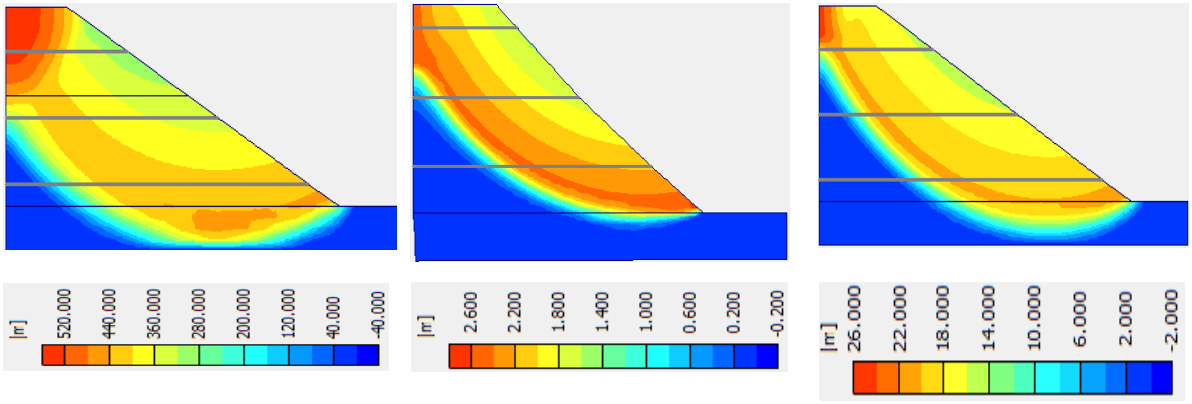

ES1 saturated with geogrid actual FOS=2.84

ES2 saturated with geogrid actual FOS=2.343

ES3 saturated with geogrid actual FOS=3.066

Figure F.12: FOS values for the existing slopes with geogrids.

Appendix G: Summary of Sensitivity Analysis Output

Table F.1 Sensitivity Analysis Output

Sensitivity Analysis											
Parameter C-value			1 46	6 51	11 56	16 61	21 66	26 71	31 76	36 81	41 86
FOS	0.806 2.32	0.964 2.445	1.111 2.568	1.263 2.693	1.406 2.818	1.545 2.941	1.681 3.065	1.815	1.945	2.072	2.196
Parameter phi-value			1 45	5 50	10 55	15 60	20 65	25	30	35	40
FOS	0.049 2.141	0.246 2.485	0.491 2.901	0.737	0.825	0.917	1.007	1.097	1.182	1.267	1.359
Parameter bulk unit weight value					9 16 23	10 17 24	11 18	12 19	13 20	14 21	15 22
FOS	1.736 1.195	1.639 1.177	1.56 1.161	1.519 1.146	1.436 1.131	1.385	1.342	1.305	1.271	1.24	1.213
Parameter K-value			2.06 0.00000206	0.206	0.0206 0.000000206	0.00206	2.06E-08	0.000206 2.06E-09		0.0000206 2.06E-10	
FOS	1.216	1.216	1.216	1.216	1.216	1.219	1.246	1.243	1.242	1.242	1.242
Parameter E-value in GPa				0.0005 0.0805	0.0105 0.0905	0.0205 0.1005	0.0305 0.1105	0.0405 0.1205	0.0505 0.1305	0.0605 0.1405	0.0705 0.2005
FOS	1.2445 1.216	1.2185 1.216	1.2155 1.216	1.2155 1.216	1.2155 1.216	1.2155	1.2155	1.2155	1.2155	1.2155	1.216
Parameter v-value			0.2	0.225	0.25	0.275	0.3	0.325	0.35		
	FOS	1.215	1.215	1.215	1.2155	1.216	1.216	1.2165			
Slope height		3	6	9	12						
FOS	2.806	1.557	1.121	0.887							

Table F.2: Sensitivity Factor Computation

Amin	A*	Amax	S(xi)		Sensitivity factor
0.806	1.111	3.188	1.869487	0.274527	1.869486949
0.049	0.825	2.901	2.516364	0.940606	2.516363636
1.131	1.213	1.436	0.183842	0.067601	0.183841715
1.216	1.216	1.246	0.024671	0	0.024671053
1.2155	1.216	1.216	0	0.000411	0.000411184
1.216	1.216	1.2165	0.000411	0	0.000411184
0.887	0.887	2.806	2.163472	0	2.163472379

Appendix H: Aerial Photographs for the Selected Study Area

a) Google Earth Photo, 5/26/2020 b) Actual Site Photo

Figure H.1: FS1 Sample Typical location from Google Earth and Actual Site Photo

a) Google Earth Photo, 5/26/2020 b) Actual Site Photo

Figure H.2: FS2 Sample Typical location from Google Earth and Actual Site Photo

a) Google Earth Photo, 5/26/2020 b) Actual Site Photo

Figure H.3: ES1 Sample Typical location from Google Earth and Actual Site Photo

Figure H.4: ES2 Sample Typical location from Google Earth Photo, 5/26/2020

a) Google Earth Photo, 5/26/2020 b) Actual Site Photo

Figure H.5: FS3 Sample Typical location from Google Earth and Actual Site Photo

a) Google Earth Photo, 5/26/2020 b) Actual Site Photo

Figure H.6: ES3 Sample Typical location from Google Earth and Actual Site Photo

a) Google Earth Photo, 5/26/2020

b) Actual Site Photo

Figure H.7: FS4 Sample Typical location from Google Earth and Actual Site Photo